UAH RESEARCH REPORT NO. 240

FINAL TECHNICAL REPORT

DYNAMIC SIMULATION OF CORONAL MASS EJECTIONS

BY:

R. S. STEINOLFSON

and

S. T. WU

The University Of Alabama In Huntsville

THIS RESEARCH WORK WAS SUPPORTED BY THE

NATIONAL AERONAUTICS AND SPACE ADMINISTRATION

CONTRACT NAS8-33216

UAH Research Report No. 240

DYNAMIC SIMULATION OF CORONAL MASS EJECTIONS

by

R. S. Steinolfson and S. T. Wu

Final Technical Report

This research work was supported by
the National Aeronautics and Space Administration
Contract NAS8-33216

Submitted by

The University of Alabama in Huntsville
P.O. Box 1247
Huntsville, Alabama 35807

April 1980

Acknowledgements

This work was supported by the National Aeronautics and Space Administration under Contract NAS8-33216. The authors would like to thank Drs. Ernie Hildner, Steve Suess, Einar Tandberg-Hanssen, and Murray Dryer for many helpful discussions during the course of this work.

Acknowledgement is made to the National Center for Atmospheric Research, which is sponsored by the National Science Foundation, for the use of its computing facilities.

The manuscript was typed by Miss Lynn Breeding and Miss Karen Goodrowe, whose services are appreciated.

Summary

A model is developed for the formation and propagation through the lower corona of the loop-like coronal transients in which mass is ejected from near the solar surface to the outer corona. The mass ejections are simulated with numerical solutions of the time-dependent, two-dimensional, dissipationless, magnetohydrodynamic equations of motion. The objective is to obtain a better understanding of the physical processes responsible for and occurring in the mass ejections.

The main difference between this model and previous similar models is that we assume that the initial state for the transient is a coronal streamer. In previous models the initial state has been taken as a hydrostatic state with a force-free magnetic field. In the coronal streamer, the atmosphere is not stationary and the magnetic field is not force-free. A coronal streamer consists of closed magnetic field lines near the solar surface with overlying and adjacent open field lines. The plasma is stationary in the closed region and flows outward in the open region.

Coronal streamers are observed to last for long periods on the solar surface and, therefore, must represent a quasi steady-state solution to the complete time-dependent equations. Since a self-consistent analytic solution for coronal streamers does not exist, a numerical solution is constructed. The initial state for the streamer is a polytropic, hydrodynamic solution to the steady-state radial equation of motion coupled with a force-free dipole magnetic field. The numerical solution of the complete time-dependent equations then gradually approaches a stationary coronal-streamer configuration. The streamer configuration becomes the initial state for the coronal

transient. The streamer and transient simulations are performed completely independent of each other. The transient is created by a sudden increase in the pressure at the base of the closed-field region in the streamer configuration. Both coronal streamers and coronal transients are calculated for values of the plasma beta (the ratio of thermal to magnetic pressure) varying from 0.1 to 100. We compare our results with similar results obtained using the previously-developed model mentioned above in which the initial atmosphere is stationary and the magnetic field is force-free. We also compare both our results and the previous results with the observed characteristics of loop-like, mass ejection coronal transients in order to evaluate the relative merits of the two models.

TABLE OF CONTENTS

I. INTRODUCTION

Coronal mass ejections are transients or disturbances in the corona in which material appears to escape from the Sun. The data obtained during the Skylab mission, by both on-board and ground-based instrumentation, have contributed significantly to the understanding of coronal mass ejections. For several ejections the coverage was complete enough that observations of the coronal transient (seen in white light and radio) could be associated with observations related to the solar phenomena, usually eruptive prominences or flares (seen in XUV, EUV, H_α and X-ray), responsible for the transient (Hildner et al., 1975a, b; Rust and Hildner, 1976; Dulk et al., 1976; Poland and Munro, 1976; Schmahl and Hildner, 1977). This complete data analysis and establishment of a cause-effect relationship are crucial in determining the physical processes in mass ejections. These associations are particularly informative for the purpose of developing dynamic models when the data can be used to infer the thermodynamic properties (temperature, density and pressure), velocities and magnetic fields of at least some portions or features of either the solar event or the transient. If the simulation can be made to reasonably reproduce the observed physical properties, then since all the above properties are included in the simulation, information will be obtained on the physics of the solar event and transient for which observations are not available.

Several models have been developed to simulate the dynamics of the transient (see, e.g., Nakagawa et al., 1975; Steinolfson and Nakagawa, 1976; Steinolfson et al., 1978; Wu et al., 1978). These models do clarify some basic physics of the observed features of mass

ejections; however, they are not able (by the very nature of the models) to simulate some other important features. The shortcomings of the current models (which will be discussed in Section V) are such that it is questionable whether they are capable of simulating the detailed structure of mass ejections; even though they may be applicable to other types of atmospheric transients. In this report we present a model which leads to a more realistic simulation of the observed features of mass ejections and, consequently, to a better understanding of the related physical processes. The particular class of ejections which we simulate is the loop-like mass ejections that tend to be associated with eruptive prominences (Hildner, 1977).

The equations used in the model and the procedure followed in solving the equations are discussed in Section II. The complete simluation consists of two parts. In the first part a coronal- or helmet-streamer configuration is established; this is discussed in Section III. A coronal-streamer configuration consists of closed magnetic loops on the solar surface that lie beneath and adjacent to an open-field region. In the second part a perturbation in the thermal pressure is introduced at the base of the closed loops which simulates the solar event. The numerical solution of the time-dependent equations then simulates the resulting coronal transient. The coronal transient is discussed in Section IV. The model is compared with a previous model in Section V and with observations in Section VI. The results are summarized and the conclusions that can be made from this study are discussed in Section VII.

II. EQUATIONS AND SOLUTION PROCEDURE

The solar atmosphere is assumed to behave as a single fluid with negligible dissipative effects. With these assumptions the time-dependent magnetohydrodynamic (MHD) equations that describe atmospheric flows in the meridional plane can be written in MKS units as follows:

$$\frac{\partial \rho}{\partial t} + \frac{\partial}{\partial r}(\rho u) + \frac{\partial}{\partial \theta}\left(\frac{\rho v}{r}\right) = -\frac{2\rho u}{r} - \frac{\rho v}{r}\cot\theta \tag{1a}$$

$$\frac{\partial u}{\partial t} + u\frac{\partial u}{\partial r} + \frac{B_\theta}{\mu\rho}\frac{\partial B_\theta}{\partial r} + \frac{1}{\rho}\frac{\partial p}{\partial r} + \frac{v}{r}\frac{\partial u}{\partial \theta} - \frac{B_\theta}{\mu\rho r}\frac{\partial B_r}{\partial \theta} = -\frac{GM_s}{r^2} + \frac{v^2}{r} - \frac{B_\theta^2}{\mu\rho r} \tag{1b}$$

$$\frac{\partial v}{\partial t} + u\frac{\partial v}{\partial r} - \frac{B_r}{\mu\rho}\frac{\partial B_\theta}{\partial r} + \frac{v}{r}\frac{\partial v}{\partial \theta} + \frac{B_r}{\mu r\rho}\frac{\partial B_r}{\partial \theta} + \frac{1}{r\rho}\frac{\partial p}{\partial \theta} = \frac{B_r B_\theta}{\mu r\rho} - \frac{uv}{r} \tag{1c}$$

$$\frac{\partial B_r}{\partial t} - \frac{\partial}{\partial \theta}\left(\frac{uB_\theta - vB_r}{r}\right) = \frac{1}{r}(uB_\theta - vB_r)\cot\theta \tag{1d}$$

$$\frac{\partial B_\theta}{\partial t} + \frac{\partial}{\partial r}(uB_\theta - vB_r) = -\frac{1}{r}(uB_\theta - vB_r) \tag{1e}$$

$$\frac{\partial p}{\partial t} + \gamma p\frac{\partial u}{\partial r} + u\frac{\partial p}{\partial r} + \frac{\gamma p}{r}\frac{\partial v}{\partial \theta} + \frac{v}{r}\frac{\partial p}{\partial \theta} = -\frac{\gamma p}{r}(2u + v\cot\theta) \tag{1f}$$

where the dependent variables are the density ρ, radial velocity u, meridional velocity v, pressure p, radial magnetic field B_r, and meridional magnetic field B_θ. The independent variables are the radius r and the latitude θ. The constants are the polytropic index γ, magnetic permeability μ, solar gravitational constant G, and solar mass M_s.

The region in which the solution to the above equations is desired is shown in Figure 1; i.e., the region bounded by the solar surface and 5 solar radii ($R_\odot$) in radial distance and by the equator and the pole in meridional distance. The solution is assumed to be symmetric about the equator. The equations are solved numerically using a modified Lax-Wendroff difference scheme given by Rubin and Burstein (1967). The grid spacings used are $\Delta r = 0.1\ R_\odot$ and $\Delta\theta = 2.5$ deg. The time step is chosen to be the maximum allowable from the usual stability criterion for Eulerian difference schemes; i.e., $\Delta t = \min(\Delta t_r, \Delta t_\theta)$ where $\Delta t_r = \Delta r/|\lambda r|$ and $\Delta t_\theta = r\Delta\theta/|\lambda_\theta|$ and $|\lambda_r|$ ($|\lambda_\theta|$) is the maximum eigenvalue (the sum of the fluid velocity and the characteristic velocity) in the radial (meridional) direction. A smoothing term suggested by Lapidus (1967) is used to reduce numerical oscillations. The amount of the smoothing is controlled by a constant. Lapidus used a value of 4; we use a value of 2. The initial conditions and the boundary conditions for this initial-boundary value problem for the coronal streamer and the coronal transient calculations are discussed in Sections III and IV, respectively.

When Equations (1) are written in conservation form, as they must be in order to solve numerically, they contain singularities at the pole due to terms of the form $v/\sin\theta$ and $B_\theta/\sin\theta$. Both the numerator and denominator of these relations vanish at the pole. In the numerical solution these singularities were overcome by setting the values of the above two relations at the pole (point 2 in Figure 1) equal to their respective values at the grid point next to the pole (point 3).

The above equations can be non-dimensionalized with respect to some selected reference values in such a way that the only parameters are γ, β (the ratio of thermal to magnetic pressure), and a parameter

involving the reference temperature. We selected the reference values as the initial values at the solar surface at the equator. Since γ and the reference temperature are kept constant, the only parameter remaining in the equations is β. A number of theoretical studies have demonstrated the importance of the value of β (see, e.g., Steinolfson and Dryer, 1978; Nakagawa et al., 1976; Steinolfson et al., 1978). The importance of β in the present problem is investigated by examining coronal-streamer and coronal-transient structures for β varying from 0.1 to 100. The results for $\beta = 4$ and $\beta = 0.5$ are discussed in the most detail.

A listing of the computer code used to numerically solve Equations (1) is included in Appendix A along with a description of the input variables for the code. A separate code is used to produce the computer-generated plots presented in this report, and this computer code and a description of the input variables for it are given in Appendix B. Appendix C contains a listing of a sample run for a coronal-streamer simulation. All of the computer simulations were performed on the CRAY-1 computer at the National Center for Atmospheric Research in Boulder, Colorado.

III. CORONAL STREAMERS

A schematic of the magnetic field lines in a coronal streamer is shown in Figure 2. The fluid velocity is essentially zero inside the closed-field region with all the outward flow occurring in the open-field region. A current sheet exists on the equator in the open region where the magnetic field reverses direction. Coronal streamers are long-lived structures (often lasting for days) and, hence, must represent, in some sense at least, a configuration approaching a solution to the steady state form of Equations (1). However, such a steady-state solution would be extremely difficult to obtain. Pneuman and Kopp (1971) have constructed a steady state solution, but they assumed that the field lines were known a priori and neglected the interaction between the field lines and the fluid. Our approach is to start with an initial state as close to a coronal streamer as feasible, numerically solve the time-dependent equations and let the solution relax with time to a coronal-streamer configuration. This approach was used by Endler (1971) and Weber (1978) for a constant temperature medium; an assumption which we do not make. The final coronal-streamer configuration serves as the initial state for the coronal transient discussed in Section IV.

A. Initial State and Boundary Conditions

The thermodynamic variables and the velocity are given initially by a radial, hydrodynamic solution to the time-independent form of Equations (1); i.e., a Parker-type solution (Parker, 1963). The reference values for the thermodynamic variables in the initial state at 1 $R_\odot$ are temperature $T = 1.8 \times 10^6$ K and electron number density $n = 2.25 \times 10^8$ cm^{-3}, where $\rho = nm_p$ and m_p is the proton mass. With these values the only solutions to the steady-state hydrodynamic equations with the critical

point beyond 1 $R_\odot$ are obtained for $1 < \gamma < 1.1$. The larger the value of γ, the more rapidly β increases with distance. Since too large an increase in β with increasing distance is unrealistic and since $\gamma = 1$ implies that the temperature is constant, we used an intermediate value for γ of 1.05. The hydrodynamic solution then gives a value for the initial radial velocity at the solar surface of 8.2 km s^{-1}. The initial meridional velocity is assumed to be zero.

The magnetic field is assumed to be force-free initially. The equations for the vanishing of the Lorentz force and the absence of free magnetic poles then determine the initial magnetic field configuration, which is given in terms of Legendre polynomials of order 1. The initial configuration selected is the dipole configuration obtained by using the Legendre polynomial of degree 1; i.e.,

$$B_r = \frac{2 B_o \cos \theta}{r^3},$$

$$B_\theta = \frac{B_o \sin \theta}{r^3}$$

where B_o is the reference magnetic field. This configuration tends to restrain material ejected near the equator and consequently is referred to as a "closed field" configuration. The reference magnetic field is selected to obtain the desired value for β. Values for the reference magnetic field of 0.83 G and 2.35 G at 1 $R_\odot$ at the equator yield values for the plasma beta of 4 and 0.5, respectively. β increases with radius and decreases away from the equator. The initial value of β at 1 $R_\odot$ at the pole is a factor of 2 less than at 1 $R_\odot$ at the equator.

The above chosen initial state does not, of course, represent a steady-state solution to the complete two-dimensional equations. Hence, when used as the initial state, the time-dependent solution to Equations (1) will evolve until the solution relaxes to or approaches a steady-state solution (the coronal streamer).

The remaining quantities that must be specified for the numerical solution are the boundary conditions at the four boundaries in Figure 1. The solution is assumed to be symmetric about the equator, and hence, the boundary conditions there become (using the notation in Figure 1):

$$u_1 = u_3 \qquad p_1 = p_3 \qquad B_{\theta_1} = B_{\theta_3}$$
$$v_1 = -v_3 \qquad \rho_1 = \rho_3 \qquad B_{r_1} = -B_{r_3} .$$

For the coronal-streamer calculation, the pole can also be considered as a symmetry boundary. The boundary conditions there then become the same as for the equator with the following exceptions:

$$B_{\theta_1} = -B_{\theta_3} \qquad B_{r_1} = B_{r_3} .$$

Note that there is no flow across either of the above two boundaries. There is flow, however, across the remaining two boundaries at 1 $R_\odot$ and 5 $R_\odot$ (the inner and outer boundaries) and this makes their treatment somewhat more difficult. The reason can best be explained using the theory of characteristics. This has been done previously for one-dimensional, hydrodynamic flow by Nakagawa and Steinolfson (1976) and Steinolfson and Nakagawa (1976). We will briefly discuss the extension of their analysis to the present problem (see also Endler, 1971). Equations (1) are a hyperbolic system of equations, and therefore, the characteristics

for the equations are all real. In this case information from any point in the flow field can only propagate in the characteristic directions. In the radial direction, then, information propagates at the six velocities equal to the sum of the radial velocity and the radial component of each of the six characteristic velocities. At the outer boundary the flow is generally supersonic and super-Alfvenic, and hence, information from the outer boundary only propagates downstream, i.e., outside the region of interest. Another way of viewing this is that all six radial characteristic directions at the outer boundary are positive. This implies that the boundary conditions at 5 $R_\odot$ can be specified arbitrarily. We choose to linearly extrapolate using the relation $Q_b = Q_n + \Delta Q$ (notation as in Figure 1) where Q is any dependent variable and ΔQ is calculated at each time step from the values at the two radial grid points adjacent to the boundary. At the inner boundary two of the six radial characteristic directions are negative, and consequently, information from the region of interest propagates upstream to the boundary. In this case four dependent variables at the lower boundary can be specified arbitrarily, and two must be calculated from some form of compatibility relations (see Steinolfson and Nakagawa, 1976). Strictly speaking, the compatibility relations are equations that can be derived from Equations (1) which must be satisfied by the dependent variables in each of the characteristic directions. Steinolfson and Nakagawa (1976) have shown that first-order or second-order (linear) extrapolation often works as well as using the more complex compatibility relations. We choose to hold the pressure, density and radial magnetic field at their initial values at the boundary and calculate the meridional velocity so that the total velocity and magnetic field are parallel at the boundary. The

radial velocity and meridional magnetic field are calculated from linear extrapolation. When the velocity approaches zero inside the closed-field region, the pressure and density at the boundary are allowed to increase accordingly by linear extrapolation.

B. Numerical Results

The initial-boundary value problem discussed above forms a well-posed problem, and the time-dependent equations are now solved numerically using the appropriate initial state and boundary conditions. It remains to select a criterion by which to determine when a steady-state, coronal-streamer configuration has been achieved. Admittedly this decision must be somewhat subjective. The criterion we used was to continue the time-dependent solution until the configuration did not change appreciably over a period of at least one hour of physical time. In general, the smaller the value of β, the more rapidly the solution evolved to a coronal-streamer configuration.

1. $\beta = 4$

The initial dipole magnetic field is shown in Figure 3(a). The field lines are spaced at 5 deg intervals at the solar surface. The curve consisting of long dashes represents the location where the radial flow velocity is equal to the sound speed (sonic curve). The radial flow velocity is equal to the Alfven velocity based on the total magnetic field along the curve composed of short dashes (Alfven curve). The evolving magnetic field is shown for three successive times in Figure 3. The numerical solution is changing so slowly with time after 24 hours that the solution at that time is selected as the final coronal-streamer configuration. Several of the dependent variables after 24 hours are shown in Figure 4. The nondimensional values given for the pressure and density are the values referenced to their respective initial values at

each point in the flow field. From Figures 3 and 4, it is easy to see the field lines evolving from a closed dipole field to a coronal-streamer configuration with the closed field lines lying beneath and adjacent to open field lines. The sonic curve is displaced inward in the final state, except for a small region around the equator, due to the general increase in velocity. The velocity decreases somewhat at the equator from that in the initial state and increases at the pole as shown in Figure 5. The changes in the pressure and density at the equator and pole referenced to their respective initial values at each point are also shown in the figure.

The top of the closed-field region in Figure 4(a) at the equator occurs at approximately the same radius at which the Alfven curve intersects the equator. The reason for this is that the magnetic field at the equator is approximately zero above the closed region, and the velocity is approximately zero in the closed region. There is one field line above the intersection of the Alfven curve with the equator that appears to be closed in Figure 4(a), but this is believed to be due to the interpolation between the relatively large grid spacing that we have used. The intersection of this field line with the equator is gradually moving outward.

The pressure and density are increased over their initial values and the velocity is approximately zero in the closed region as indicated in Figures 4 and 5. The temperature is proportional to the ratio of the pressure to the density, and hence, it is evident that the temperature also increases throughout the flow field. The increments in pressure and density between the contour lines in Figure 4 are equal so more tightly grouped curves denote larger gradients. The velocity vectors closely parallel the magnetic field lines in Figure 4 despite the relatively large value of β. The open field lines never become completely radial; not even the field lines next to the pole. Hence, assuming that the flow

does follow the field lines, the flow near the pole is in a region where the cross-sectional area of an infinitesimal flow tube increases more rapidly than as the radius squared. Several steady-state studies for flow in coronal holes where the cross-sectional area of a flow tube is specified to increase more rapidly than as the radius squared have appeared in the literature (see, e.g., Kopp and Holzer, 1976, and Steinolfson and Tandberg-Hanssen, 1977). These steady-state studies conclude that the velocity increases in coronal holes, but that the temperature and density decrease, which is in contrast with the present results. The reason for the discrepancy is not immediately apparent, but it is most likely related to the different boundary conditions applied at the solar surface in the two studies and to the inclusion of the meridional terms in the equations used in our study.

The results discussed above for $\beta = 4$ display several of the characteristics expected of coronal streamers (correct magnetic field configuration, higher pressure and density and zero velocity in the closed region, etc.) in spite of the fact that $\beta = 4$ is larger than would be expected in coronal streamers. We now consider a reference plasma beta almost an order of magnitude smaller ($\beta = 0.5$) which is a value more consistent with observations.

2. $\beta = 0.5$

The initial dipole magnetic field configuration and the location of the sonic curve are the same regardless of the value of the reference magnetic field as can be seen by comparing Figures 6(a) for $\beta = 0.5$ and 3(a) for $\beta = 4$. The only difference in the two figures is that the Alfven velocity increases with the magnetic field causing the Alfven curve to move outward as β is decreased (magnetic field increased). As the magnetic field evolves in this case, as shown in Figure 6, the Alfven curve moves inward throughout the flow field as does the sonic curve except for a

small region around the equator. Some of the variables in the final coronal-streamer configuration are presented in Figure 7. The sonic curve intersects the equator in Figure 7(a) at approximately the same radius as for $\beta = 4$ in Figure 4(a) indicating that the sonic Mach number near the equator must be similar for the two cases. The radial velocities along the equator are about the same as can be seen by comparing Figures 5 and 8, and therefore, the temperatures along the equator must be similar. The temperature distribution along the pole is clearly quite different for the two values of β with the temperature for $\beta = 0.5$ being considerably larger. The velocity in the open region near the pole for $\beta = 0.5$ is more than a factor of two larger than the velocity over the closed region near the equator. The velocity in the closed region is again approximately zero as would be expected, but the pressure and density in the closed region are increased considerably more for $\beta = 0.5$ than they were for the larger value of β.

The distribution of β throughout the flow field is shown in Figure 9 for both the initial state and the coronal streamer. For the initial state β increases from 0.5 (0.25) at the solar surface to 10.2 (2.6) at 5 $R_\odot$ along the equator (pole). In the coronal streamer the value of β increases at the equator and becomes infinite along the neutral line above the closed region. Since β is so large near the equator and since the incremental spacing between the curves in Figure 9(b) is fixed, the β distribution is not shown within 10 deg of the equator in order to show the distribution in the remainder of the flow field. β is decreased at the pole near the solar surface and increased at 5 $R_\odot$ at the pole compared to the corresponding values in the initial state. Throughout most of the flow field, β is lower in the coronal streamer than for

the initial state. Because of this and since the thermal pressure is higher in the coronal streamer than initially, the magnetic pressure in the coronal streamer is also higher than the initial value throughout most of the flow field.

As for the previous example, the velocity flows more or less along the field lines. Also, none of the field lines becomes exactly radial. The radial location of the top of the closed field region is not changed appreciably from that for the higher value of β. The dimensions of the closed-field region are considered below for a wider range of β.

3. Coronal-Streamer Structure

As the magnitude of the reference magnetic field is increased in studies such as the above two, one would expect that the field lines would remain closed to a higher altitude in the solar atmosphere. That this indeed happens is illustrated in Figure 10 where the dimensions of the height and the base at the solar surface for the closed region are plotted as a function of β. The circles indicate values obtained from individual computer runs. A closed region is not achieved for $\beta = 100$. The base dimension of the closed region is relatively unaffected by the values of β unless β becomes larger than about 5. The maximum values of the pressure and density (referenced to their respective initial values at each point) in the closed region are plotted as a function of β in Figure 11. The large increase in the pressure and density with decreasing β is due partly to the increased Lorentz force which is directed inward on the closed region and partly to the increased magnetic field strength which increases the tensile strength of the field lines and makes it more difficult to open the closed field lines. This latter effect has been demonstrated by Steinolfson

et al. (1978). Both of these effects must be balanced by an increase in thermal pressure in the closed region, and both effects also tend to compress the fluid in the closed region. For $\beta = 100$ the magnetic field is so weak ($B = 0.17$ G) that the solution remains essentially unchanged.

The velocity and the thermodynamic variables at 5 $R_\odot$ are presented as a function of meridional angle in Figures 12 and 13, respectively, for several values of β. The velocity is consistently larger over the pole than the equator with the velocity differential between the two regions increasing dramatically as β decreases. The pressure and density are highest near the equator and the temperature is highest at the pole for each value of β. The temperature distribution for β equal to 4,10 and 100 are so close to being the same that the curves cannot be resolved in Figure 13. For the two lowest values of β (0.5 and 0.1), the density decreases and the velocity increases from their respective initial values in the polar region in analogy with flow in coronal holes (Kopp and Holzer, 1976). However, according to the study of Steinolfson and Tandberg-Hanssen (1977) the temperature and pressure should also decrease in coronal holes, while in the present study both variables increase. Hence, although the open magnetic field in the present study is diverging as would be expected in coronal holes, it appears that the flows in the open regions in the present study are not analogous to previous steady-state studies of flows in coronal holes. As mentioned earlier, the discrepancy may be due to the different boundary conditions in the two studies, but it may also be partially due to the meridional gradients in the equations that we use which are neglected in the steady-state studies.

IV. CORONAL TRANSIENTS

The coronal-streamer configurations discussed in the previous section are long-lasting structures which may remain virtually unchanged on the solar surface for periods up to several days. These configurations are often observed to exist prior, both spatially and temporally, to the occurence of mass ejections or, as they are often referred to, coronal transients. We now simulate a coronal transient by using the final state for the coronal streamer as the initial state for the coronal transient.

A. Initial State, Boundary Conditions and Perturbation

As mentioned above, the final state for the coronal streamer is used as the initial state for the coronal transient. The reference β referred to in this section (and all other reference conditions) is the reference value used for the coronal streamer. Naturally, all the dependent variables may have a different value in the final streamer simulation than they did in the corresponding initial state.

The boundary conditions applied at the equator, pole and 5 $R_\odot$ for the coronal transient are the same as those used for the coronal streamer. At the solar surface a perturbation in the thermodynamic variables from their initial values (the final values for the coronal streamer) is introduced near the equator to simulate the solar event that produces the resulting coronal transient. The perturbation is assumed to occur instantaneously, to be symmetric about the equator, and to extend in the meridional direction over a total of 10 deg (5 deg on each side of the equator) or 1.22×10^5 km. The perturbed values are maintained for the duration of the calculation. The magnitude of the perturbation varies with each simulation and is discussed along with the corresponding numerical results. The pressure and density are assumed to be constant throughout the perturbed region. Outside this region they are calculated from linear extrapolation as for the streamer

simulation. The remaining variables at the solar surface are simply set equal to the value at the grid point next to the boundary at each time step; i.e., $Q_b = Q_n$ (first-order extrapolation).

For the streamer simulation the computation had to be carried out for the entire flow regime at each time step. In this section we only compute the solution from the solar surface to the leading edge of the coronal transient.

B. Numerical Results

The coronal transients for the two values of β used in the previous section ($\beta = 0.5, 4$) are investigated. The transient for the lower value of β is examined in more detail since, as will be shown later, it agrees more closely with observations. Some of the more important results for other values of β are also discussed.

1. $\beta = 4$

The thermal pressure in the perturbation is increased by a factor of 2.6 above the initial value at the solar surface for the streamer calculation which, as discussed in the previous section (see Figure 5), remained unchanged throughout that calculation. The pressure increase results from a factor of 2 increase in temperature and a factor of 1.3 increase in density. Some of the variables in the resulting coronal transient are shown in Figure 14 after 60 minutes and in Figure 15 after 120 minutes. The corresponding variables for the initial state for the transient are those in Figure 4. The time is now referenced to the start of the transient simulation. The pressure and density are referenced to their initial values for the streamer calculation at each point in the flow field.

The large velocity that develops at the solar surface in the vicinity of the perturbed region causes the flow to become super-Alfvenic there after 60 minutes and both supersonic and super-Alfvenic after 120 minutes as seen in Figures 14(a) and 15(a). The coronal transient is preceded by an MHD shock which has the characteristics of a fast shock since it increases the meridional component in both the velocity and magnetic field. It is not clear from the figures that the shock normal (or the direction of shock propagation) lies directly along the magnetic field, except, of course, when the shock propagates into the open region along the equator. Note that a meridional velocity component cannot be produced by the shock along the equator because of the boundary conditions there. When the shock normal and magnetic field are parallel for some finite length of the shock, the fast shock becomes a switch-on shock since it produces a meridional component in the magnetic field and velocity when neither was present ahead of the shock. The numerical shock is necessarily spread over a few grid points due to the relatively large grid spacing that we used. Hence the shock location shown in the figures is selected to be approximately at the mid-point of the jump in the dependent variables produced by the shock. The shock has not completely formed at large meridional angles near the pole after 60 minutes. The shock velocity along the equator increases from 306 km s^{-1} at 2 $R_\odot$ to 584 km s^{-1} at 4 $R_\odot$ implying that the shock travels considerably faster in the initially open region than it does in the initially closed region. One reason for this is that there is an ambient outward flow in the open region which tends to increase the shock velocity in the laboratory frame.

The contact surface separates the initial coronal plasma from that which has been emitted from the perturbed region. The maximum increase in pressure lies along the equator below the contact surface while the maximum increase

in density is between the contact surface and the shock. Due to the relatively large value of β used for this simulation, the magnetic field does not have a large effect on guiding the outward-propagating plasma and is, to a large extent, essentially carried along with the plasma. As can be seen in the figures, the contact surface travels outward both radially and meridionally. It appears from the figures that the fluid is propagating across the field lines (which should not occur due to the infinite conductivity) since the contact surface at 120 minutes encloses more field lines than at the earlier time. That this is not actually happening is a result of the method used to calculate the field lines. The field lines are calculated by starting at the same location on the solar surface at each time step and using the magnitude and direction of the magnetic field at that time as the starting values. Since the magnitudes of both components of the magnetic field at the solar surface are allowed to change with time, different field lines may be traced out from each starting location at each time.

2. $\beta = 0.5$

The thermal pressure in the perturbation is increased by a factor of 10, the temperature by a factor of 5, and the density by a factor of 2. All of these increases are with respect to the corresponding final values at the solar surface for the streamer calculation. Some of the variables in the coronal transient produced by this perturbation are shown in Figure 16 after 80 minutes and in Figure 17 after 180 minutes. The corresponding variables for the initial state for this transient are given in Figure 7.

The relatively low velocities and large magnetic field prevent the flow from becoming either supersonic or super-Alfvenic at the solar surface near the perturbed region as it did for $\beta = 4$. The transient

is again preceded by a fast MHD shock which may, over a portion of its extent, be a switch-on shock. The shock velocity along the equator increases from 397 km s^{-1} at 2 $R_\odot$ to 517 km s^{-1} at 4 $R_\odot$. Hence, as for the results at $\beta = 4$, the shock travels faster in the initially open region than in the initially closed region. However, the shock velocity is now larger at 2 $R_\odot$ and smaller at 4 $R_\odot$ than it was for $\beta = 4$. The shock velocities for these two values of β and for other values of β will be discussed in more detail later.

The contact surface does not travel as far in the meridional direction as for $\beta = 4$. This is due to the larger magnetic field in this case which tends to restrict the meridional movement of the plasma. Along the equator the maximum increase in pressure again occurs below the contact surface and the maximum increase in density between the contact surface and the shock. This is shown better in Figure 18 which gives the radial profiles of the radial velocity, pressure and density along the equator initially and at two subsequent times. The mass excess initially in the closed region of the coronal streamer (illustrated by the increase in density between 1 and 2 $R_\odot$ in the figure) is at the later times distributed between the shock and the contact surface. The fluid ahead of the contact surface (including the fluid initially in the closed region) has been heated, compressed and accelerated by the shock. This figure also demonstrates how the shock is spread over a number of grid points. At t = 80 minutes, the shock, which should be a sharp discontinuity, extends approximately from 3.75 $R_\odot$ to 4.25 $R_\odot$.

The curves consisting of the dark shorter dashes in Figures 16 (d) and 17 (d) enclose a region in which the density is higher than in the adjacent regions in the meridional direction. That is, in a scan from

the equator to the pole at a fixed radius, an increase in density would be found in this region. This is illustrated by the meridional scans of pressure and density at 4 $R_\odot$ for three times in Figure 19. The density has a definite peak at approximately 30 degrees at 180 minutes where the scan is now through the "leg" of the high density region in Figure 17 (d). At the previous times the scans are partially through the top of the high density region. The pressure, on the other hand, does not have a peak away from the equator at 180 minutes and decreases more or less monotonically for all three times from the equator to the pole. The curves with the dark longer dashes in Figures 16 (d) and 17 (d) represent the approximate locations of the maximum in the high-density region. The importance of this dense region will be discussed in the following sections.

The distribution of β throughout the flow field (except near the equator, since β again becomes very large there) for the two times in Figures 16 and 17 are given in Figure 20. The initial distribution of β is shown in Figure 9 (b). The β contours are very similar to those of the pressure -- especially after 180 minutes when the magnetic field is almost radial. These plots illustrate that for the region shown, β remains relatively small during and following the passage of the coronal transient.

3. Other Pertinent Results

The shock velocities along the equator at various values of β are shown in Figure 21. A wide range of perturbations in the thermodynamic variables was used to obtain these results as shown in Table I. The

shock velocities for the $\beta = 4$ and $\beta = 0.5$ studies discussed above are represented by the dashed curves. There are several important results that should be noted from the figure. First of all, despite more than an order of magnitude change in both β and the magnitude of the pressure perturbation, the shock velocities for all simulations do not vary that much in magnitude; at 4 $R_\odot$, the velocities are all within 200 km s^{-1} of each other. Note also that at a fixed β, a reduction in the magnitude of the pressure perturbation reduces the shock velocity although the shape of the curve remains generally the same. This is true for both $\beta = 4$, where both runs have the same density perturbations, and $\beta = 0.5$, where the two runs have different density perturbations. One would expect that if the density perturbation was varied over a wide range this result may be altered. Finally, as β is decreased, the shock velocity curves tend to become flatter until for $\beta = 0.1$ the shock velocity is essentially constant over the radius range considered. If the results had been extended to a larger radius, the curves for $\beta = 4$ would certainly approach a constant velocity also although the final velocity in this case may be somewhat larger.

The fact that a larger pressure perturbation was used to obtain the results in Figure 21 as β decreases is not coincidental. In fact, at each value of β there is a value of the magnitude of the pressure perturbation (at a fixed value of the density perturbation) below which a physically realistic solution (in the sense that the flow along the equator is outward) is not obtained. This would be expected since the perturbation is in a closed-field region, and a certain pressure force is required to open the field lines so the fluid can flow outward. As the strength of the magnetic field increases (β decreases), one would expect that a larger

force would be required. The approximate minimum pressure perturbation for a fixed density perturbation of 1.3 is shown in Figure 22 for the range of β used for the results in Figure 21. The circles indicate the runs used to obtain the curve. Hence, it is clear that as β is decreased below 0.5, the required pressure perturbation increases very rapidly.

V. COMPARISON WITH OTHER APPLICABLE MODELS

The other models which we will consider here are those which are similar to the one we have developed in the sense that they consider the transient to be the coronal response to a simulated solar event near the solar surface. That is, the driving force responsible for the transient originated and remains near the solar surface. We do not consider the magnetically-driven model proposed by Mouschovias and Poland (1978) and further studied by Anzer (1978). They assume that the driving force is the magnetic force produced by the interaction of currents flowing in the loops with their self-induced magnetic fields. Yeh and Dryer (1980) have attempted to show that coronal loop transients cannot be driven by such magnetic forces.

All similar models that have appeared in the literature which purport to be applicable to the formation and propagation of coronal transients in the lower corona (with the inner boundary inside the critical points near the solar surface) in either the meridional or latitudinal plane and including the magnetic field have assumed that the atmosphere is initially stationary. On the surface this appears to be a reasonable assumption since the kinetic energy in the inner corona is certainly less than either the thermal or magnetic energies. It is definitely simpler to assume an initially stationary atmosphere since an analytic planar solution including the magnetic field (other than a purely radial field, which is unrealistic in the lower corona) and a finite velocity has not been obtained for the lower corona to the author's knowledge. In addition to including the velocity in the initial streamer for the transient in the present study, the magnetic field in the streamer decreases with radius similar to a dipole field. This offers the

advantage of producing a reasonable increase in β with radius. For any higher order field β increases too rapidly with radius to be reasonable. We first present some results for an initially stationary atmosphere and then compare these and other similar results from the literature with our results obtained using a coronal streamer as the initial state.

A. A Model with an Initially Stationary Atmosphere

The initial state for this model is taken to be an initially hydrostatic atmosphere for the thermodynamic variables and a dipole magnetic field. This initial state represents a solution to the steady-state form of the complete set of time-dependent equations (Equations (1)). The reference conditions for the thermodynamic variables and the magnetic field are the same as used for the streamer simulations. Again we will consider the $\beta = 4$ and $\beta = 0.5$ simulations. The boundary conditions, grid spacings and spatial distribution of the perturbation are also the same as used above. Hence the simulations considered here are in every way as close as possible to the same as those done for the coronal transients in the previous section.

The spatial distribution of some of the variables for the coronal transient for $\beta = 4$ are shown in Figure 23 after 120 minutes. The magnitudes of the pressure and density perturbations used for this simulation are the same as those used in the previous section for $\beta = 4$. Similar results for $\beta = 0.5$ are presented in Figure 24 after 80 minutes. The pressure in the perturbation is now increased by a factor of 6 and the density by 1.3, which is not the same as those used in the previous

section for $\beta = 0.5$. The corresponding results obtained when the initial atmosphere is a coronal streamer are given in Figure 15 for $\beta = 4$ and in Figure 16 for $\beta = 0.5$. The pressure and density along a meridional scan at 4 $R_\odot$ for the present simulation with $\beta = 0.5$ are illustrated in Figure 25. These results are analagous to those in Figure 19 for the streamer initial configuration. All the above results for the initially stationary atmosphere will now be discussed vis-à-vis the results from the previous section.

B. Comparisons

For convenience, the results obtained in this section and other previously published results for an initially stationary atmosphere will be referred to as the "stationary" results, while those in the previous section for an initial atmosphere consisting of a coronal streamer will be referred to as the "streamer" results. The figure numbers of the results presented in this paper will only be referred to when some confusion may arise.

Since the perturbations are identical for both the stationary and streamer results for $\beta = 4$ and since the magnetic field in this case is relatively small, a comparison of the results should be similar to what one would expect from a similar hydrodynamic study. Indeed they are, as will soon become apparent. The shock travels more rapidly and the fluid velocity is larger for the streamer results due to the initial fluid velocity. The shape of the shock curves in Figure 23(a) and 15(a) are also similar, which would be expected since the shock velocity in a lab-

oratory frame depends to a large extent on the characteristic speeds in the ambient medium through which it is propagating (in addition to its dependence on the velocity in the ambient medium). As the magnetic field is relatively small in this case the sound speed dominates, and, of course, this speed is approximately the same for the two sets of results. The separation between the shock and contact surface is larger in the stationary results since the velocity of the contact surface depends entirely on the fluid velocity which is smaller for the stationary results. The general shape of the pressure and density profiles for the two cases are quite different with the higher pressure and density values being confined to a region closer to the equator for the streamer results. The maxima of the pressure and density are larger for the streamer results because of the increased values in the initial closed magnetic field region near the equator and the solar surface.

The magnetic field would be expected to have a larger effect on the results for $\beta = 0.5$. Note that a larger pressure pulse was used for the streamer results when $\beta = 0.5$ than for the stationary results. This difference is not expected to affect the comparisons. The shock travels faster along the equator (despite a smaller pressure perturbation) and slower at the pole for the stationary results as compared to the streamer results (Figures 24 (a) and 16 (a)). This result is reasonable since shocks with a given initial strength always travel faster across field lines than along them. This effect is not important for $\beta = 4$ since the field is so small. The other results mentioned above for $\beta = 4$ remain much the same at the lower β. It is important to note that the high pressure and density region near the equator for the streamer results is even more exaggerated at $\beta = 0.5$.

The curves consisting of heavy short dashes in Figure 24 (d) enclose the high density region that would be observed in a meridional scan at a fixed radius in analogy with the similiar curves in Figures 16 (d) and 17 (d). A curve with heavy longer dashes again identifies the approximate center of the maxima of this high-density region. The density peaks away from the equator for the stationary results show up on the meridional scans at 4 $R_\odot$ in Figure 25; however, they are much further from the equator than for the streamer results in Figure 19.

The maxima of the high density region (the curves consisting of the heavy longer dashes in Figures16 (d), 17 (d), and 24 (d) are shown for several times for β = 0.5 and for both the stationary (dashed curves) and streamer results in Figure 26. The maxima for the streamer results are contained within 30 deg of the equator, while the maxima for the stationary results extends to the pole. A plot similiar to that in Figure 26 is shown in Figure 27 for only the streamer results for β = 0.1. This plot demonstrates that as β is decreased below 0.5 the angle of confinement of the density maxima decreases. The variation of the density along a meridional scan at 4 $R_\odot$ for β = 0.1 corresponding to the results in Figure 27 is presented in Figure 28. This result is in comparison with that in Figure 19 and shows that as β decreases the density peak becomes more prominent. The importance of these results will be discussed in comparing the results with observations in the following section.

VI. COMPARISON WITH OBSERVATIONS

Among the several classes into which coronal transients in general tend to be grouped (Hildner, 1977), the type we have attempted to simulate is the loop-like transients in which mass is ejected from near the solar surface to the outer corona. The major observed characteristics of this type of transient will first be discussed followed by a comparison with the calculated results. We concentrate on attempting to simulate just the characteristics for this single class of transient since it is extremely difficult to simulate all observed aspects of one particular transient (due to inhomogenieties, non-planar effects, dissipative effects, etc.). One would also expect that different physical processes are involved in the different classes of transients.

A. Observed Characteristics of Coronal Transients

The velocity of the leading edge of a transient is a relatively simple quantity to determine from the white-light observations. These velocities generally lie in the range of 100-1200 km s^{-1} with an average value of 470 km s^{-1} (Gosling et al., 1976). The velocity tends to increase or remain about constant between approximately 2.5 - 5 $R_\odot$.

The reason that coronal transients are observed by the white-light coronagraph is that the density in the transients exceeds that in the surrounding medium. Hence it is necessary that the simulated transient produce a density enhancement similar to that observed. It should be pointed out that the coronagraph only observes the projection of the

transient in the meridional plane so it is certainly possible that they do not lie in that plane. For the purpose of the following discussion we will assume that the observed transients do lie in or near the meridional plane. As shown by Hildner (1977), the observed transient tends to take the shape of a loop, with the loop extending from near the solar surface, out to some maximum height (which increases with time) in the atmosphere, and back to the solar surface. The northern and southern edges (the legs) of the loop generally remain stationary so the loop just stretches outward with time. The centers of the loops usually lie within 40 deg of the equator with a symmetrical distribution about a maximum at the equator. The latitudinal extents of the transients are usually less than 65 deg.

The coronal magnetic field cannot be measured directly so other means are necessary to infer its value. Dulk et al. (1976) used data from type IV radio bursts along with white-light data to calculate the magnetic field for the loop-shaped mass ejection of 15 September 1973. They calculated a value of 2.6 G at a height of 3.1 $R_\odot$ and a β at that height of 0.007. Further evidence for expecting relatively large fields near transients is due to the observations that at least three-quarters of the transients occur over active regions (Hildner, 1977) where the magnetic field is larger than elsewhere on the sun. Mass ejections also tend to be associated with magnetic phenomena (flares, eruptive prominences, etc.) which occur near lines on the solar surface which separate uni-polar regions of the photospheric magnetic field.

The mass associated with a mass ejection generally lies in the range $1 - 24 \times 10^{15}$ g with an average of 6.2×10^{15} g while the energy ranges from $1.6 - 69.8 \times 10^{30}$ erg with an average of 11.9×10^{30} erg (Hildner, 1977).

In order to obtain these values it is necessary to make some rather speculative assumptions concerning the size of the transient.

B. Comparisons

The radial velocity of the leading edge of the transient can be easily simulated by the model proposed herein, as shown in Figure 21, or by any of the previous models which do not use the streamer configuration as the initial state. Larger velocities than those in Figure 21 can be obtained in our present model by increasing the magnitude of the pressure perturbation. The observed increase in velocity with radius, however, is generally between that shown in Figure 21 for $\beta = 0.5$ and $\beta = 0.1$, implying that the lower β results are more realistic in this sense. The fact that previous models also reproduce the observed velocities (as demonstrated by the one-dimensional study by Steinolfson and Nakagawa, 1977, and the two-dimensional study by Dryer et al., 1979) makes the leading-edge velocity a poor quantity by which to judge the relative merits of various models.

One observed characteristic that previous models cannot adequately simulate (at least not for any of the results published to date) is the shape of the loop as given by the density enhancement. This is seen quite clearly for the calculations presented in Section V for a non-streamer, stationary initial state (see Figures23(d) and 24(d)). The enhanced density region moves both radially and laterally away from the simulated solar event similar to the motion of an expanding bubble. Similiar results for a non-streamer, stationary initial state have been obtained in all previous two-dimensional studies (see eg. Dryer et al., 1979; and Nakagawa,

Wu and Han, 1978). These previous results are obtained regardless of whether the initial magnetic field configuration is assumed to be closed over the location of the simulated solar event (as for the initial dipole configuration for the streamer calculation in Figure 3(a)) or open (as if the configuration in Figure 3(a) was rotated 90 deg so the configuration originally at the pole was at the equator). The edges of the loop do not move laterally in the present model as seen in Figures 16(d) and 17(d). The most graphic comparison of the present model with previous models is shown in Figure 26 which shows the outward motion of the high density regions near the outer edge of the transient. The latitudinal extent of the transient for the present model is 60 deg which lies within the observed latitudinal extent of 65 deg. The results in Figure 27 show that if β is decreased the latitudinal extent of the transient decreases. Hence it is obvious that the present model agrees considerably better than the previous models with the observed density enhancement which is certainly one of the more important observed characteristics.

Since the coronal magnetic field cannot be measured directly, a direct comparison cannot be made between observed and calculated magnetic field magnitudes at various points in the flow field. The inferred value of the magnetic field of 2.6 G at 3.1 $R_\odot$ made by Dulk et al. (1976) agrees closely with the values at that height in our model for the $\beta = 0.1$ calculation. Dulk, however, obtained a β of 0.007 at that height which is about an order of magnitude less than what we calculated indicating a difference in thermal pressure. Although the magnetic field cannot be measured, it is reasonable to expect that if the β is relatively small (as observations indicate it should be) it may be important in guiding

the fluid; that is, in determining the shape of the expanding loop. Thus it is logical to assume that the magnetic field prevents the lateral expansion of the loop, as has been done by several authors. This assumption would agree with our model since it is the magnetic field that contains the lateral expansion in Figures 26 and 27. The fact that mass ejections generally originate near lines separating uni-polar regions on the solar surface implies that previous studies using open field lines do not apply to mass ejections.

We have not attempted to calculate the mass or energy associated with the mass ejections in our simulations. Due to the assumptions that must be made for the dimensions of the transient both in the observations and in the simulation, it is not felt that a direct comparison of the absolute magnitudes would be meaningful.

VII. DISCUSSION AND CONCLUSIONS

The main objective for developing self-consistent models such as the one we have presented herein is to attempt to gain a better understanding of the physical mechanisms occurring in and responsible for observed coronal transients. As such, it is necessary that the simulations reproduce the available observations as well as possible in order that valid conclusions regarding the behavior of transient quantities that are not observed can be made from the simulations. From the previous section it is apparent that the present model does reproduce the observations better than similar models published previously. Again we should point out that the only other models we are considering here assume that a sudden disturbance near the solar surface produced the transient.

The major difference between the present models and previous ones is the initial state for the coronal transient. While previous models simply use a stationary atmosphere with a force-free magnetic field, we have used a coronal-streamer configuration in which the atmosphere is not stationary (except in the closed-field region) nor is the magnetic field force-free. Coronal streamers are frequently observed in the lower solar corona and are observed to occur over uni-polar regions of the photospheric magnetic field. As mentioned previously, this is the region in which mass ejections commonly originate. We should also mention that the class of transients which we are concerned with is the loop-like transient in which mass is ejected to the outer corona. Although it does not appear likely that previous models apply to these transients, they may certainly be applicable to other classes of transients or other solar

phenomena.

The magnetically-driven models studied by Mouschovias and Poland (1978) and Anzer (1978) may also merit some consideration as the mechanism involved in mass ejections. However, the simplifications made in their analysis and the fact that their study is confined to just the top of the loop limit the application of their results. A more complete study of magnetically-driven models may prove worthwhile.

In the present and previous similar models, the radially-propagating, leading edge of the transient is a shock wave. This shock wave certainly agrees with observations in that it travels radially outward and produces the necessary density enhancement. The fact that both type II and type IV radio bursts (which are indicative of shocks) are often observed in transients substantiates the possibility that the leading edge may be a shock. Other than the frequent observation of radio bursts there is no a priori reason why the leading edge should be a shock. In fact, in the magnetically-driven models, it is not. The lateral edges of previous models are also shock waves (which travel laterally as well as somewhat radially), while in the present model they are due to plasma confinement by the magnetic field. Since the lateral edges of observed transients do not travel laterally, they, of course, cannot be shocks.

The available observations imply that the magnetic field associated with mass ejection coronal transients would be expected to be relatively large. The plasma beta is certainly less than one and may be one or two orders of magnitude smaller. This conclusion being due to the usual occurance of mass ejections over active regions and their association with

magnetic phenomena. The present study supports this view since the best agreement with the well-observed, leading-edge velocities of transients is obtained for $\beta \leq 0.5$. The lower beta results in the simulation also produced better lateral confinement of the edges of the transient.

As β is decreased, the more the simulated coronal transients with a coronal streamer initial state differ from those with an initially stationary, force-free initial state - as shown in the results in Section V. One reason for this is that - as discussed in Section III - the coronal streamer diverges more from the initially stationary, force-free state with decreasing β. For the coronal streamer, as β decreases the following changes occur in the variables: (1) the pressure and density in the closed-field region increase, (2) the velocities increase throughout the open region and the gradient in the velocities between the values at 4 $R_\odot$ at the equator and at the pole increases, and (3) larger changes occur in all the thermodynamic variables and, as for the velocity, the gradients in all the thermodynamic variables between the values at 4 $R_\odot$ at the equator and at the pole increase. Hence the meridional inhomogeneities in the streamer increase with decreasing β.

For a constant reference temperature, as we have assumed, the only other parameter in our model besides β is the polytropic index γ. We used a value of 1.05 which is not much different than the constant temperature value of 1. From the results in Sections III and IV it appears that the temperature does not change much in our simulation of either the streamer or transient providing $\beta \geq 1$. Hence for a large β, the constant temperature solution should not be much different than ours.

However, as β is decreased below 1, the temperature changes more and more from the steady-state value indicating that a constant temperature solution is no longer valid.

The mass that is contained in the expanding loop in our model (i.e.; the enhancement that would be observed by a white-light coronagraph) is entirely composed of mass which was in the corona prior to the occurance of the solar event responsible for the transient. Part of the mass was initially in the closed region and part in the open region of the coronal streamer. In this respect our model contrasts with other more approximate one-dimensional models where the mass is assumed to initially reside in a loop without any consideration given to how the mass-filled loop was formed (Mouschovias and Poland, 1978; and Anzer, 1978). The transient in these simplified models consists of an expansion of the top section of the initial loop outward through the corona, while in our model both the formation and propagation of the loop are calculated self-consistently throughout the meridional plane.

REFERENCES

Anzer, U., Can coronal transients be driven magnetically?, Solar Phys. 57, 111, 1978.

Dryer, M., S. T. Wu, R. S. Steinolfson, and R. M. Wilson, Magnetohydrodynamic models of coronal transients in the meridional plane. II. Simulation of the coronal transient of August 21, 1973, Astrophys. J. 227, 1059, 1979.

Dulk, G. A., S. F. Smerd, R. M. MacQueen, J. T. Gosling, A. Magun, R. T. Stewart, K. V. Sheridan, R. D. Robinson, and S. Jacques, White light and radio studies of the coronal transient of 14-15 September 1973, I. Material motions and magnetic field, Solar Phys. 49, 369, 1976.

Endler, F., Interaction between the solar wind and coronal magnetic fields, unpublished, 1971.

Gosling, J. T., E. Hildner, R. M. MacQueen, R. H. Munro, A. I. Poland, and C. L. Ross, The speeds of coronal mass ejection events, Solar Phys. 48, 389, 1976.

Hildner, E., J. T. Gosling, R. M. MacQueen, R. H. Munro, A. I. Poland, and C. L. Ross, The large coronal transient of 10 June 1973, I. Observational description, Solar Phys. 42, 163, 1975a.

Hildner, E., J. T. Gosling, R. T. Hansen, and J. D. Bohlin, The sources of material comprising a mass ejection coronal transient, Solar Phys. 45, 363, 1975b.

Hildner, E., Mass ejections from the solar corona into interplanetary space, Proceedings of L. D. deFeiter Memorial Symposium on Study of Travelling Interplanetary Disturbances (STIP), published by Air Force Geophys. Lab., Bedford, Mass., 1977.

Kopp, R. A. and T. E. Holzer, Dynamics of coronal hole regions, I. Steady polytropic flows with multiple critical points, Solar Phys. 49, 43, 1976.

Lapidus, A., A detached shock calculation by second-order finite differences, J. Comp. Phys. 2, 154, 1967.

Mouschovias, T. Ch., and A. I. Poland, Expansion and broadening of coronal loop transients: A theoretical explanation, Astrophys. J. 220, 675, 1978.

Nakagawa, Y., S. T. Wu, and E. Tandberg-Hanssen, Dynamic response of an isothermal static corona to finite-amplitude disturbances, Solar Phys. 41, 387, 1975.

Nakagawa, Y., and R. S. Steinolfson, Dynamical response of the solar corona, I. Basic formulations, Astrophys. J. 207, 296, 1976.

Nakagawa, Y., R. S. Steinolfson, and S. T. Wu, On build-up of magnetic energy in the solar atmosphere, Solar Phys. 47, 193, 1976.

Nakagawa, Y., S. T. Wu, and S. M. Han, Magnetohydrodynamics of atmospheric transients. I. Basic results of two-dimensional plane analyses, Astrophys. J. 219, 314, 1978.

Parker, E. N., Interplanetary Dynamical Processes, Interscience, New York, 1963.

Pneuman, G. W., and R. A. Kopp, Gas-magnetic field interactions in the solar corona, Solar Phys. 18, 258, 1971.

Poland, A. I., and R. H. Munro, Interpretation of broadband polarimetry of solar coronal transients: Importance of Hα emission, Astrophys. J. 209, 927, 1976.

Rubin, E. L., and S. Z. Burstein, Difference methods for the inviscid and viscous equations of a compressible gas, J. Comp. Phys. 2, 178, 1967.

Rust, D. M., and E. Hildner, Expansion of an X-ray coronal arch into the outer corona, Solar Phys. 48, 381, 1976.

Schmahl, E., and E. Hildner, Coronal mass ejections - kinematics of the 19 December 1973 event, Solar Phys. 55, 473, 1977.

Steinolfson, R. S. and Y. Nakagawa, Dynamical response of the solar corona II. Numerical simulation near the sun, Astrophys. J. 207, 300, 1976.

Steinolfson, R. S. and Y. Nakagawa, Dynamical response of the solar corona III. Numerical simulation of the 1973 June 10 coronal transient, Astrophys. J. 215, 345, 1977.

Steinolfson, R. S. and E. Tandberg-Hanssen, Thermally conductive flows in coronal holes, Solar Phys. 55, 99, 1977.

Steinolfson, R. S. and M. Dryer, Numerical simulation of MHD shock waves in the solar wind, J. Geophys. Res. 83, 1576, 1978.

Steinolfson, R. S., S. T. Wu, M. Dryer, and E. Tandberg-Hanssen, Magneto-hydrodynamic models of coronal transients in the meridional plane I. The effect of the magnetic field, Astrophys. J. 225, 259, 1978.

Weber, W. J. , The dynamics of coronal magnetic structures, Ph.D. thesis, University of Utrecht, Holland, 1978.

Wu, S. T., M. Dryer, Y. Nakagawa, and S. M. Han, Magnetohydrodynamics of atmospheric transients. II. Two-dimensional plane numerical results for a model solar corona, Astrophys. J. 219, 324, 1978.

Yeh, T., and M. Dryer, Magnetic force in a coronal loop transient, submitted, 1980.

Table I. Perturbation parameters used to obtain the results in Figure 21.

β	curve	δ_p	$\delta\rho$	δ_T
4	solid	2.0	1.3	1.54
4	dashed	2.6	1.3	2.0
1	solid	5	1.3	3.85
0.5	solid	8	1.3	6.15
0.5	dashed	10	2	5.00
0.1	solid	30	1.3	23.10

FIGURE CAPTIONS

1. A schematic of the portion of the meridional plane in which the solution is calculated. The grid spacings are also sketched (not to scale) along with the nomenclature used for the boundary conditions.

2. A schematic of the magnetic field lines in a coronal streamer.

3. The evolution of the coronal magnetic field for $\beta = 4$. The sonic curve is represented by the curve with long dashes and the Alfven curve by the curve with shorter dashes.

4. Planar maps of several of the dependent variables in the coronal streamer for $\beta = 4$. The maximum values given are the maximum values throughout the regions shown. The velocity vectors point in the direction of the velocity at their base and their length is proportional to the magnitude of the velocity. The pressure and density are referenced to their respective initial values at each point in the flow field.

5. Radial distributions of the density, pressure, and radial velocity initially (solid curve) and in the coronal streamer for $\beta = 4$ (Figure 4) at the pole (shorter dashes) and equator (long dashes).

6. The evolution of the coronal magnetic field for $\beta = 0.5$. See the caption for Figure 3.

7. Planar maps of several of the dependent variables in the coronal streamer for $\beta = 0.5$. See the caption for Figure 4.

8. Radial distributions of the density, pressure, and radial velocity initially (solid curve) and in the coronal streamer for $\beta = 0.5$ (Figure 7) at the pole (short dashes) and at the equator (long dashes).

9. Planar maps of the plasma beta for the $\beta = 0.5$ simulation initially and in the coronal streamer.

10. The dependence of the dimensions of the closed region on the reference beta. A closed region is not obtained for $\beta = 100$.

11. The dependence of the maximum pressure and density in the closed region on the reference beta.

12. The meridional distribution of the radial velocity at 5 $R_\odot$ as a function of the reference beta.

13. The meridional distribution of the thermodynamic variables at 5 $R_\odot$ as a function of the reference beta.

14. Planar maps of several dependent variables in the coronal transient for $\beta = 4$ after 60 min. The approximate locations of the shock (double lines) and contact surface (heavy dashed lines) are indicated. See the caption for Figure 4.

15. Planar maps of several dependent variables in the coronal transient for $\beta = 4$ after 120 min. See the caption for Figure 4.

16. Planar maps of several dependent variables in the coronal transient for $\beta = 0.5$ after 80 min. The short dashed curves in (d) enclose the maximum density region and the curve with longer dashes traces out the approximate location of the maximum density in this region. See the caption for Figure 4.

17. Planar maps of several dependent variables in the coronal transient for $\beta = 0.5$ after 180 min. See the captions for Figures 4 and 16.

18. Radial distributions of the density, pressure, and radial velocity initially and at two later times in the coronal transient for $\beta = 0.5$.

19. Meridional distribution at 4 $R_\odot$ of the pressure and density in the coronal transient for $\beta = 0.5$ at three times.

20. Planar maps of the plasma beta for the coronal transient for $\beta = 0.5$ after 80 and 180 min.

21. The variation of the shock velocity along the equator with radius for several values of the reference beta.

22. The magnitude of the pressure perturbation required to produce a mass ejection coronal transient for a fixed value of the density perturbation as a function of the reference beta.

23. Planar maps of several dependent variables in the coronal transient for $\beta = 4$ after 120 min for an initially stationary atmosphere with a force-free magnetic field. See the caption for Figure 4.

24. Planar maps of several dependent variables in the coronal transient for $\beta = 0.5$ after 80 min. for an initially stationary atmosphere with a force-free magnetic field. See the captions for Figure 4 and 16.

25. Meridional distributions at 4 $R_\odot$ of the density and pressure at three times in the coronal transient for $\beta = 0.5$ for an initially stationary atmosphere with a force-free magnetic field.

26. The maxima of the high density regions at several times in the coronal transient with $\beta = 0.5$ for an initial state consisting of a coronal streamer (solid curves) and an initially stationary, force-free atmosphere (dashed curves).

27. The maxima of the high density regions at serveral times in the coronal transient with $\beta = 0.1$ for an initial state consisting of a coronal streamer.

28. Meridional distributions at 4 $R_\odot$ of the density at two times in the coronal transient for $\beta = 0.5$ for an initial state consisting of a coronal streamer.

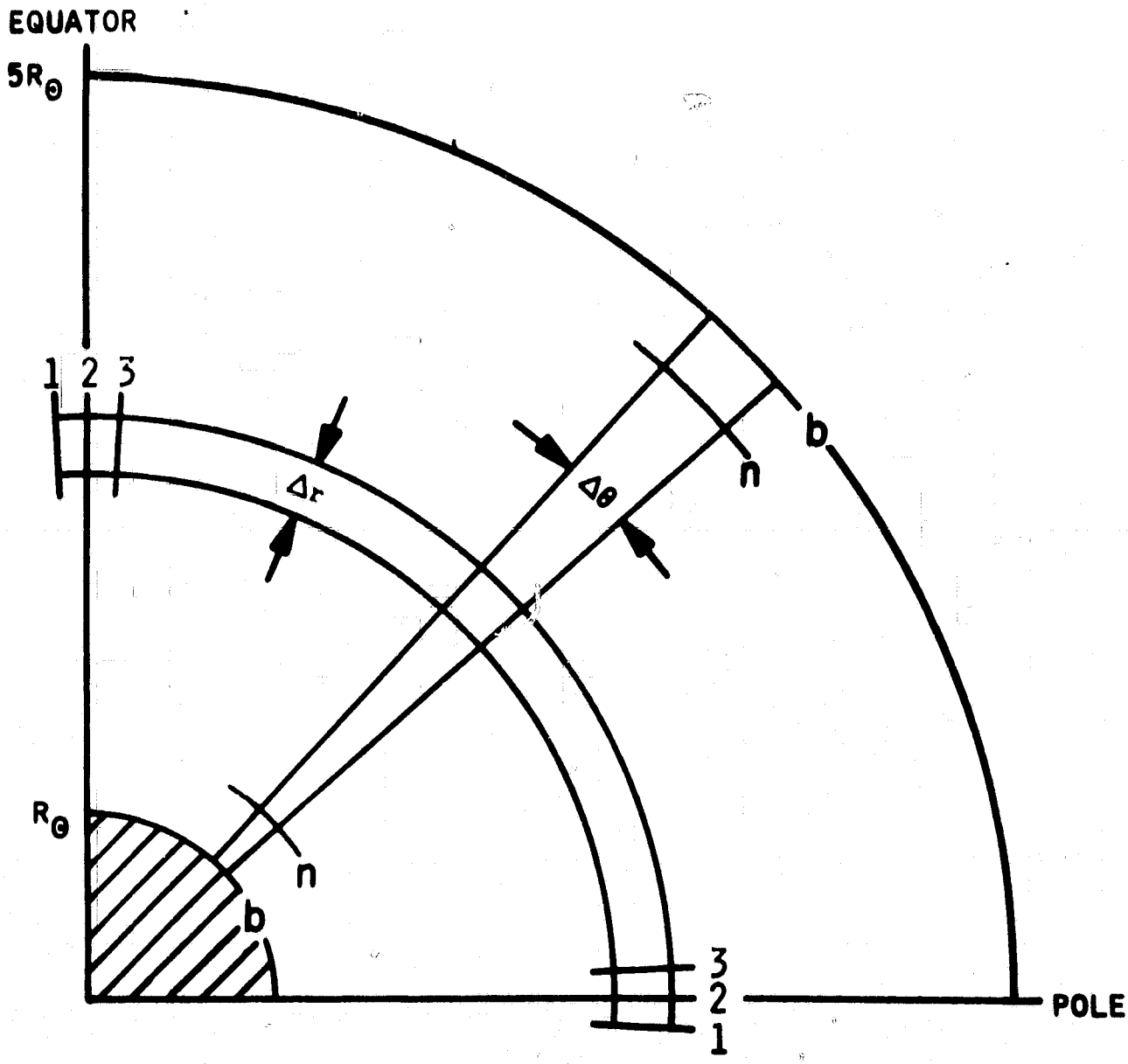

Figure 1

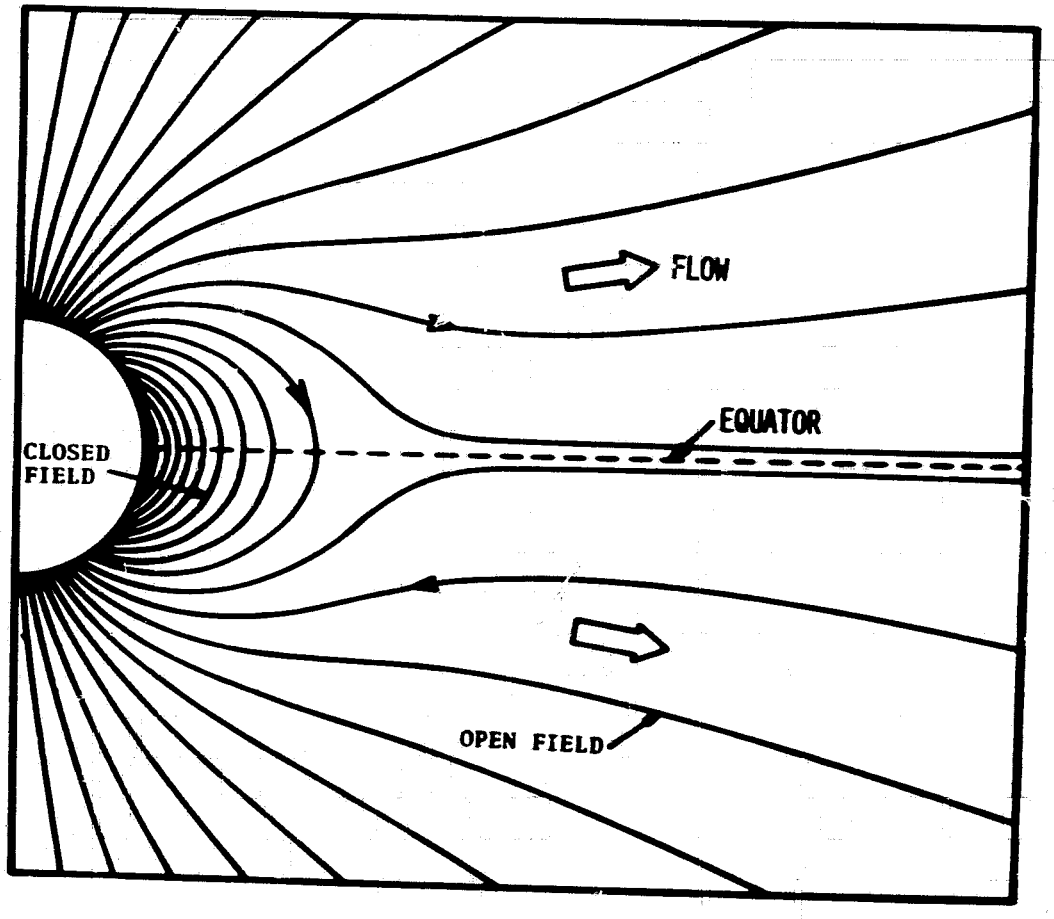

Figure 2

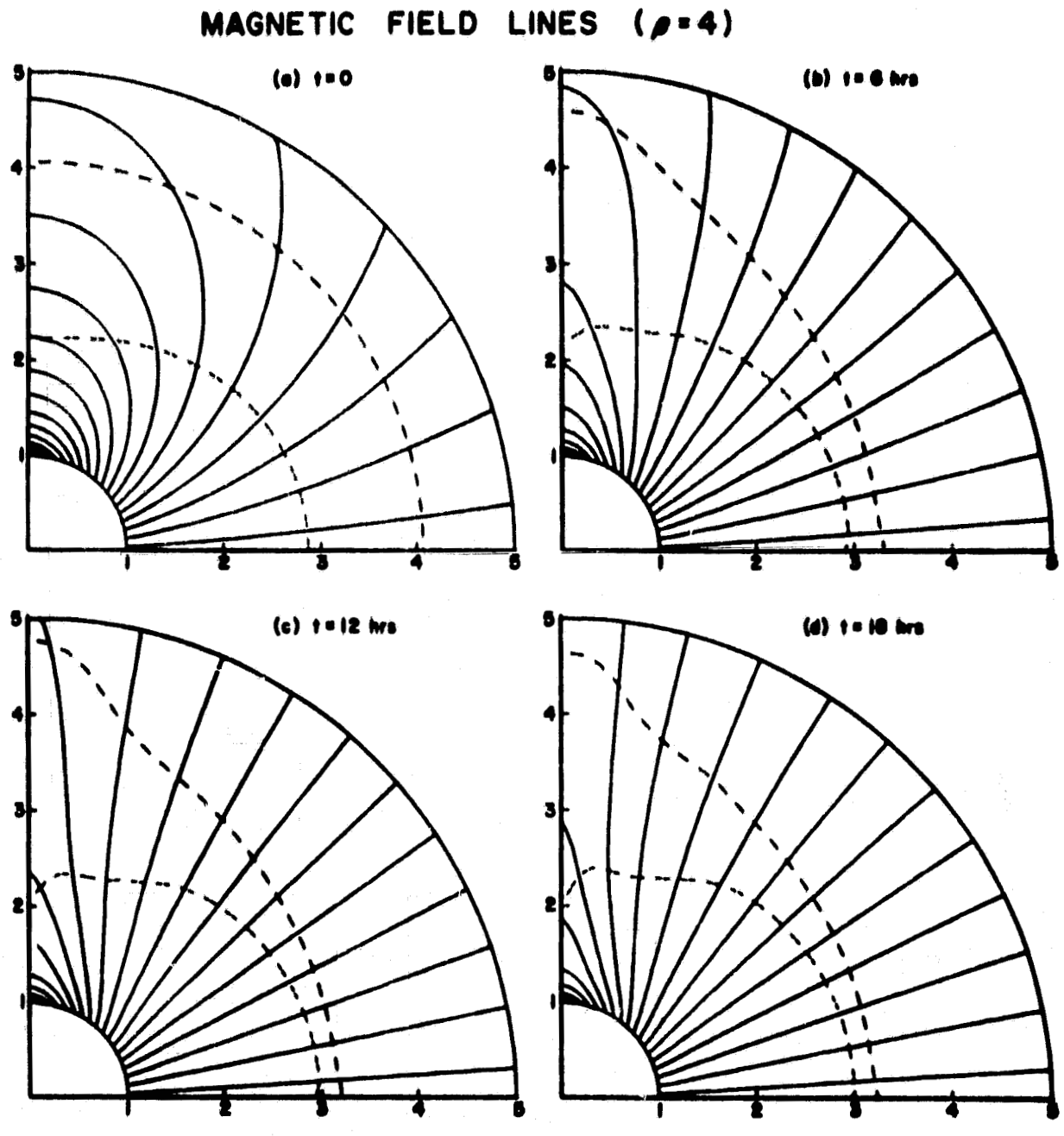
MAGNETIC FIELD LINES (ρ = 4)
(a) t = 0
(b) t = 6 hrs
(c) t = 12 hrs
(d) t = 18 hrs
1
2
3
4
5

Figure 3

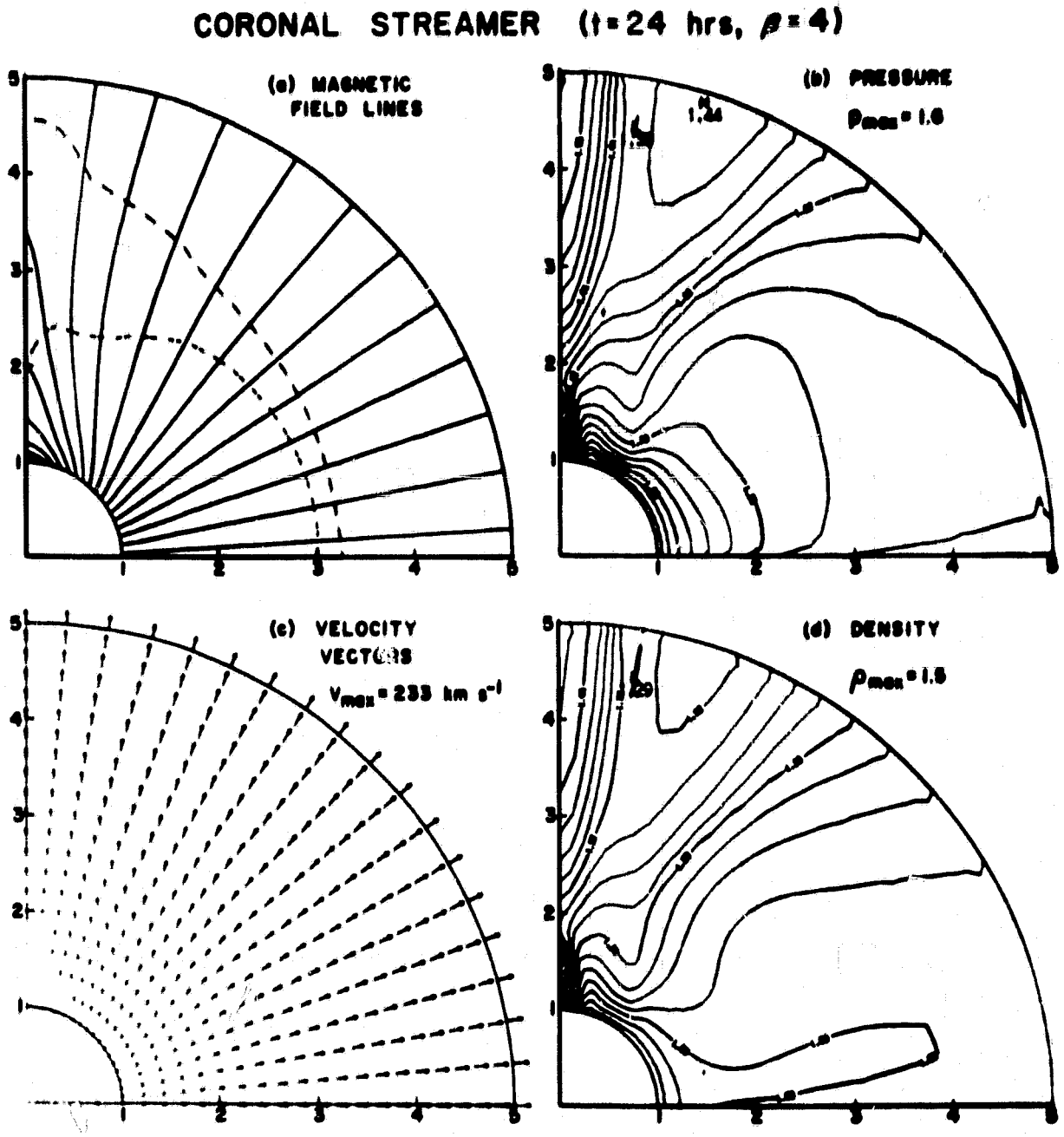
CORONAL STREAMER (t = 24 hrs, β = 4)
(a) MAGNETIC FIELD LINES
(b) PRESSURE
p_max = 1.6
(c) VELOCITY VECTORS
V_max = 233 km s⁻¹
(d) DENSITY
ρ_max = 1.5

Figure 4

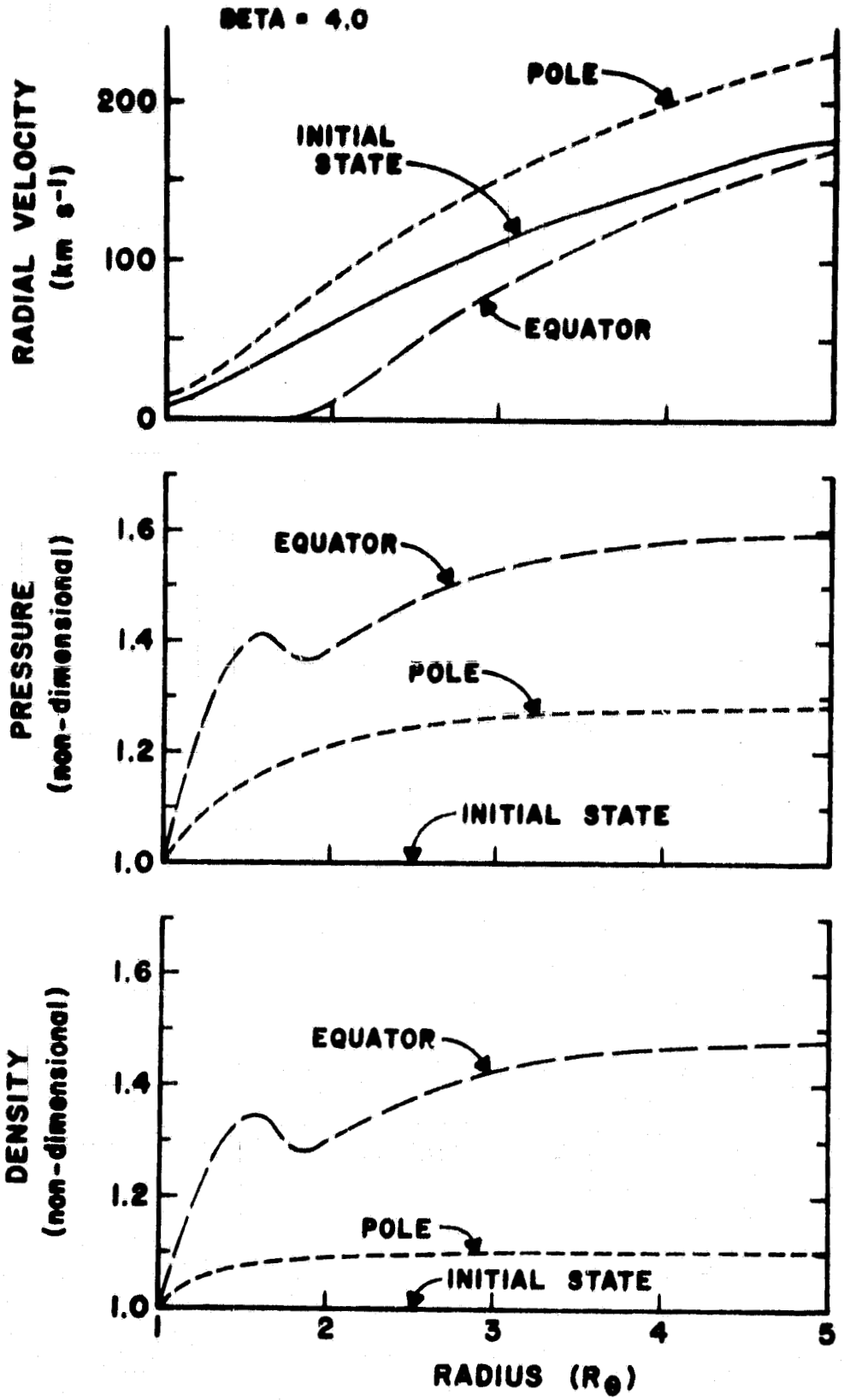
BETA = 4.0
RADIAL VELOCITY (km s⁻¹)
200
100
0
POLE
INITIAL STATE
EQUATOR
PRESSURE (non-dimensional)
1.6
1.4
1.2
1.0
EQUATOR
POLE
INITIAL STATE
DENSITY (non-dimensional)
1.6
1.4
1.2
1.0
EQUATOR
POLE
INITIAL STATE
1
2
3
4
5
RADIUS (R⊙)

Figure 5

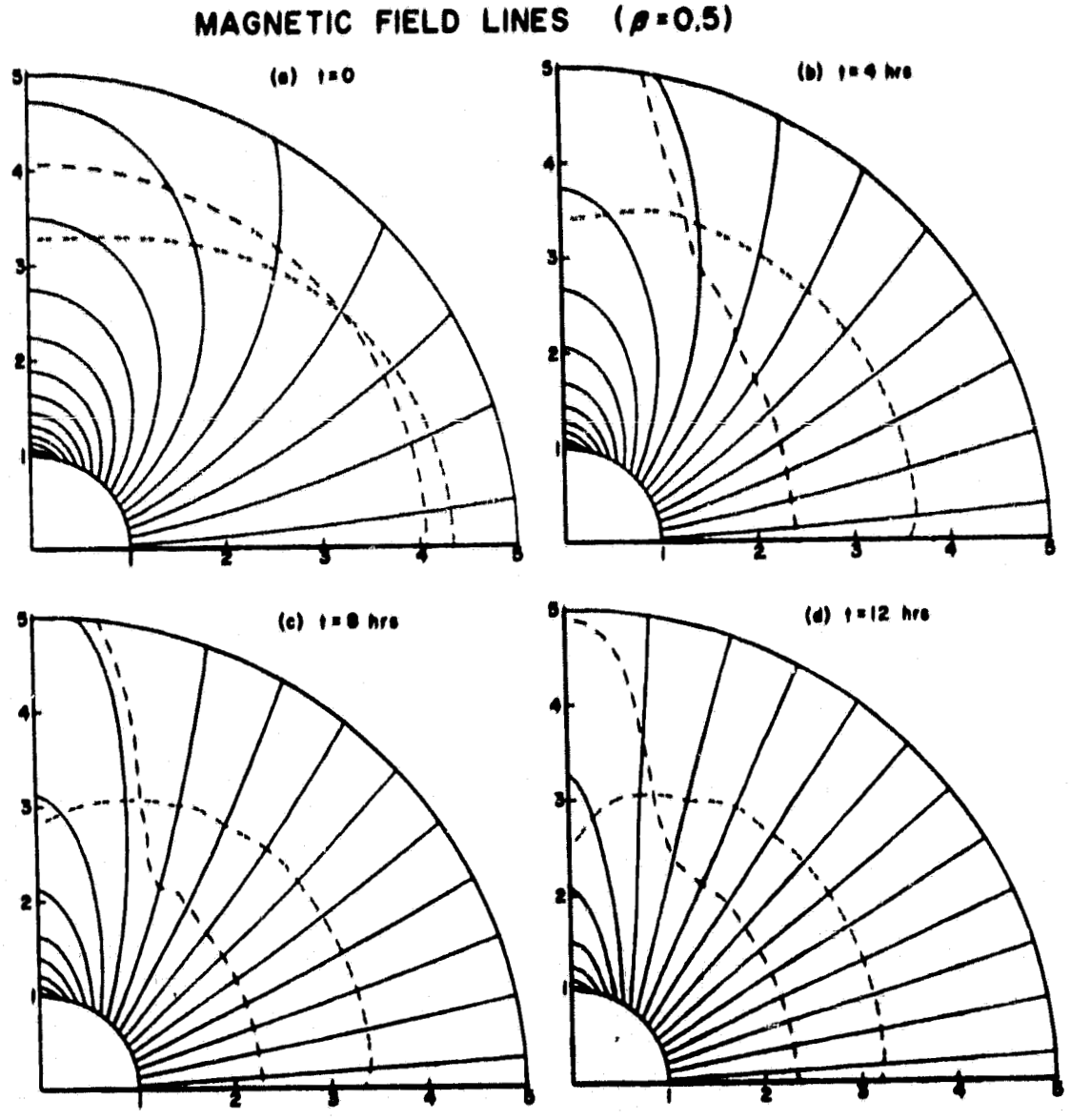

Figure 6

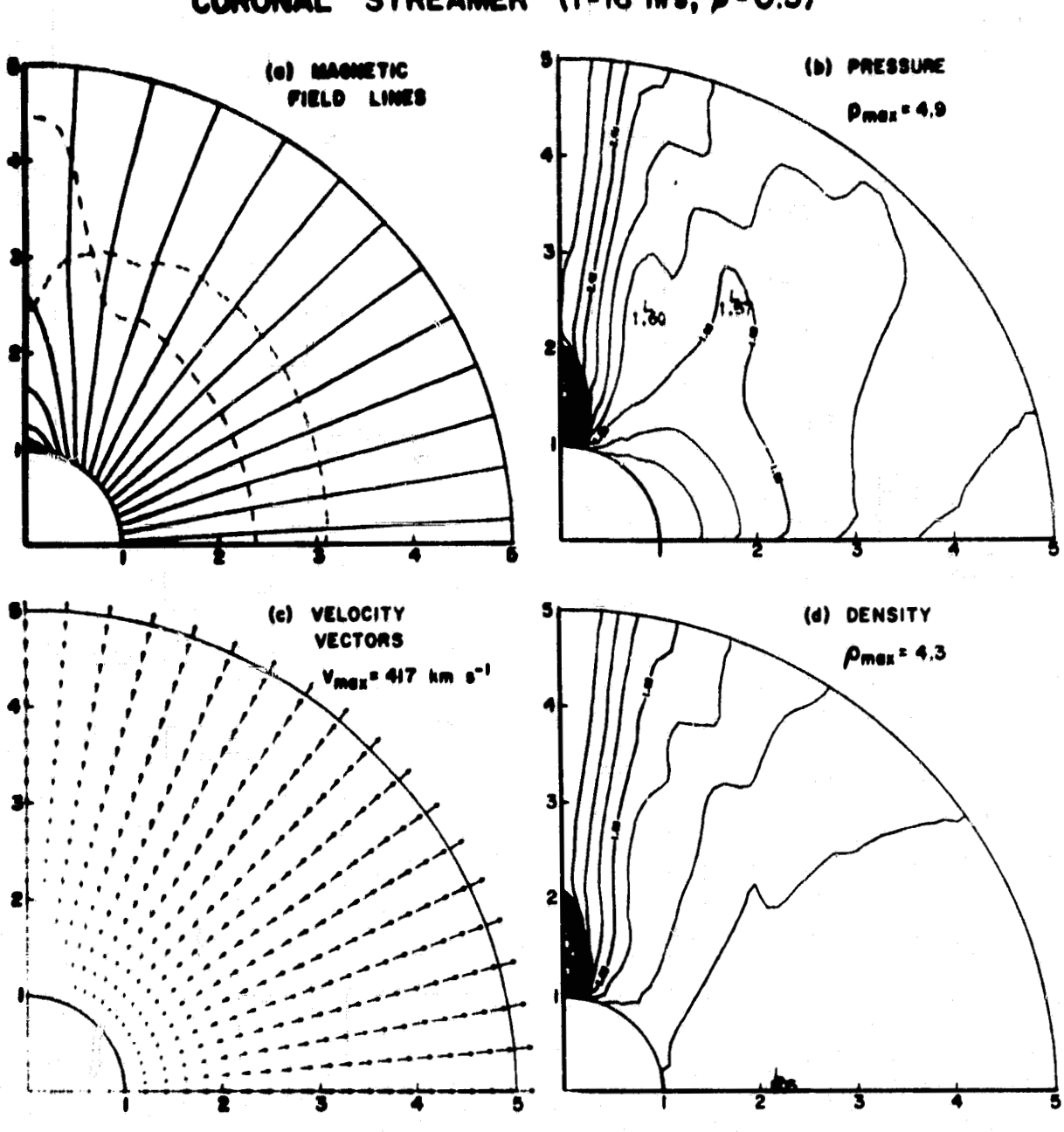
CORONAL STREAMER (t=16 hrs, ρ=0.5)
(a) MAGNETIC FIELD LINES
(b) PRESSURE
ρmax = 4.9
1.80
1.87
(c) VELOCITY VECTORS
Vmax = 417 km s⁻¹
(d) DENSITY
ρmax = 4.3

Figure 7

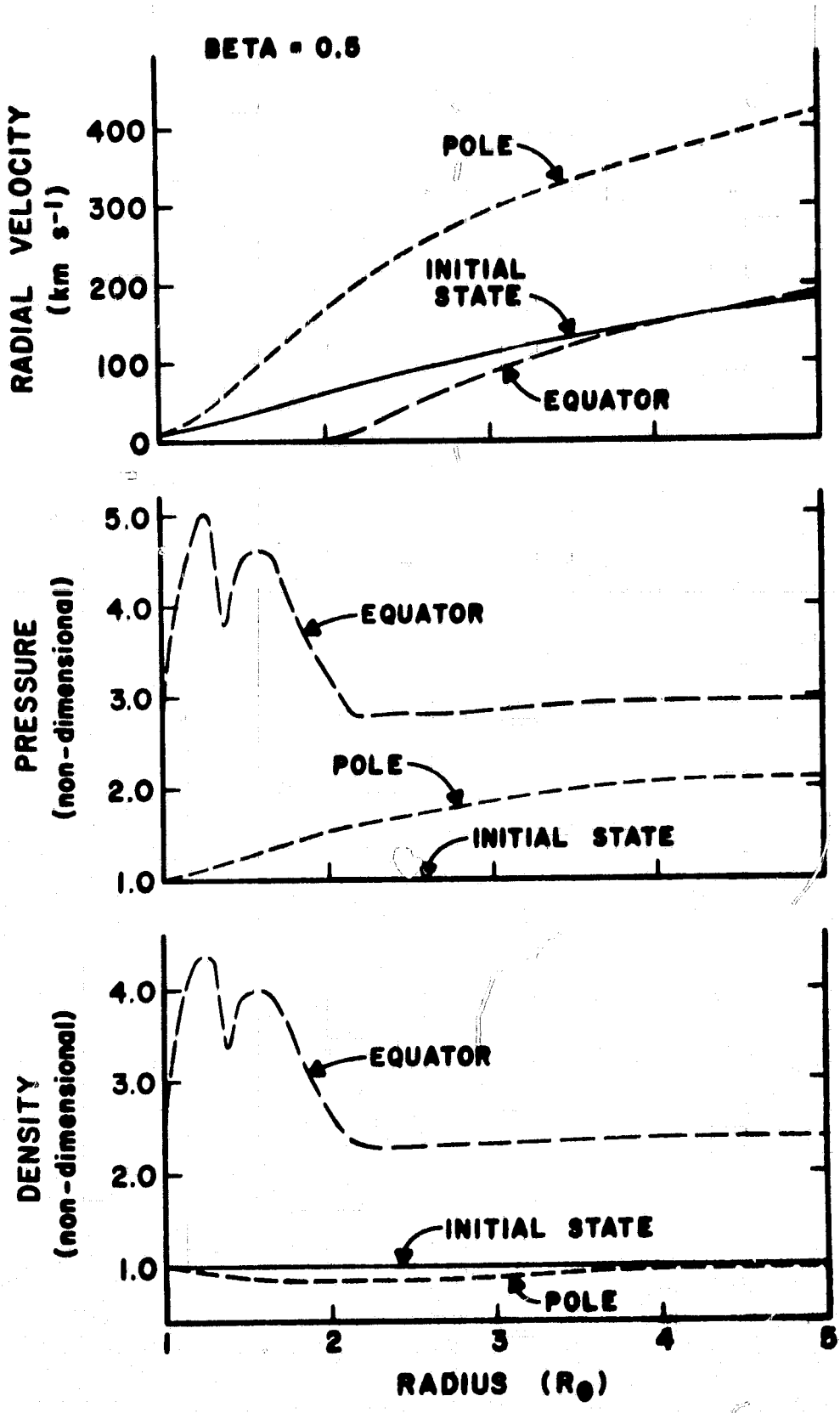
BETA = 0.8
RADIAL VELOCITY (km s⁻¹)
400
300
200
100
0
POLE
INITIAL STATE
EQUATOR
PRESSURE (non-dimensional)
5.0
4.0
3.0
2.0
1.0
EQUATOR
POLE
INITIAL STATE
DENSITY (non-dimensional)
4.0
3.0
2.0
1.0
EQUATOR
INITIAL STATE
POLE
1
2
3
4
5
RADIUS (R⊙)

Figure 8

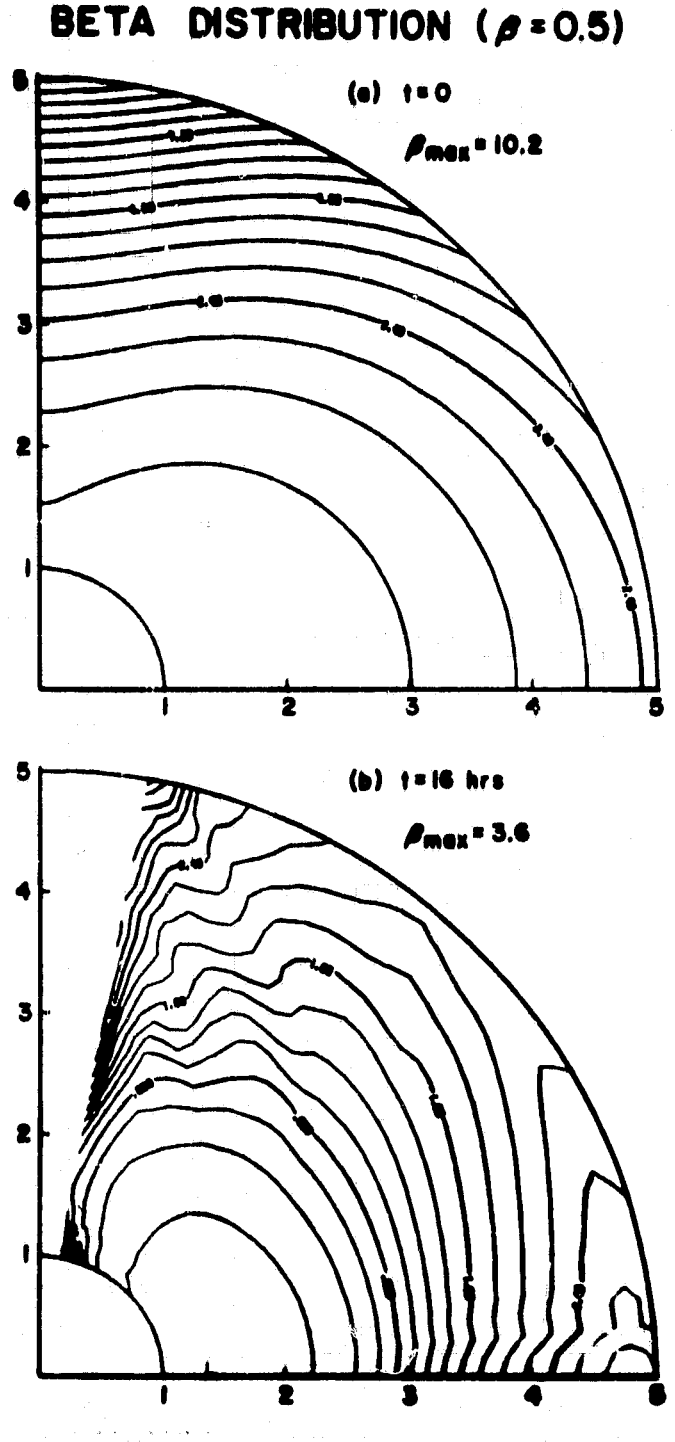
BETA DISTRIBUTION (β = 0.5)
(a) t = 0
β_{max} = 10.2
(b) t = 16 hrs
β_{max} = 3.6

Figure 9

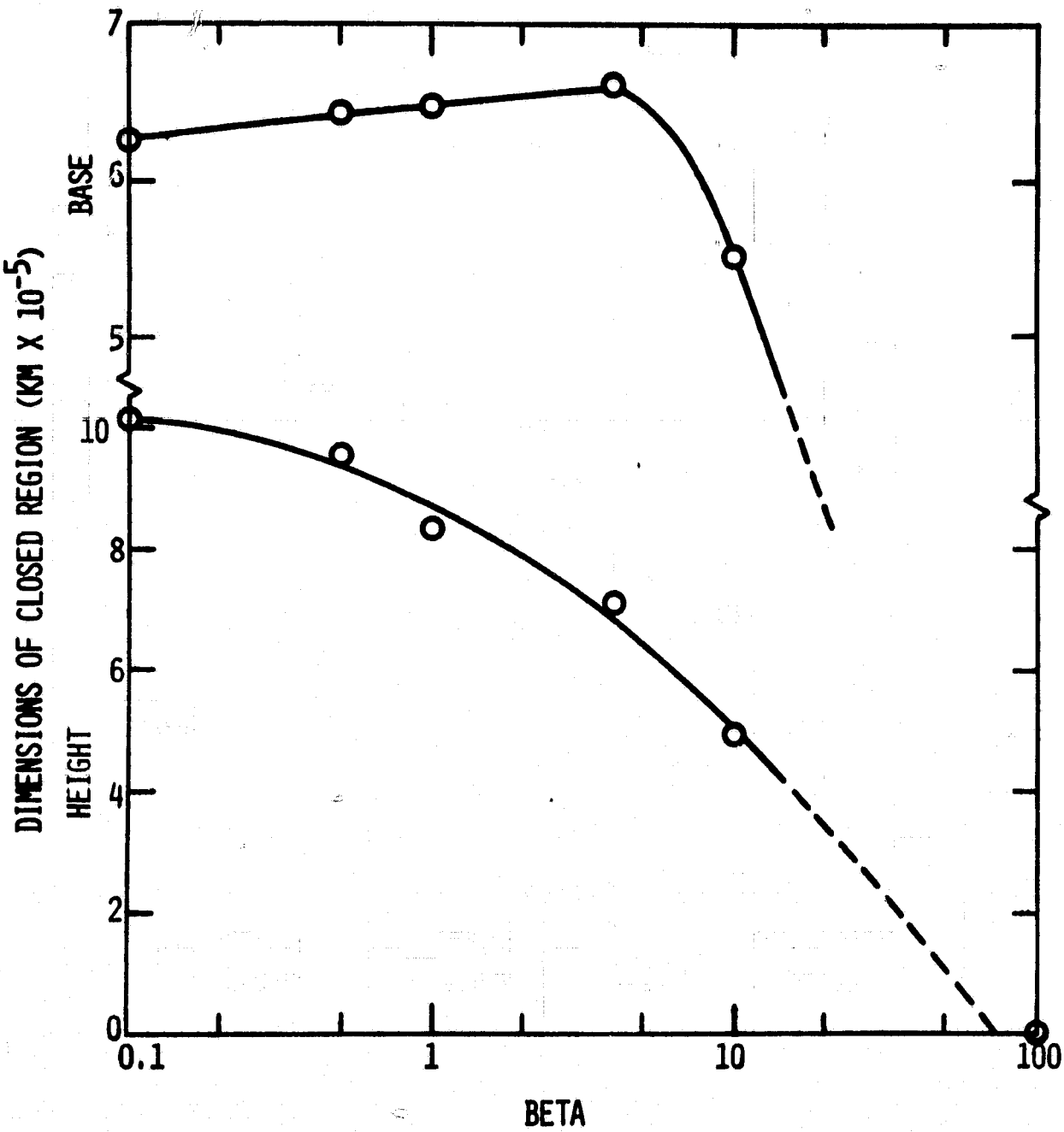
DIMENSIONS OF CLOSED REGION (KM X 10^{-5})
BASE
HEIGHT
7
6
5
10
8
6
4
2
0
0.1
1
10
100
BETA

Figure 10

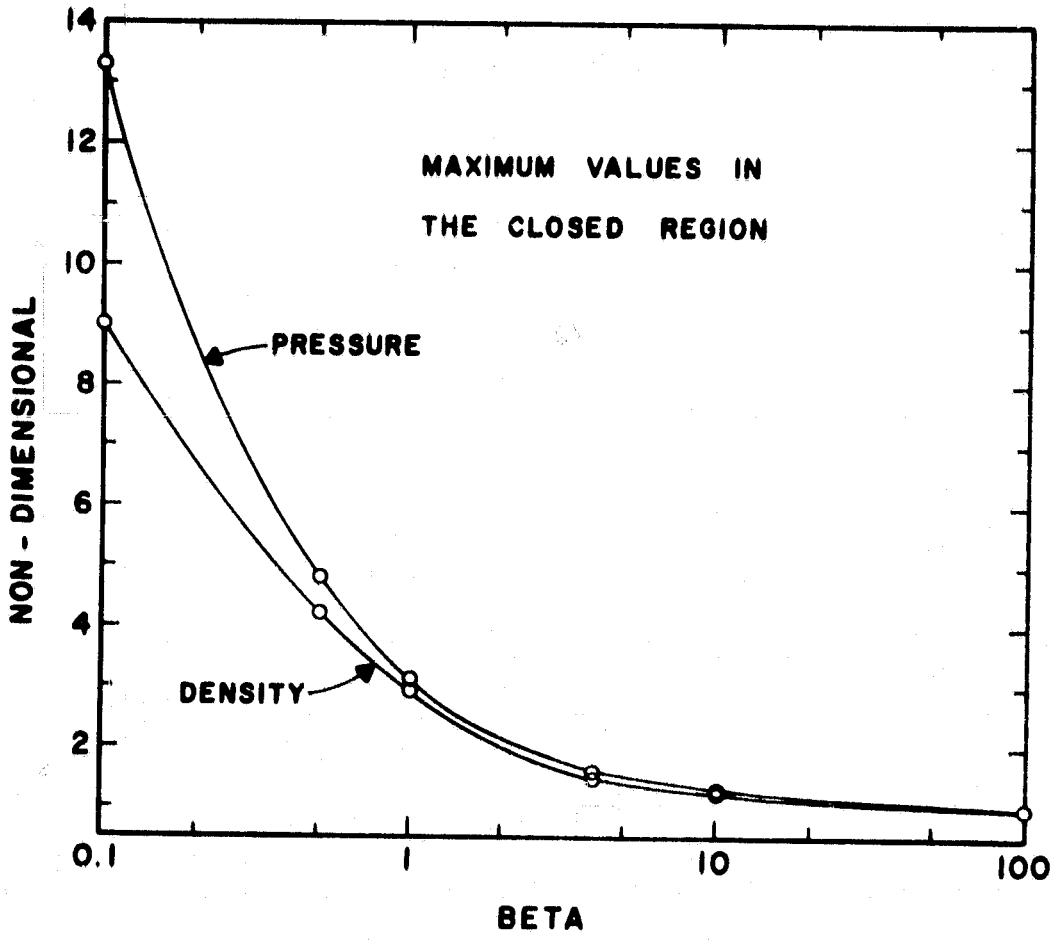
MAXIMUM VALUES IN
THE CLOSED REGION
PRESSURE
DENSITY
NON - DIMENSIONAL
BETA
14
12
10
8
6
4
2
0.1
1
10
100

Figure 11

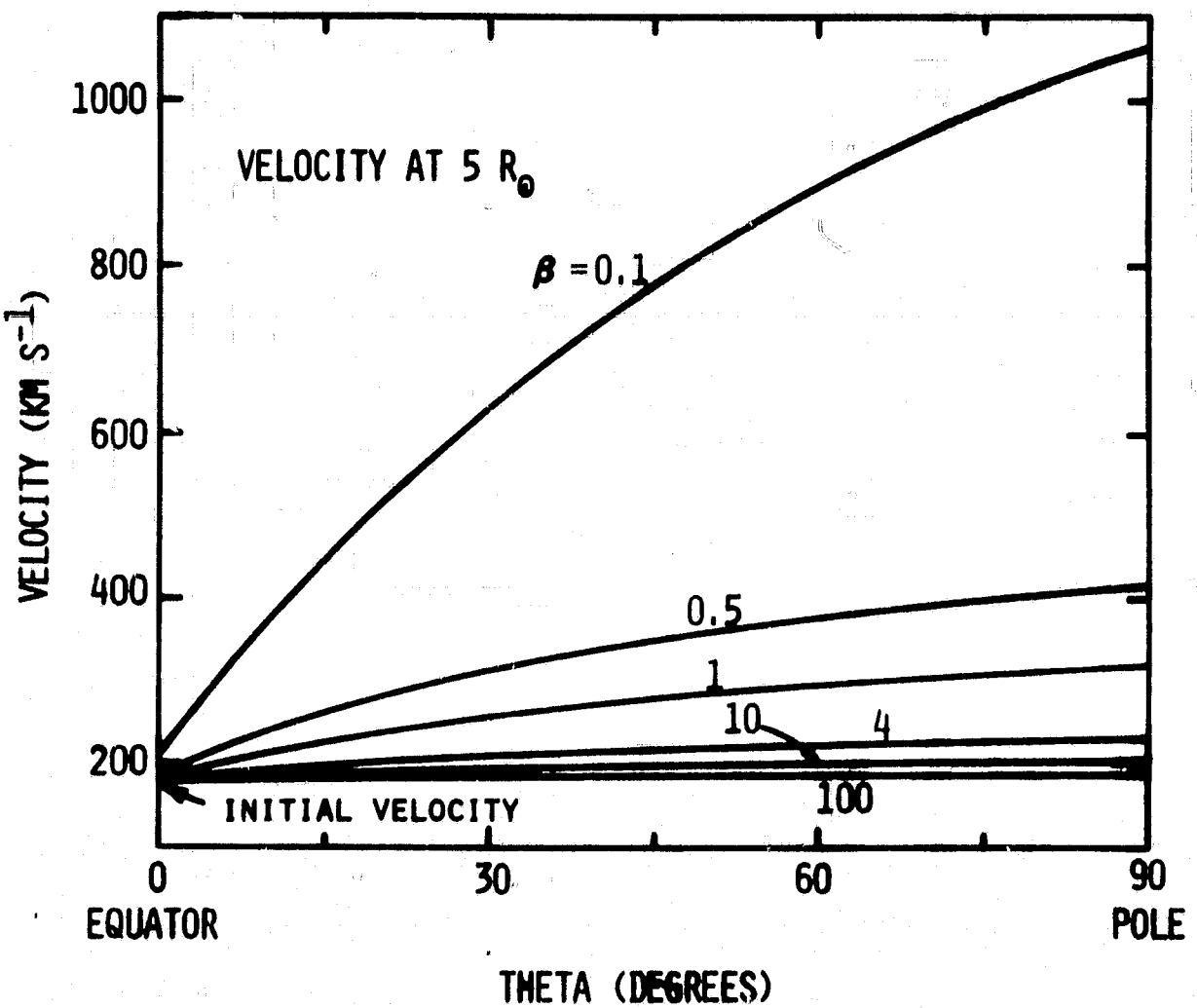
VELOCITY AT 5 $R_\odot$
β =0.1
0.5
1
4
10
100
INITIAL VELOCITY
1000
800
600
400
200
VELOCITY (KM S^{-1})
0
EQUATOR
30
60
90
POLE
THETA (DEGREES)

Figure 12

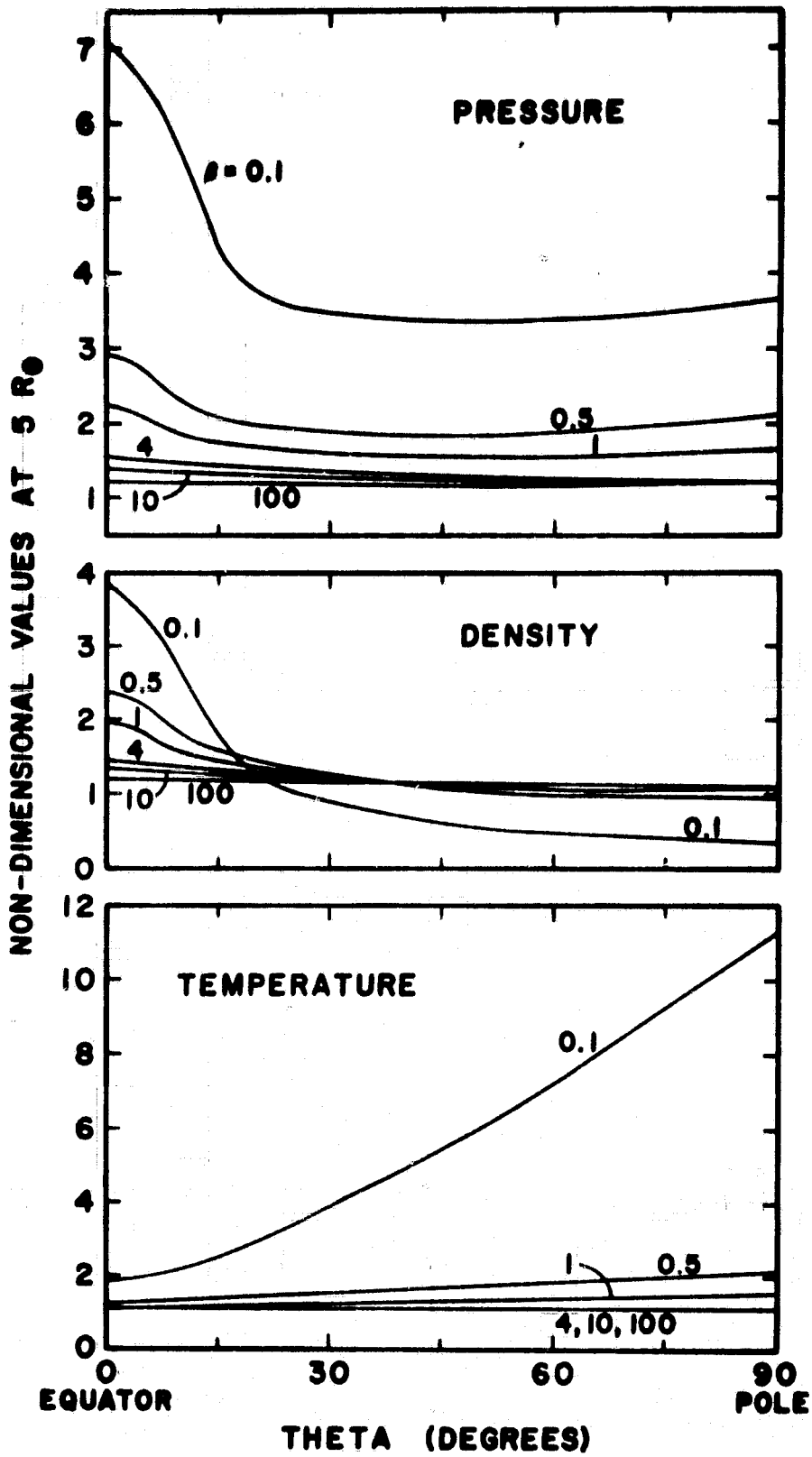
PRESSURE
β = 0.1
0.5
1
4
10
100
DENSITY
0.1
0.5
1
4
10
100
0.1
TEMPERATURE
0.1
1
0.5
4, 10, 100
NON-DIMENSIONAL VALUES AT 5 R⊕
0
30
60
90
EQUATOR
POLE
THETA (DEGREES)

Figure 13

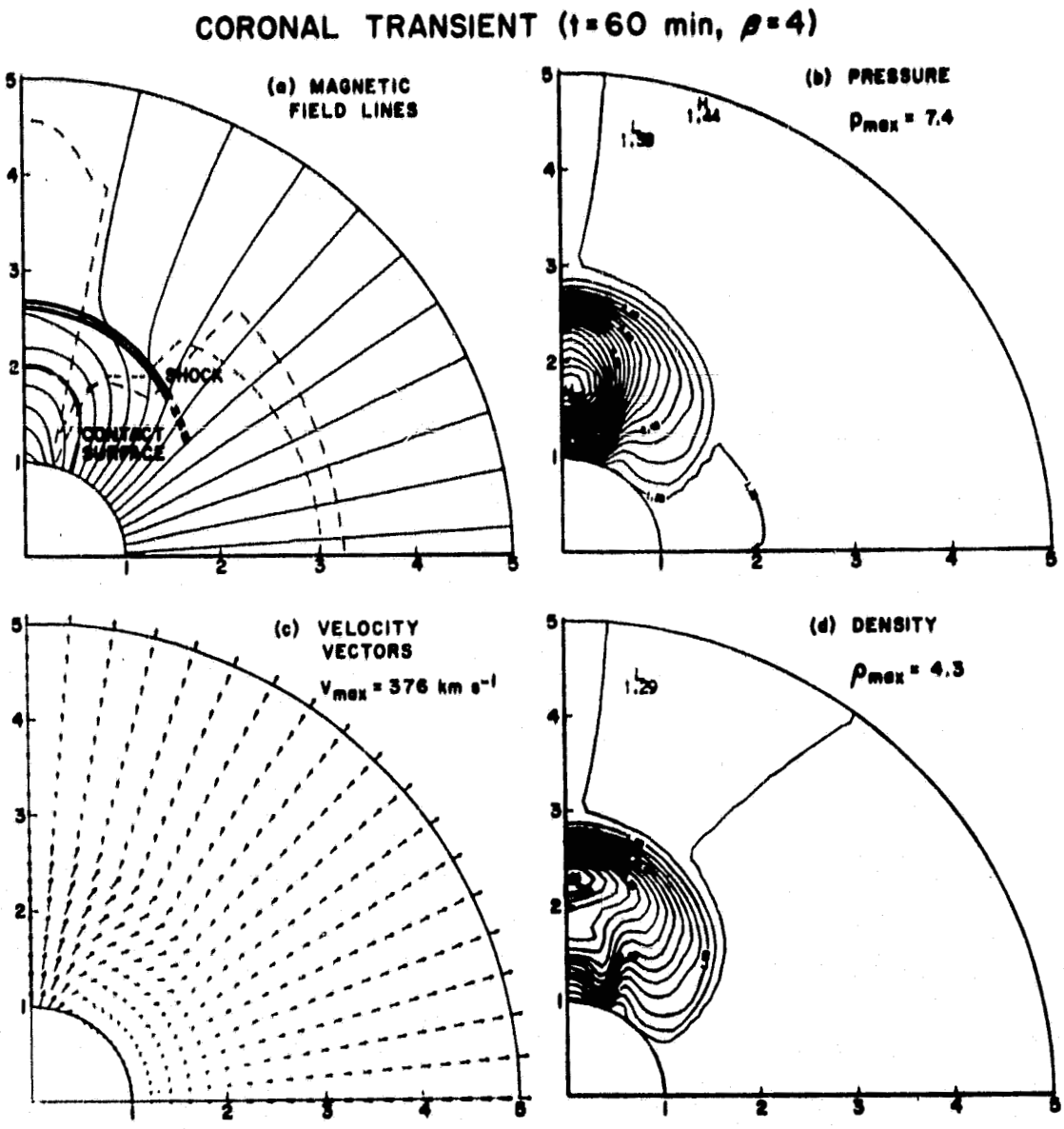
CORONAL TRANSIENT (t = 60 min, β = 4)
(a) MAGNETIC FIELD LINES
SHOCK
CONTACT SURFACE
(b) PRESSURE
ρmax = 7.4
(c) VELOCITY VECTORS
Vmax = 376 km s⁻¹
(d) DENSITY
ρmax = 4.3

Figure 14

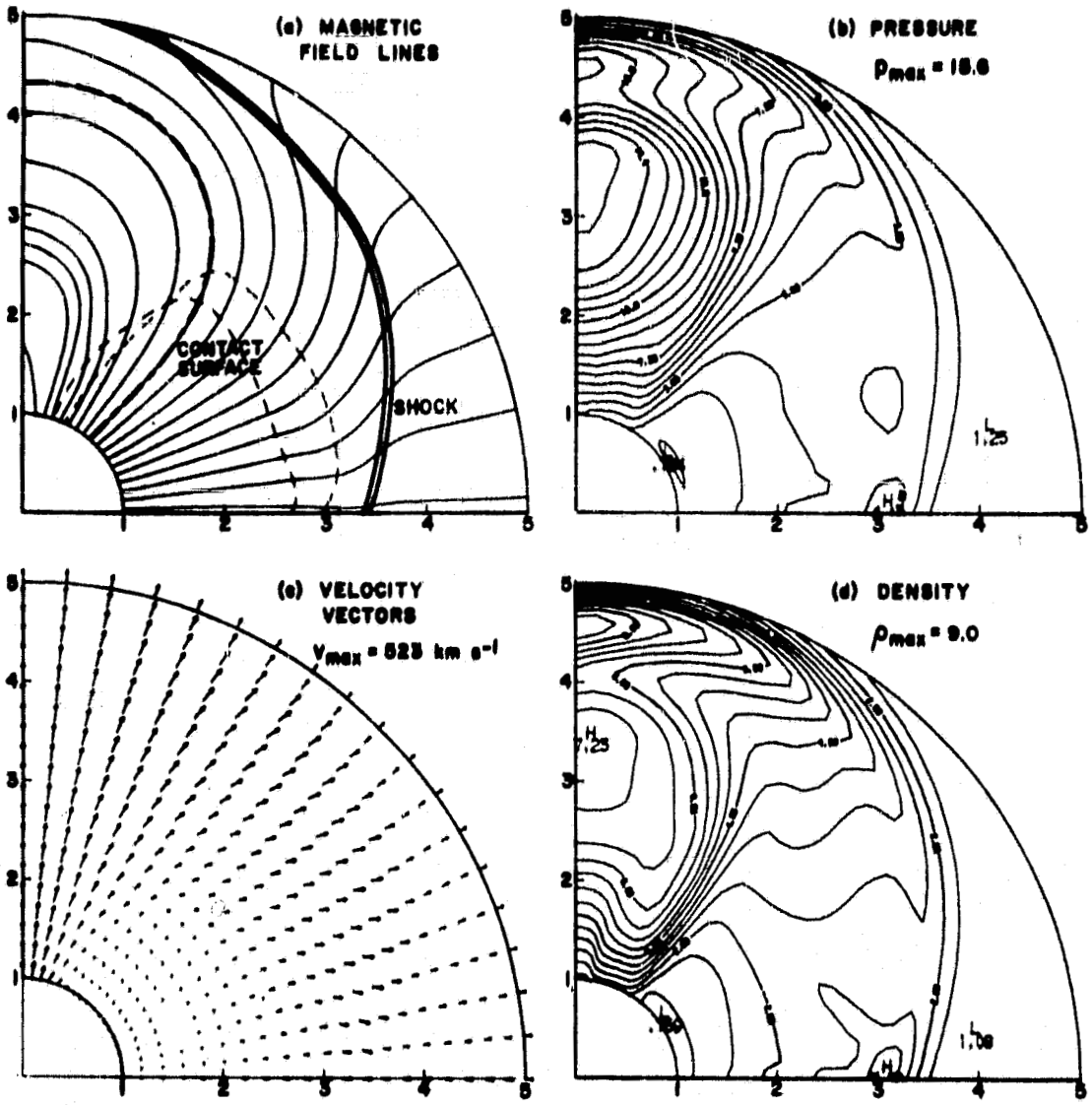
CORONAL TRANSIENT (t = 120 min, β = 4)
(a) MAGNETIC FIELD LINES
CONTACT SURFACE
SHOCK
(b) PRESSURE
p_{max} = 18.6
(c) VELOCITY VECTORS
V_{max} = 525 km s^{-1}
(d) DENSITY
ρ_{max} = 9.0

Figure 15

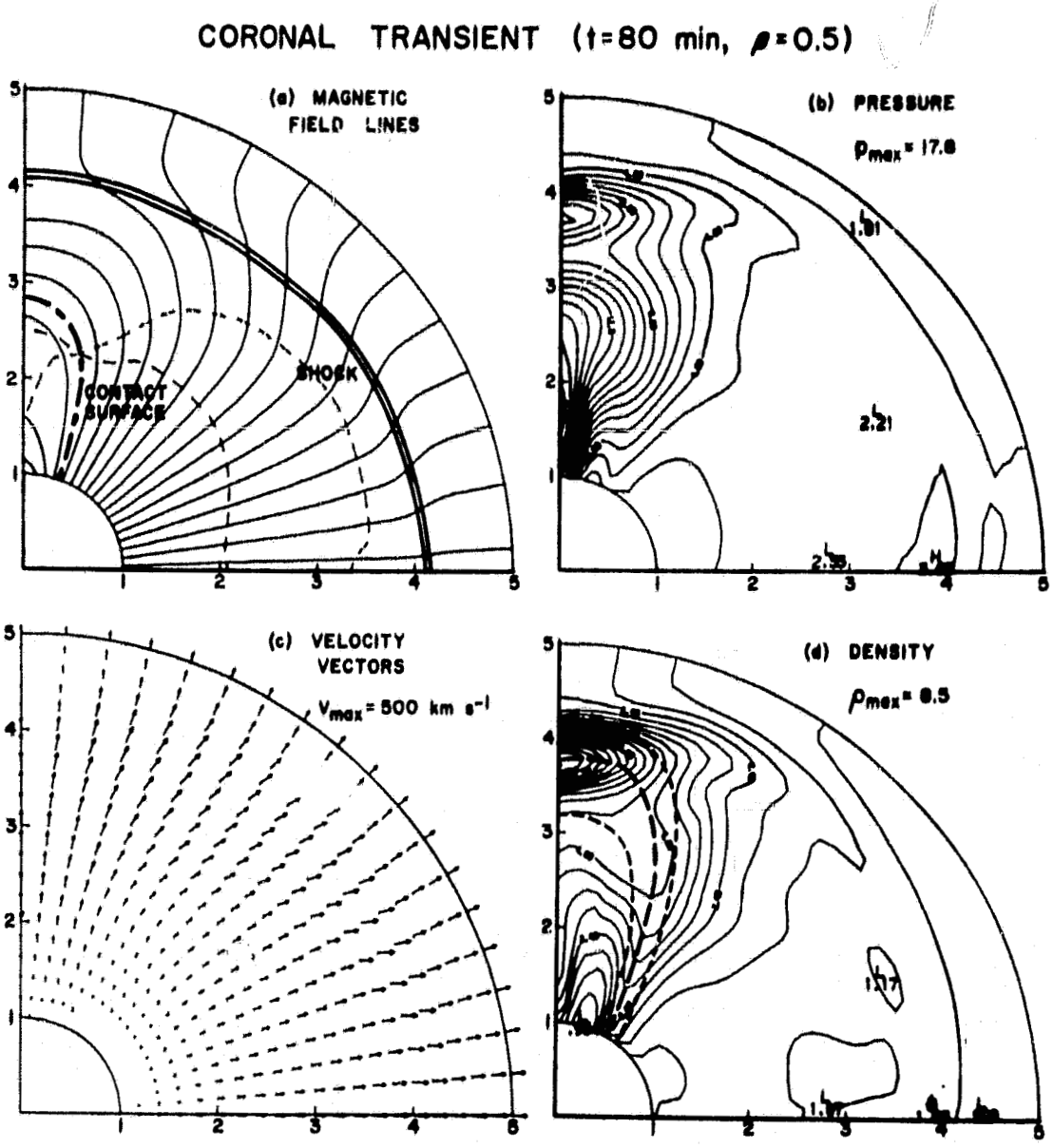
CORONAL TRANSIENT (t=80 min, β=0.5)
(a) MAGNETIC FIELD LINES
CONTACT SURFACE
SHOCK
(b) PRESSURE
p_{max} = 17.8
1.81
2.21
2.35
(c) VELOCITY VECTORS
V_{max} = 500 km s^{-1}
(d) DENSITY
ρ_{max} = 8.5
1.17
1.47

Figure 16

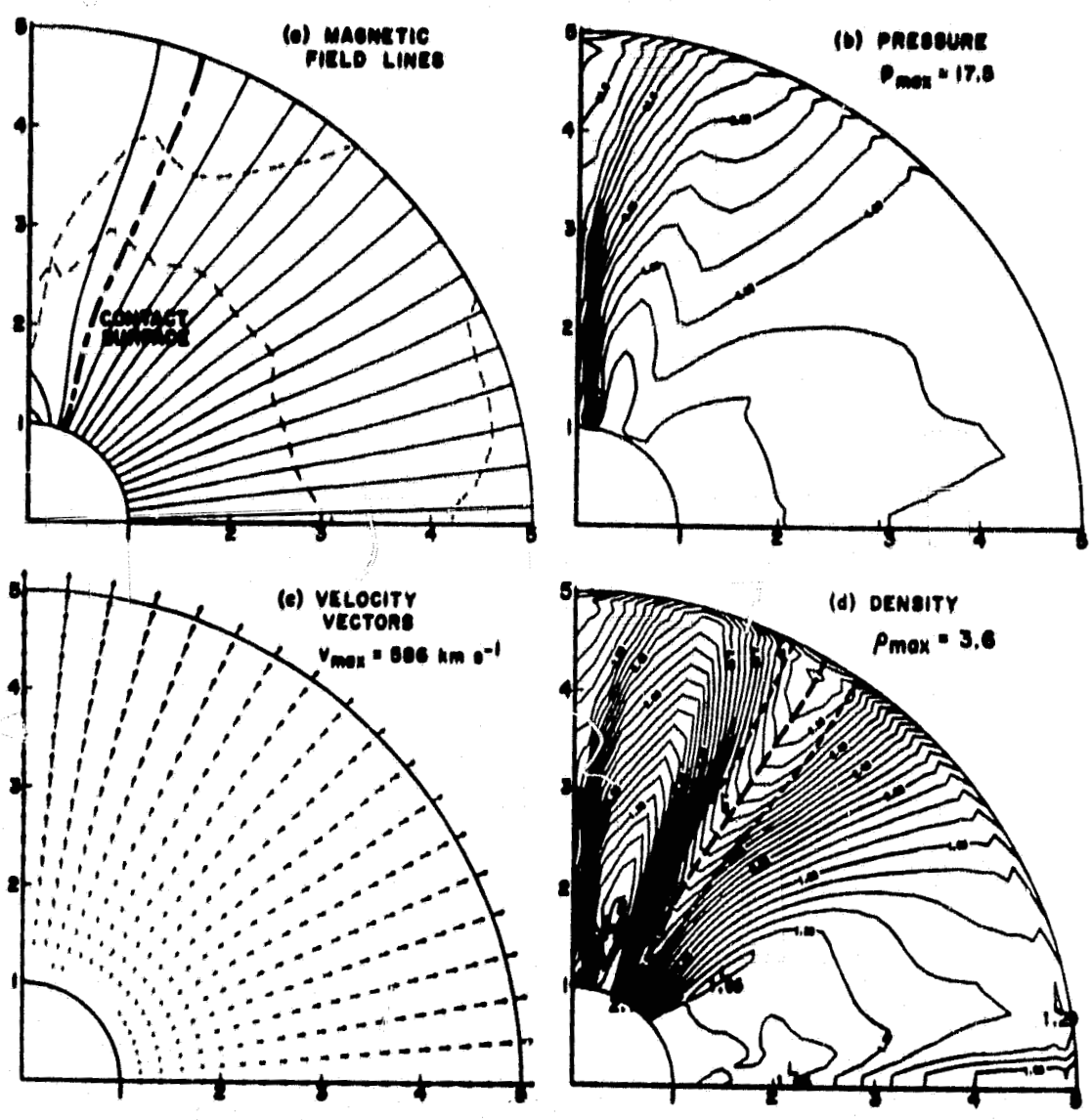
CORONAL TRANSIENT (t=180 min, β=0.5)
(a) MAGNETIC FIELD LINES
CONTACT DISCONTINUITY
(b) PRESSURE
p_{max} = 17.8
(c) VELOCITY VECTORS
v_{max} = 886 km s^{-1}
(d) DENSITY
ρ_{max} = 3.6

Figure 17

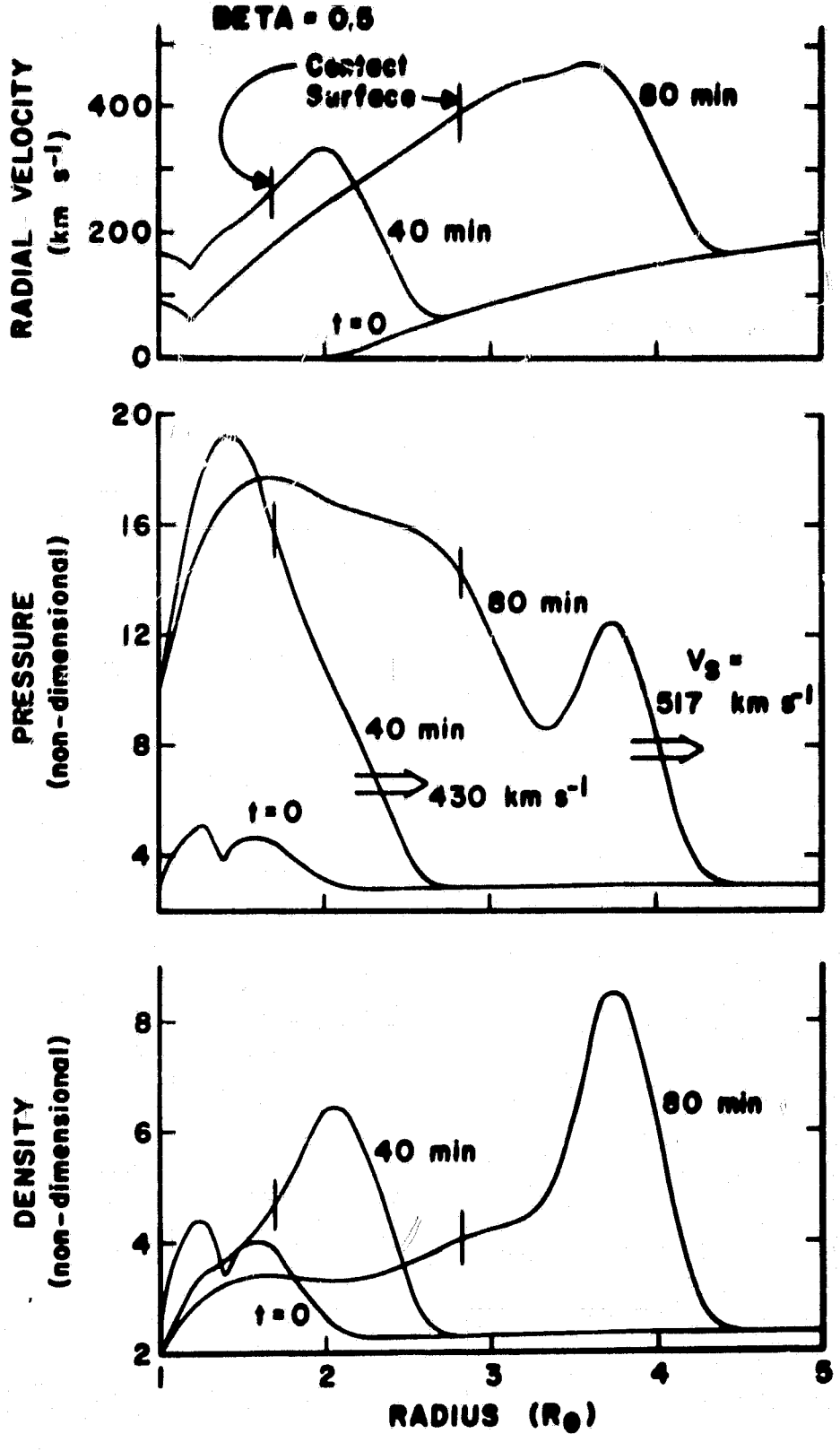
BETA = 0.5
Contact Surface
80 min
40 min
t = 0
RADIAL VELOCITY (km s⁻¹)
400
200
0
PRESSURE (non-dimensional)
20
16
12
8
4
80 min
V_s = 517 km s⁻¹
40 min
430 km s⁻¹
t = 0
DENSITY (non-dimensional)
8
6
4
2
80 min
40 min
t = 0
1
2
3
4
5
RADIUS ($R_\odot$)

Figure 18

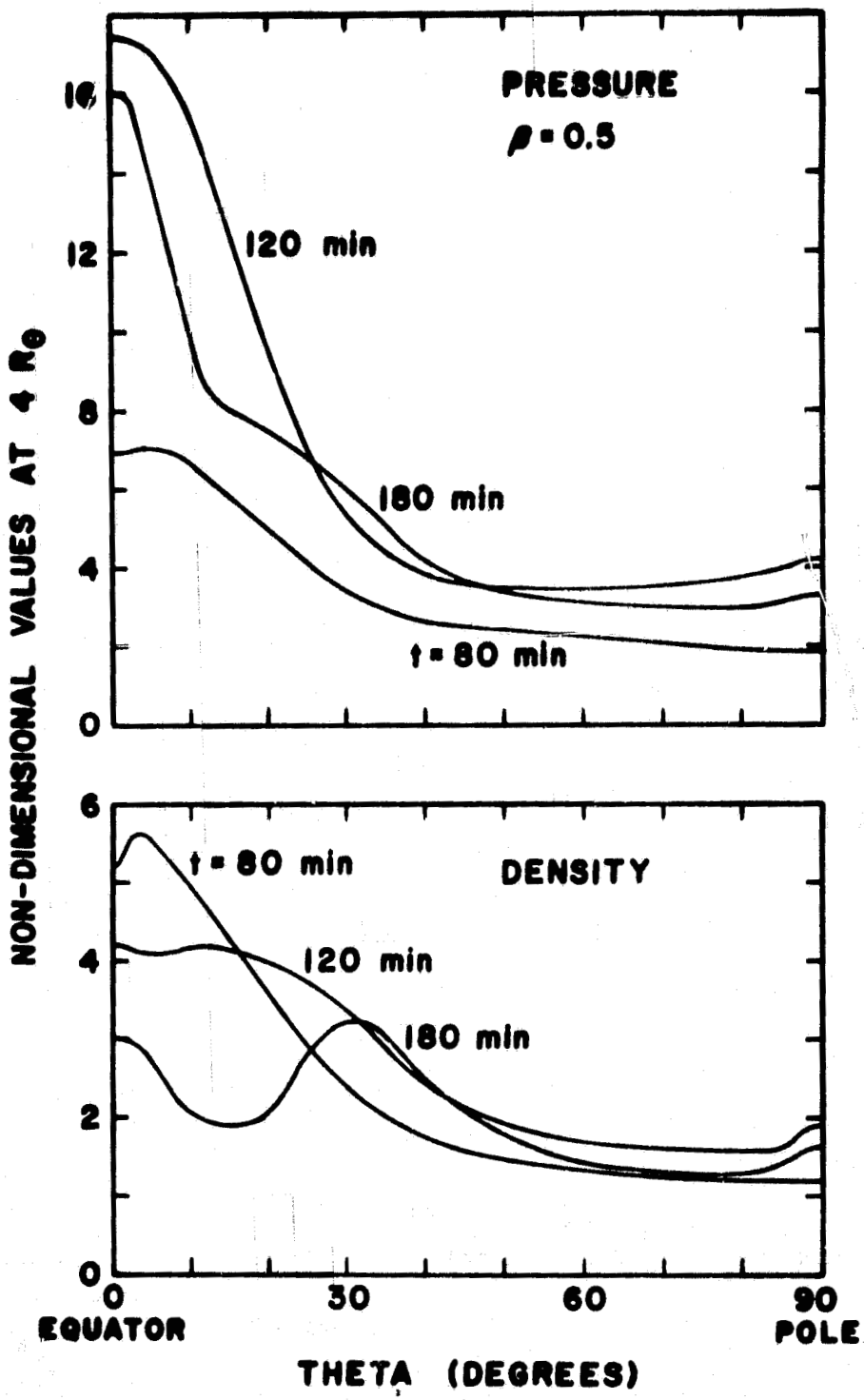
PRESSURE
β = 0.5
120 min
180 min
t = 80 min
DENSITY
t = 80 min
120 min
180 min
NON-DIMENSIONAL VALUES AT 4 R₀
0
2
4
6
8
12
16
0
30
60
90
EQUATOR
POLE
THETA (DEGREES)

Figure 19

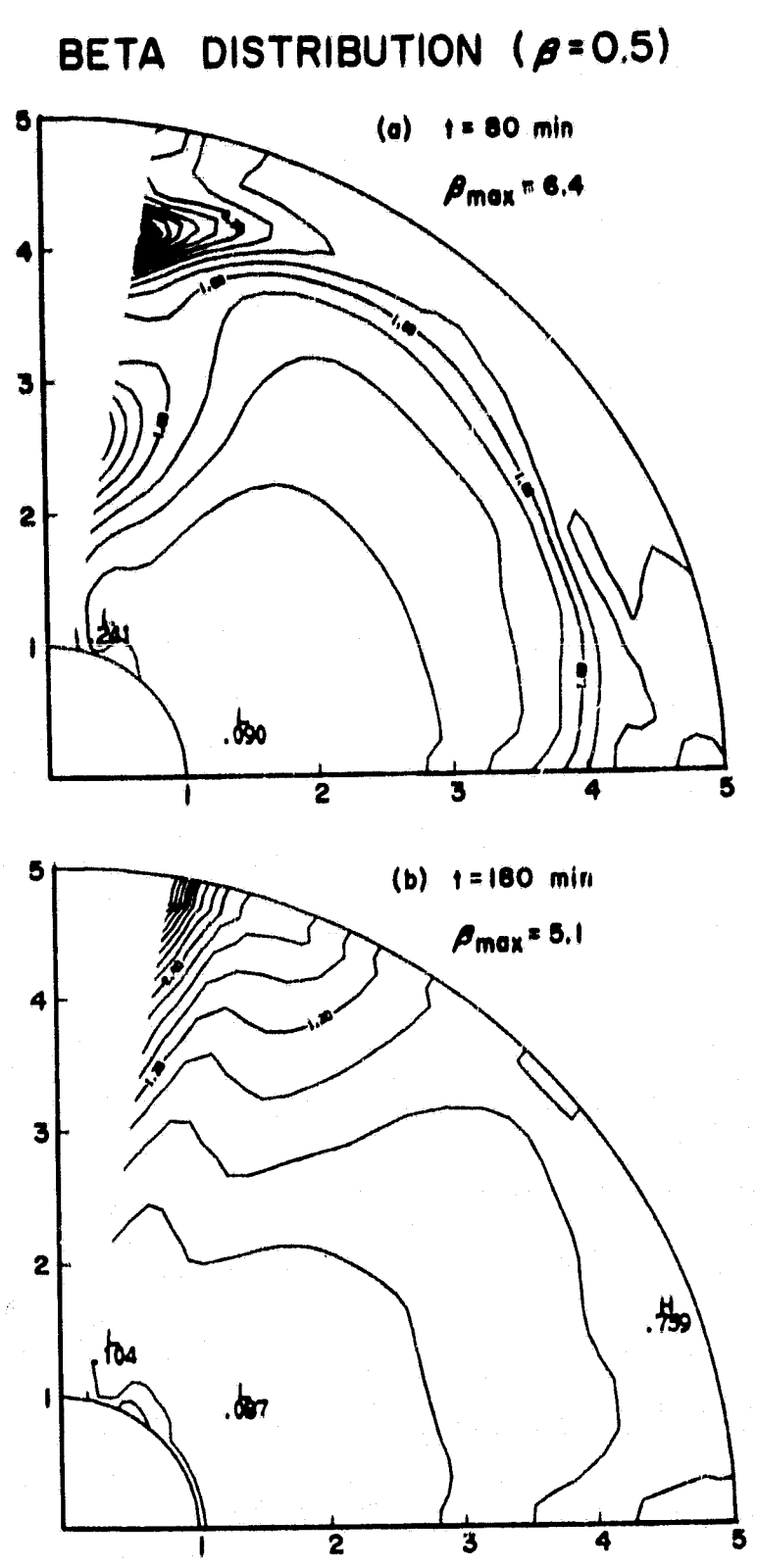
BETA DISTRIBUTION (β=0.5)
(a) t = 80 min
β_{max} = 6.4
.890
(b) t = 180 min
β_{max} = 5.1
.759
.804
.887
1
2
3
4
5

Figure 20

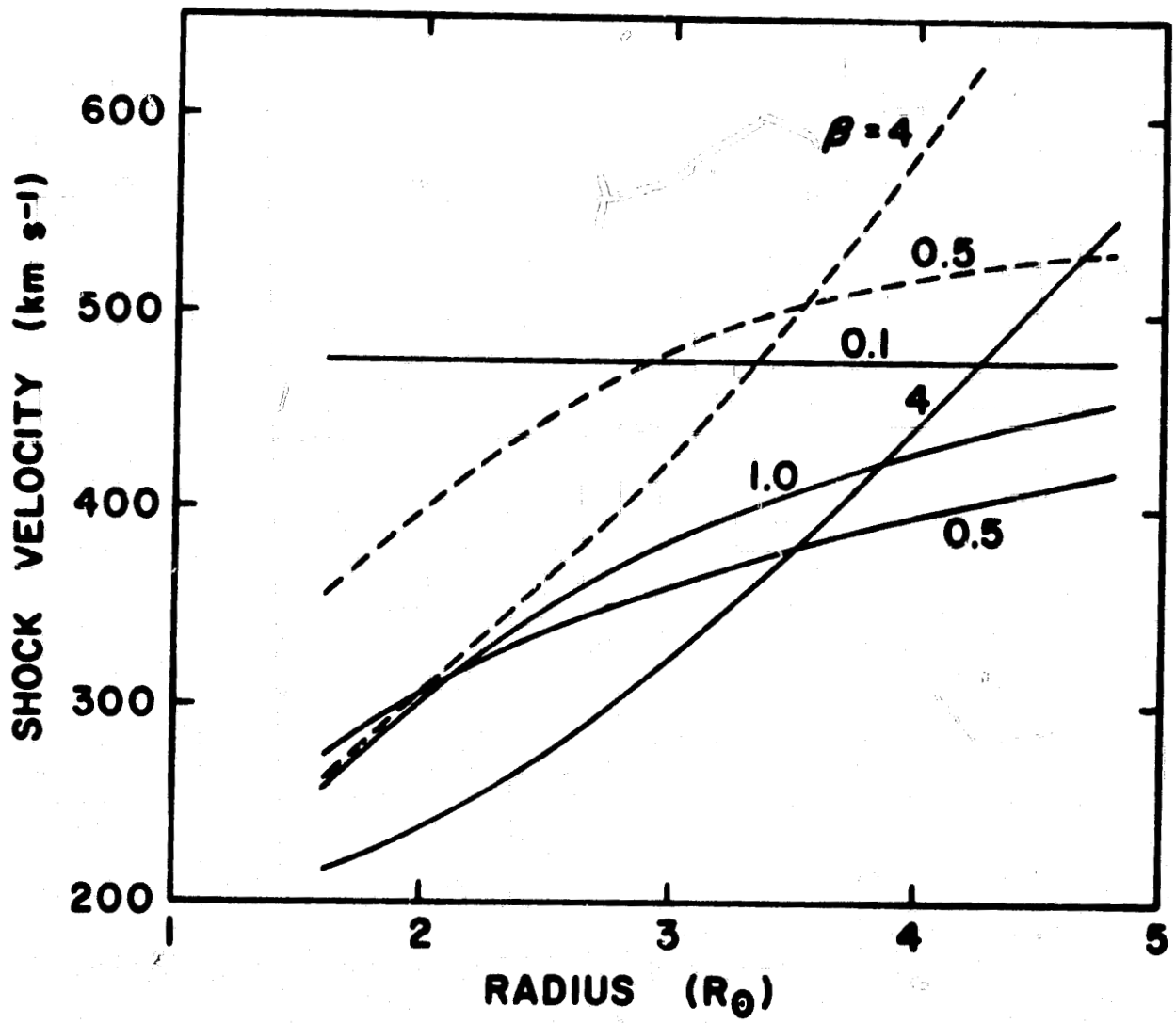
SHOCK VELOCITY (km s-1)
600
500
400
300
200
1
2
3
4
5
RADIUS (R⊙)
β=4
0.5
0.1
4
1.0
0.5

Figure 21

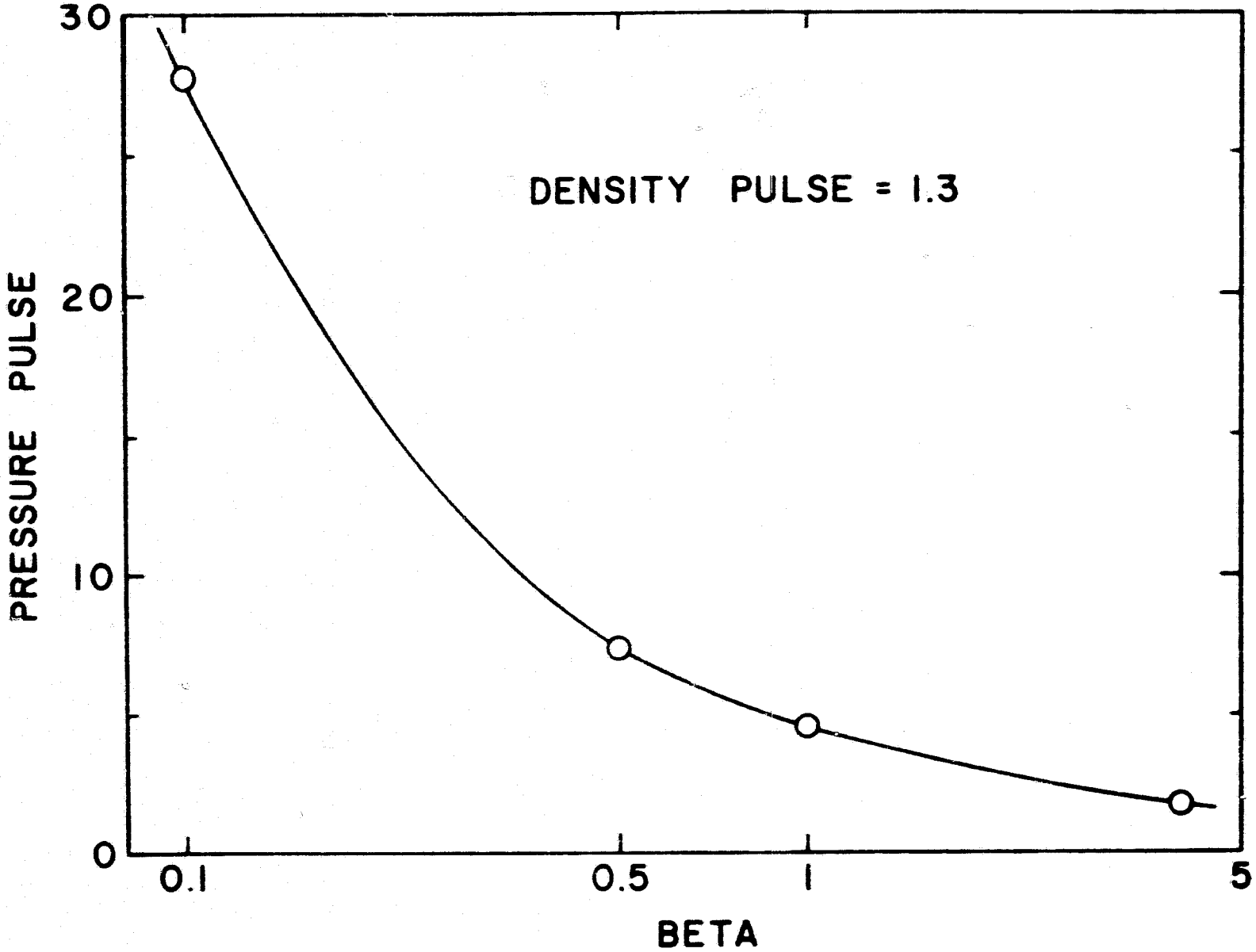

Figure 22

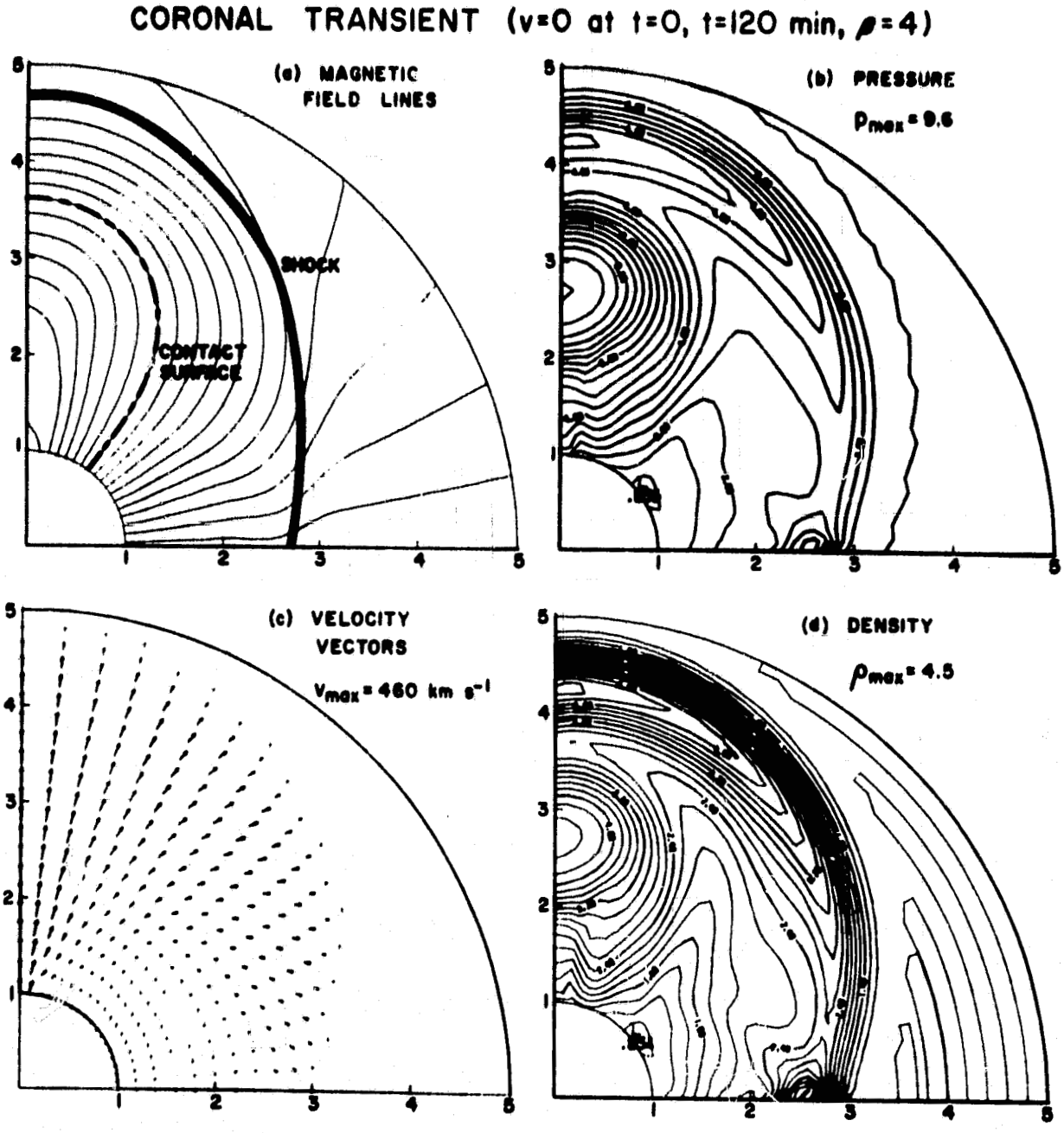
CORONAL TRANSIENT (v=0 at t=0, t=120 min, ρ=4)
(a) MAGNETIC FIELD LINES
SHOCK
CONTACT SURFACE
(b) PRESSURE
Pmax = 9.6
(c) VELOCITY VECTORS
Vmax = 460 km s⁻¹
(d) DENSITY
ρmax = 4.5

Figure 23

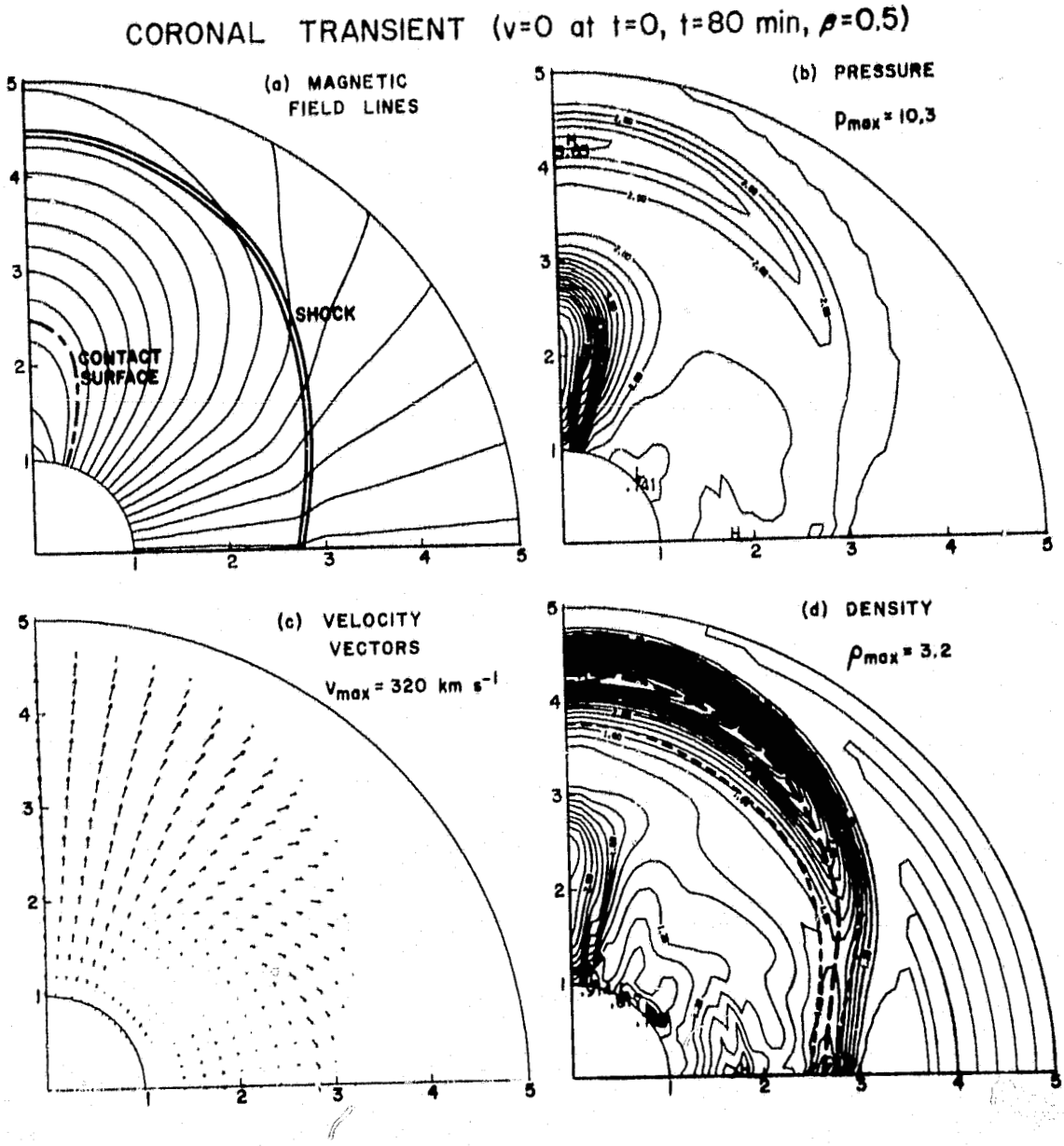
CORONAL TRANSIENT (v=0 at t=0, t=80 min, ρ=0.5)
(a) MAGNETIC FIELD LINES
SHOCK
CONTACT SURFACE
(b) PRESSURE
Pmax = 10.3
(c) VELOCITY VECTORS
Vmax = 320 km s⁻¹
(d) DENSITY
ρmax = 3.2

Figure 24

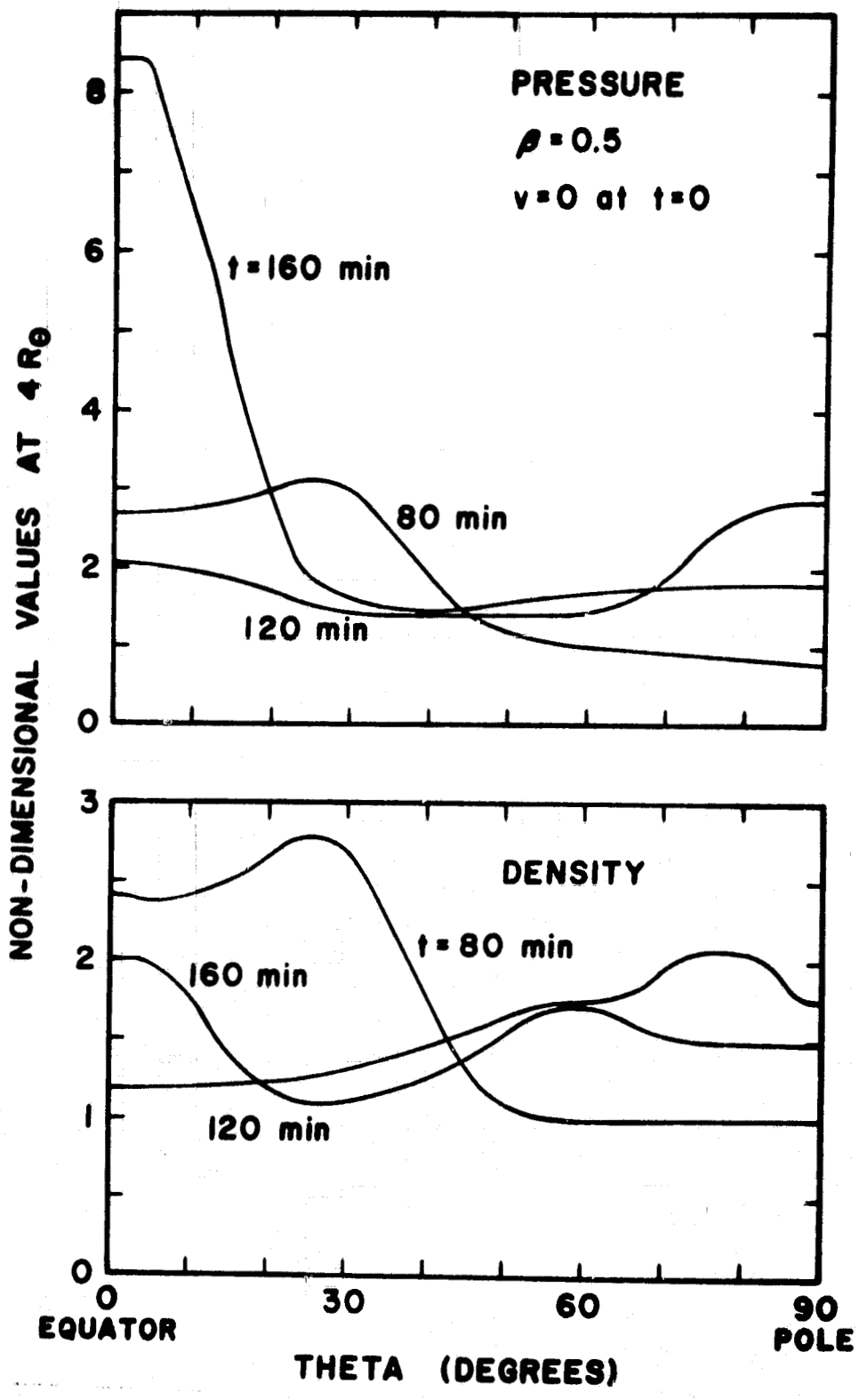
PRESSURE
β = 0.5
v = 0 at t = 0
t = 160 min
80 min
120 min
DENSITY
t = 80 min
160 min
120 min
NON-DIMENSIONAL VALUES AT 4 R₀
0
2
4
6
8
1
3
0
30
60
90
EQUATOR
POLE
THETA (DEGREES)

Figure 25 .

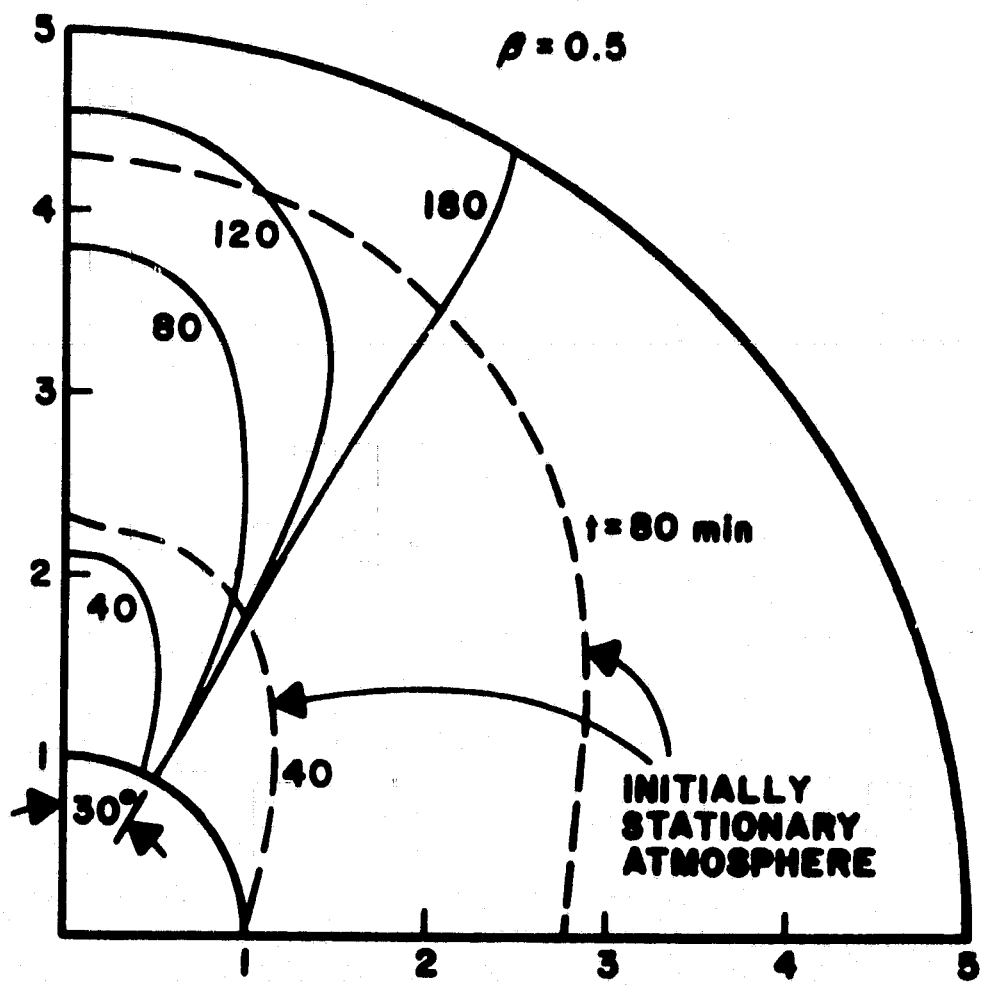
β = 0.5
180
120
80
40
t = 80 min
40
30°
INITIALLY
STATIONARY
ATMOSPHERE
5
4
3
2
1
1
2
3
4
5

Figure 26

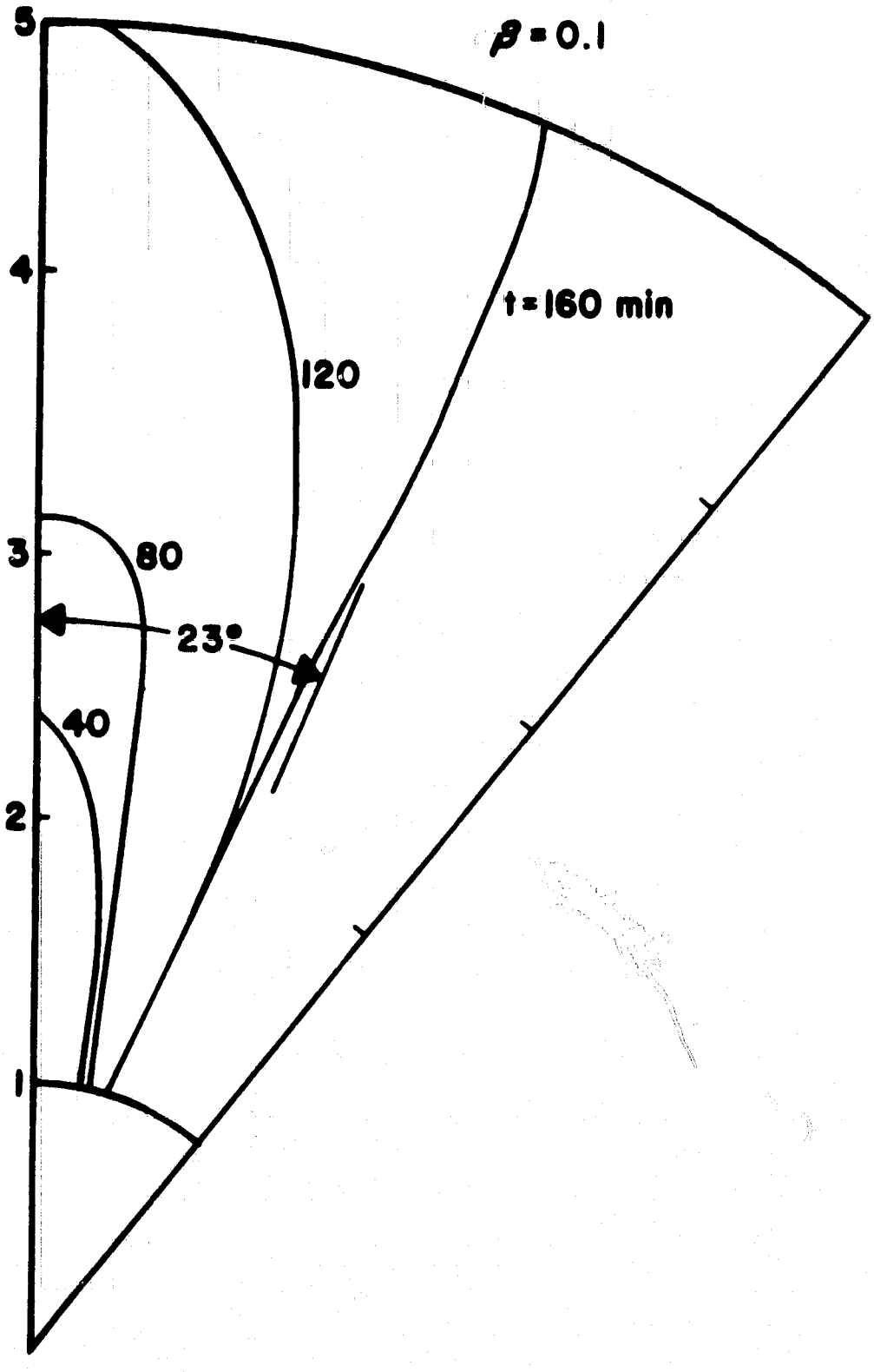

Figure 27

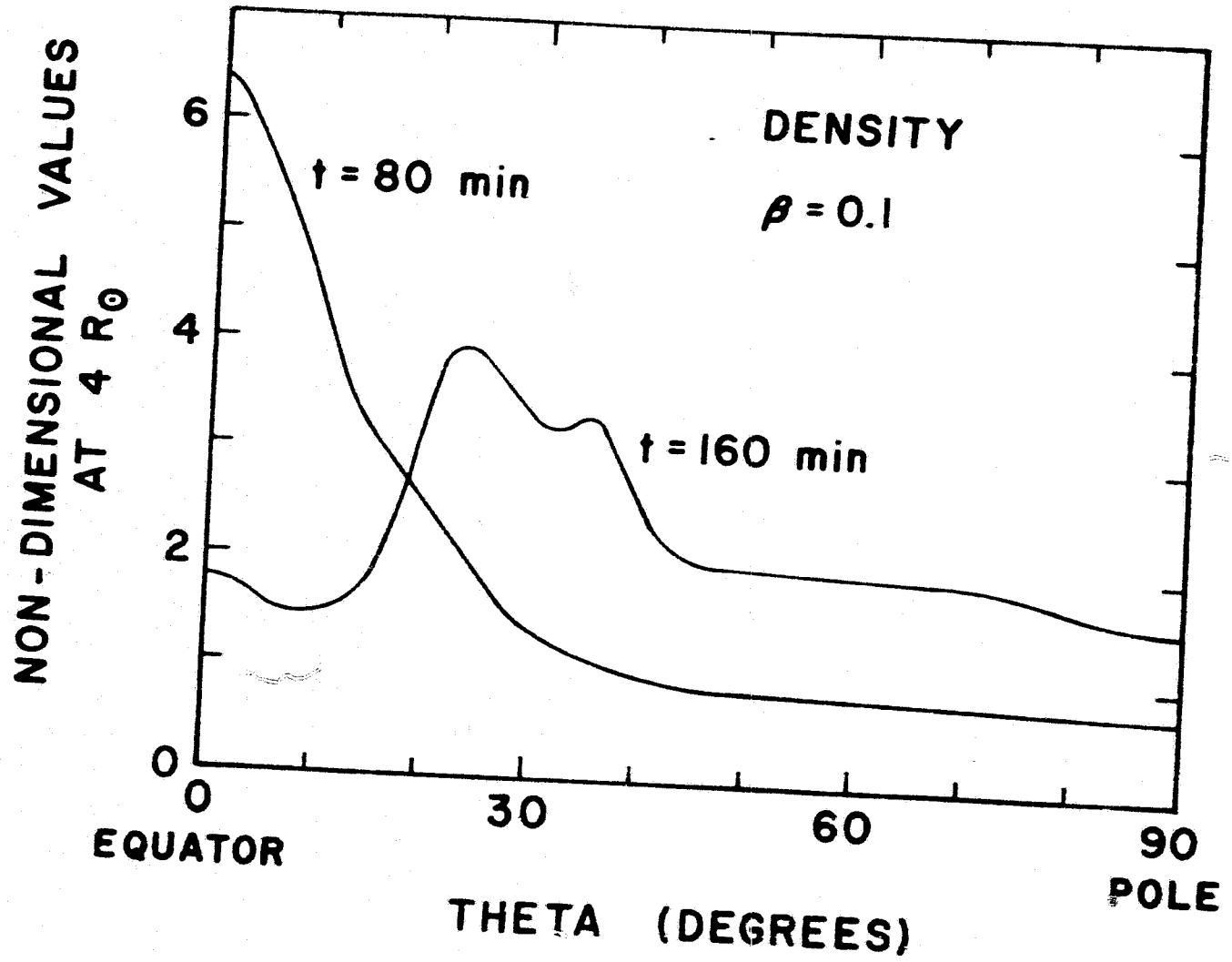
NON-DIMENSIONAL VALUES AT 4 R_0
6
4
2
0
DENSITY
β = 0.1
t = 80 min
t = 160 min
0
EQUATOR
30
60
90
POLE
THETA (DEGREES)

Figure 28

APPENDIX A. COMPUTER CODE FOR NUMERICAL SOLUTION

The simulations of the coronal streamer and the coronal transient are performed in two separate computer runs. The numerical solutions for the streamer simulation at each value of β are output to mass storage devices at selected time intervals. These solutions can then be recalled by the plotting routine in Appendix B and plotted in various formats by the computer. The streamer simulation at the last time for which it is calculated is then used as the initial state for the transient simulation. The transient solutions are also output to mass storage devices at selected time intervals, and plots can again be produced.

As an example of the computer time required, the streamer simulation for $\beta = 0.5$ required 6 min and 45 sec on the CRAY-1 computer to simulate 16 hrs of physical time. The transient simulation for $\beta = 0.5$ required 40 sec on the same computer to simulate 2 hrs of physical time.

Since the codes for the streamer and transient simulations are essentially identical, only the code for the streamer simulation is presented here. The variables that must be input to the code are given first followed by a listing of the code.

R. S. Steinolfson
25 April 1980

Description of Input Variables for Computer Code MHDHS*(CRAY-1)

Variable	Columns	Definition	Comments	Units
		Run Identification (Card 1)		
RN	1-4	Run number	Right-adjusted integer	
Title	5-80	Run title	Any alphanumeric information	
		Steady-State Parameters (Card 3)		
RØ	1-8	Reference radius	a. The time-dependent solution is computed for $r \geq$ RØ b. The values of the remaining variables on this card must be the values at this radius	solar radii
T	9-16	Temperature		K
D	17-24	Electron (or proton) density		no/cm^3
PI	25-32	Polytropic index	Constant everywhere ($1 < PI \leq 5/3$). If input as 0, set to 5/3.	
B	33-40	Magnetic field	The reference value at RØ and theta = 90^o.	
		Pulse Parameters (Card 4)		
TAU	1-8	Pulse duration		minutes
DMG(I), I = 1,9	9-16 17-24 . . . 73-80	Determine the dependent variables in the pulse at RØ.	The values input depend on the type of pulse being considered - see IPULS on the option card	

*This code is two-dimensional and is applicable to the meridional or r-θ plane in spherical coordinates. The azimuthal components of the velocity and magnetic field are neglected. This code does not use the large core memory.

Variable	Columns	Definition	Comments	Units
		Numerical Solution Parameters (Cards 5 and 6)		
		- Card 5 - Steady State		
REND	1-8	Maximum radius		solar radii
DR	9-16	Grid spacing in radial direction		
		Time Dependent		
DTT	17-24	Grid spacing in theta direction	It is best to select DTT such that R*DTT is about equal to DRT at (RMAX+RØ)/2	degrees
DRT	25-32	Grid spacing in radial direction		solar radii
TMAX	33-40	Maximum distance in theta direction	The solution is computed from the equatorial plane (theta = 90°) to TMAX > 90°.	degrees
RMAX	41-48	Maximum distance in radial direction	The solution is computed from RØ to RMAX.	solar radii
DTTP	49-56	Theta increment at which solution printed out	If either (or both) is input as 0, every grid point is printed out in that (or both) direction at each specified time increment (DTP).	degrees
DRTP	57-64	Radial increment at which solution printed out		solar radii
TMAX	65-72	Time limit	The solution is calculated until the simulated time exceeds TMAX.	minutes
DTP	73-80	Time increment at which solution printed out	If input as 0, the solution is printed out at every time increment.	
		- Card 6 -		
DTPT	1-8	Time increment at which solution is written out on a plot file	If input as 0, the solution is written out at every time increment	
STBY	9-16	Stability constant	a. STBY $\leq$ 1.0 b. Recommend using a value as near 1.0 as possible without numerical instabilities developing.	

Variable	Columns	Definition	Comments	Units
SMTH	17-24	Smoothing constant	a. Removes some numerical instabilities. b. Recommended using SMTH 1.0 if possible. c. Only used if ISMTH = 1 and ICHCK = 0.	
TSTR	25-32	Times at which solution written on mass storage	The solution can then be used as the initial state for restart in a separate program.	Minutes

Variable	Columns	Definition	Value	Description
				Options (Card 2)
ISTST	1-4	Steady-state solution	1	**Isothermal solar wind.**
			2	**Polytropic solar wind.**
IPULS	5-8	Pulse		The pulse depends on the particular study being conducted. The types of pulses currently available are the following (all symmetrical about theta = 90°):
			1	Pulse in temperature and density. DMG(L)=TM (Meridional extent of pulse in degrees), DMG(2)=δT, DMG(3)=$\delta\rho$. The maximum pulse in T and ρ is at theta = 90°, and it falls off sinusoidally to ambient values at theta = TM. See IPULS = 2 also.
			2	Pulse in the magnetic field. DMG(1) as for IPULS=1, DMG(2)=$(B_\theta)_p$ gauss, DMG(3)=$(B_r)_p$ where $(B_\theta)_p$ and $(B_r)_p$ are the maximum values of the latitudinal and radial components, respectively, in the pulse. Input 0 if no pulse desired in one of the components. The theta dependence is the same as for IPULS=1. For both IPULS=1 and =2, DMG(4)=DTI where DTI is the time in minutes for the pulse to reach maximum magnitude. The pulse increases linearly in magnitude with time.
ICHCK	9-12	Time-dependent solution check	0	Do not check the time-dependent solution.
			1	Check the time-dependent solution by starting it with the steady-state solution. The space terms are handled properly (and the steady-state solution is correct) if the time-dependent solution does not deviate appreciably from the steady-state solution after a sufficiently long time.
IBDRY	13-16	Boundary treatment at RØ		The boundary treatment depends on the type of pulse (IPULS) being used. See the subroutine BDRY. The current options are:

Variable	Columns	Definition	Value	Description
			0	No boundary treatment
			1	v_r and v_θ at RØ set to value at adjacent radial grid point (RØ+DRT).
IMAGF	17-20	Steady-state magnetic field calculation	1	Closed dipole
			2	Open quadrupole
			3	Open dipole
			4	Closed hexapole
			5	Open hexapole
			6	Closed decapole
			7	Open decapole
				If IMAGF = 1, 4 or 6 (2, 3, 5 or 7), the option IBDXØ is set to 2(3) internally.
IFWCS	21-24	Contact surface calculation	0	Follow the contact surfaces along r at $\theta = 90°$
			1	Do not follow the contact surfaces along r at $\theta = 90°$
IPTFL	25-28	Print out radii at which sound and Alfvén Mach numbers are one initially and at each time print out solution	0	Print out
			1	No print out
IPTVR	29-32	Dependent variable plots	0	No plots of the dependent variables
			1	Produce plots of the dependent variables (UAH)
			2	Produce plots of the dependent variables (NCAR)
ISTSL	33-36	Store solution at time TSTR on mass storage for restart	0	Do not store solution
			1	Store solution
ISMTH	37-40	Smoothing	0	No smoothing applied.
			1	Lapidus smoothing method applied.
NTMSM	41-44	Smoothing		The input value minus one is the number of time cycles that are skipped before smoothing. Only used if ISMTH=1.
IBDXØ	45-48	Boundary treatment at $\theta = 90°$.		The nomenclature is: $(\ )_1$ = value at 90-DTT, $(\ )_2$ = value at 90+DTT. For all cases $\rho_1 = \rho_3$, $P_1 = P_3$, $u_1 = u_3$, $v_1 = -v_3$, $B_{\theta 1} = B_{\theta 3}$, $B_{r1} = -B_{r3}$
			1	

Variable	Columns	Definition	Value	Description
			2	$u_1 = -u_3$, $v_1 = v_3$, $B_{\theta 1} = B_{\theta 3}$, $B_{r1} = -B_{r3}$
			3	$u_1 = -u_3$, $v_1 = v_3$, $B_{\theta 1} = -B_{\theta 3}$, $B_{r1} = B_{r3}$
			4	No boundary treatment
IBDXM	49-52	Boundary treatment at TMAX		The nomenclature is: $(\ )_1$ = value at TMAX-DTT, $(\ )_2$ = value at TMAX, $(\ )_3$ = value at TMAX+DTT.
			0	No boundary treatment, calculation stops when reach TMAX.
			1	$Q_3 = Q_2$, where Q is any dependent variable
			2	$Q_3 = 2Q_2 - Q_1$, where Q is any dependent variable
			3	$Q_3 = Q_1$, where Q is any dependent variable
IBDYM	53-56	Boundary treatment at RMAX		The nomenclature is: $(\ )_1$ = value at RMAX-DRT, $(\ )_2$ = value at RMAX, $(\ )_3$ = value at RMAX+DRT.
			0	No boundary treatment, calculation stops when reach RMAX.
			1	$Q_3 = 2Q_2 - Q_1$, where Q is any dependent variable
			2	$Q_3 = Q_1$, where Q is any dependent variable
IRDTN	57-60	Radiation-Not included in these codes	0	Neglect radiation
			1	Calculate radiation (Cox-Tucker), but don't allow it to effect the solution
			2	Calculate radiation (Cox-Tucker) and include it in equations.
ILØWB	61-64	Application of numerical differencing procedure	0	Use usual method with equations in conservation form.
			1	Use modified method. This method is often necessary when β is small ($\beta \approx 0.1$) and the magnetic field is essentially radial.

FORTRAN CODING FORM

ANALYST R. S. Steinolfson ENGINEER

JOB NO. MHDHS Input Format - 25 April 1980 COST CONTROL NO

C NO. | X | FORTRAN STATEMENT | LABEL

Run Identification (Card 1):

RN	title

Options - All right-adjusted integers (Card 2):

ISTST	IHULS	ICHCK	IBDRY	IMAGF	IFWCS	IPTFL	IPTVR	ISTSL	ISMTH	NTMSM	IBDXO	IBDXM	IBDYM	IRDTN	ILOWB

Steady State Parameters (Card 3):

RØ	T	D	PI	B

Pulse Parameters (Card 4):

TAU	DMG(1)	DMG(2)	DMG(3)	DMG(4)	DMG(5)	DMG(6)	DMG(7)	DMG(8)	DMG(9)

Numerical Solution Parameters (Card 5):

REND	DR	DTT	DRT	TMAX	RMAX	DTTP	DRTP	TMAX	DTP

Numerical Solution Parameters (Card 6):

DTPT	STBY	SMTH	TSTR

```
@ELT,IDL .SAMPLE,,STOP
ELT 8R1 S7491C 04/25/80 09:38:19 (->()
      @JOB,5143,36471701,S-RICH     STEINOLFSON, MHDHS
      @FORTRAN,REPLIB,DMEPHIT01,PL
            PROGRAM MHDMP
C  THIS CODE IS APPLICABLE TO THE MERIDIONAL PLANE IN SPHERICAL
C  COORDINATES.  IT IS MODIFIED FROM A CODE APPLICABLE TO THE CARTESION
C  (X,Y) PLANE.  THE TERMINOLOGY IS - X REFERS TO THETA (T), Y TO R,
C  U TO VT, V TO VR, BX TO BT, BY TO BR, IX7 TO T, IY7 TO R.
            PARAMETER (IX7=59,IY7=31)
            COMMON X(IX7),Y(IY7),U(IX7,IY7,2),V(IX7,IY7,2),D(IX7,IY7,2),
           1P(IX7,IY7,2),LDISMY(IX7),BY(IX7,IY7,2),BX(IX7,IY7,2),AZB(IX7,IY7),
           2AZZ(IX7,IY7)
            COMMON /COMM1/ YO,TO,DO,     IO,AO,RNO,PO,SG,TIO,YEND,DXT,DYT,XMAX,
           1YMAX,TAU,TMAX,DTP,RS,VO,WO,FO,AFO,AREAM,AREAT
            COMMON /COMM2/ LDISMX,LMX,LMY,ICHCK,IPULS,XMP,WMP,DTT,STEY,PI,DMP
            COMMON /COMLX/ ISMTH,SMTH,NTMSM,ILOWB
            COMMON /COMOBD/IBDXO,IBDXM,IBDYM
            COMMON /COMFDN/IRDTN,RADTN(IY7),CRADN,RADTNC(IX7,IY7)
            COMMON /COMBDY/IMBDY
            DIMENSION TIT(19)
          1 FORMAT ('1')
          2 FORMAT (I4,19A4 / 13I4)
          3 FORMAT (' INPUT -' // 3X'RUN IDENTIFICATION' / 5X'RUN NUMBER =',
           1I3 / 5X19A4 // 3X'OPTIONS' / 5X'ISTST =',I3 / 5X'IPULS =',I3 /
           25X'ICHCK =',I3 / 5X'IBDRY =',I3 / 5X'IMAGF =',I3/5X'IFMCS =',I3/
           35X'IPTFL =',I3/5X'IPTVR =',I3/5X'IPTVV =',I3/5X'ISMTH =',I3/5X
           4'NTMSM =',I3/5X'IBDXO =',I3 / 5X'IBDXM =',I3 / 5X'IBDYM =',I3/
           55X'IRDTN =',I3 / 5X'ILOWB =',I3 / 5X'IMBDY =',I3)
          4 FORMAT (5E6.0)
          5 FORMAT ( / 3X'STEADY-STATE PARAMETERS AT RO' /
           1                          5X'RO =',1PE12.5,' SOLAR RADII'/5X'T =',
           1E13.5,' K'/5X'D =',E13.5,' ELECTRONS/CM3' / 5X'PI =',0PF12.5/5X
           2'B =',1PE13.5,' GAUSS')
          6 FORMAT (7E6.0)
          7 FORMAT ( / 3X'PULSE PARAMETERS' / 5X'TAU =',1PE10.3,' MINUTES'/
           15X'TM =',E11.3,' DEGREES' / 5X'DT =',E11.3/5X'DD =',E11.3/5X
           2'DTI =',E10.3,' MINUTES')
          8 FORMAT (1258.0 /3F8.6)
          9 FORMAT ( / 3X'STEADY-STATE SOLUTION PARAMETERS' / 5X'REND =',1PE11
           *.5,  ' SOLAR RADII' / 5X'DR =',E13.5,' SOLAR RADII' // 3X
           2'TIME-DEPENDENT SOLUTION PARAMETERS' / 5X'DTT =',E12.5,
           3' DEGREES'      / 5X'DRT =',E12.5,' SOLAR RADII' / 5X'TMAX =',
           4E11.5,' DEGREES'      / 5X'RMAX =',E11.5,' SOLAR RADII' / 5X
           6'DTTP =',E11.5,' DEGREES'      / 5X'DRTP =',E11.5,' SOLAR RADII' /
           75X'TMAX =',E11.5,' MINUTES'/ 5X'DTP =',E12.5,' MINUTES' / 5X
           8'DTPT =',E11.5,' MINUTES'/5X
           9'STEY =',E11.5/5X'SMTH =',E11.5)
         13 FORMAT (/3X'PULSE PARAMETERS'/5X'TAU =',1PE10.3,' MINUTES'/5X
           1'TM =',E11.3,' DEGREES'/5X 'BT =',E11.3,' GAUSS'/5X'BR =',E11.3,
           2' GAUSS'/5X'DTI =',E10.3,' MINUTES')
            IO = 5
         16 FORMAT (/3X'PULSE PARAMETERS'/5X'TAU =',1PE10.3,' MINUTES'/5X
           1'TM =',E11.3,' DEGREES'/5X'BT =',E11.3,' GAUSS'/5X'DD =',E11.3,
           2' KM'/5X'DTI =',E10.3,' MINUTES')
            IO = 5
         10 WRITE (IO,1)
```

```
      READ (IN,2) NORUN,TIT,ISTST,IPULS,ICHCK,IRDRY,IMAGF,IFWCS
     1,IPTFL,IPTVH,IPTVV,ISMTH,NTMSM,IBDXO,IBDXM,IBDYM,IRDTN
     2,ILOW2,IREDY
C
      IF (IPTVH.EQ.1) IPTVH=2
      IF (IMAGF.EQ.1.OR.IMAGF.EQ.4.OR.IMAGF.EQ.6) IBDXO=2
      IF (IMAGF.EQ.2.OR.IMAGF.EQ.3.OR.IMAGF.EQ.5.OR.IMAGF.EQ.7) IBDXO=3
      WRITE (IO,3)NORUN,TIT,ISTST,IPULS,ICHCK,IRDRY,IMAGF,IFWCS
     1,IPTFL,IPTVH,IPTVV,ISMTH,NTMSM,IBDXO,IBDXM,IBDYM,IRDTN
     2,ILOW2,IREDY
      READ (IN,4) YO,TO,DO,PI,EO
      WRITE (IO,5)YO,TO,DO,PI,EO
      IF (PI.EQ.0.0) PI=5./3.
      READ (IN,6) TAU,XMP,WMP,DMP,YMXP1,YMXP2,TAU1
      GO TO(11,12,15),IPULS
   11 WRITE (IO,7)TAU,XMP,WMP,DMP,YMXP1
      GO TO 14
   12 PRINT 13,TAU,XMP,WMP,DMP,YMXP1
      WMP=WMP/EO
      DMP=DMP/DO
      GO TO 14
   15 PRINT 16,TAU,XMP,WMP,DMP,YMXP1
      WMP=WMP/EO
   14 READ (IN,8) YEND,DY,DXT,DYT,XMAX,YMAX,DXTP,DYTP,TMAX,DTP,DTPTL,
     1STPY,SMTH
      WRITE (IO,9)YEND,DY,DXT,DYT,XMAX,YMAX,DXTP,DYTP,TMAX,DTP,DTPTL,
     1STPY,SMTH
      CALL STST (ISTST,DY,IMAGF,AREAR,AREAD,IPTFL,IPTVH,DYTP)
      CALL TIMDEP (IRDRY,DXTP,DYTP,YMXP1,YMXP2,TAU1,IFWCS,AREAS,AREAD,
     1IPTFL,IPTVH,IPTVV,DTPTL,IMAGF)
      STOP
      END
      SUBROUTINE TIMDEP (IRDRY,DXTP,DYTP,YMXP1,YMXP2,TAU1,IFWCS,AREAS,
     1AREAD,IPTFL,IPTVH,IPTVV,DTPTL,IMAGF)
C   CONTROL TIME-DEPENDENT SOLUTION CALCULATION
      PARAMETER (IX7=79,IY7=51)
      COMMON X(IX7),Y(IY7),U(IX7,IY7,2),V(IX7,IY7,2),R(IX7,IY7,2),
     1P(IX7,IY7,2),LDISMY(IX7),BY(IX7,IY7,2),BX(IX7,IY7,2),AZZ(IX7,IY7),
     2AZZ(IX7,IY7)
C   MATCH DIMENSIONS OF ILMY IN COMMON/COBDRY/ AND LDIYM1 IN DIMENSION
      COMMON /COMM1/ YO,TO,DO,    IO,AO,RHO,PO,SO,TIO,YEND,DXT,DYT,XMAX,
     1YMAX,TAU,TMAX,DTP,RS,[illegible],TC,APO,AREAM,AREAT
      COMMON /COMM2/ LDISMX,LMX,LMY,ICHCK,IPULS,XMP,WMP,DTT,STPY,PI,DMP
      COMMON /COBDRY/ LKEEP,ILMY(IY7),ILMYT
      COMMON /COMRDN/IRDTN,RADTN(IY7),GRADN,RADTNC(IX7,IY7)
      DIMENSION IHD2(2),          LDIYM1(IY7)
   11 FORMAT(/10X27H*************************** / 10X27H  TIME-DEPENDENT
     1 SOLUTION  / 10X27H*************************** / )
   12 FORMAT (1X'TIME =',
     1                 1PE10.3,' =',E10.3,' MINUTES, TIME CYCLE NO',I5,
     1', DTT =',E10.3)
   13 FORMAT (5X'T =',1PE10.3,' [illegible] ='
     1                       E10.3,' DEG',', [illegible] NO',I4 /
     1                                      [illegible]
     [illegible]
   14 FORMAT (I7,11(1PE11.4))
   23 FORMAT (5X'ENERGY BUILD-UP (ERGS/KM2):  MAGNETIC =',1PE11.4,
```

```
      113.          00          1', THERMAL =',E11.5,', KINETIC =',E11.5,', GRAVITATIONAL =',E11.5
      114.          00          2/ 5X'MASS BUILD-UP =',E11.5,' GMS/KMZ =',E11.5,' PARTICLES/<<Z')
      115.          00        27 FORMAT (5X'P CHARACTERISTIC DIRECTIONS AT RO'  / 14X'T'10X'L3'
      116.          00          110X'L4'10X'L5'1 X'L6')
      117.          00        28 FORMAT (7X,3(1PE12.4))
      118.          00        39 FORMAT (5X'RCONTS-RO =',1PE10.4,' SOLAR RADII =',E10.4,
      119.          00          1' KM, RCONTSR-RO =',
      120.          00          2   E10.4,' SOLAR RADII =',E10.4,' KM')
      121.          00        45  FORMAT (5X'NPTVR =',I3)
      122.          00        62 FORMAT (5X'NO'5X'R'7X'SR-GRO')
      123.          00        63 FORMAT (I7,2(1PE11.4))
      124.          00        95 FORMAT (/5X'RADII AT WHICH SOUND AND ALFVEN MACH NUMBERS ARE ONE'
      125.          00          1/5X'NO'3X'TH(DEG)'5X'RS'10X'RA')
      126.          00        94 FORMAT (I7,3(1PE12.4))
      127.          00        47 FORMAT ('T=',1PE9.5,' ')
      128.          00           KTIME = 0
      129.          00           IEND1 = 0
      130.          00           IEND = 1
      131.          00           ILMX = 0
      132.          00           YCONTS=Y(1)
      133.          00           YCTSR=Y(1)
      134.          00           LCONT=1
      135.          00           LCONT1=2
      136.          00           LCTR=1
      137.          00           LCTR1=2
      138.          00           NPTVR=0
      139.          00           IF (IPTVR.EQ.1) NPTVR=1
      140.          00           IPULSE=0
      141.          00           XTP = X(2)-1.E-10
      142.          00           YTP = Y(1)-1.E-10
      143.          00           PM = 1.67259E-24
      144.          00           GRA=6.67E-8
      145.          00           SUNM=1.99E33
      146.          00           RADDG=.0174533
      147.          00           PIEC2=3.141593/2.
      148.          00           DY02=DXT/2.
      149.          00           DY02=DYT/2.
      150.          00           DXTT2=DXT*2.
      151.          00           DYTT2=DYT*2.
      152.          00           AREA2=AREA**2
      153.          00           BETA0=2./(PI*AR(1)
      154.          00           PRNO2=PI/RNO**2
      155.          00           LMXM1 = LMX-1
      156.          00           LMYM1=LMY-1
      157.          00           TIM = 0.0
      158.          00           TIMP = DTP
      159.          00           DTPTL=DTPTL/TIO
      160.          00           TIMPL=DTPTL
      161.          00           CALL LAX (IPP,IP,DTTK,ILMX,IPPX,IPPY1,IPPY2)
      162.          00           IF (IBDRY.NE.0)
      163.          00          1CALL BDRY(IP,NTIME,IBDRY,ILMX,TIM,IPP,LMXPY)
      164.          00           CALL BCDRY(ILMX,IEND,IPP,IP)
      165.          00           IF (ICHCK.EQ.0)  C TO 1
      166.          00           ILMX=1
      167.          00           LBISMX = LMX-1
      168.          00           DO 2 I=1,LMX
      169.          00           ILMY(I)=1
```

```
00        2 LBISNY(I) = LMY-1
00          CALL HSEDY(IP)
00          GO TO 3
00        1 CALL PULSIN (IEND1,TIM,IP,YMXP1,YMXP2,LMXPY,LMXPY1,TAU1)
00          IF (IPTVR.EQ.0) GO TO 3
00          IPULS6=1
00          GO TO 56
00       56 IPULS6=0
00        3 WRITE (IO,11)
00       16 TIM = TIM+DTT
00          NTIME = NTIME+1
00          IF(ICHCK.EQ.1) GO TO 25
00          IF (                   IEND1.EQ.1) CALL PULSIA(IEND1,TIM,IP,YMXP1,
00         1YMXP2,LMXPY,LMXPY1,TAU1)
00       25 IF (TIM.LT.TMAX) GO TO 5
00          IEND = 2
00        5 IF (ICHCK.EQ.1) GO TO 15
00          IF (NTIME.GT.1)
00         1CALL BDRY1(IP,NTIME,INDFY,ILMX,TIM,IPP,LMYPY)
00          IF (NTIME.GT.1) CALL ODRRY1(ILMX,IEND,IPP,IP)
00       15 CALL LAX1 (IPP,IP,DTTK,ILMX,IFFX,IFFY1,IFFY2)
00          IF (ICHCK.GT.1) CALL HSEDY1(IP)
00          DTTK2=DTTK/2.
00          DO 69 J=1,LMY,LMYM1
00          DO 69 I=2,LMXM1
00          IM=I-1
00       69 AZD(IM,J)=AZD(IM,J)+DTTK2*(V(I,J,IP)*EX(I,J,IP)-U(I,J,IP)*
00         1EY(I,J,IP)+V(I,J,IPP)*EX(I,J,IPP)-U(I,J,IPP)*EY(I,J,IPP))
00     C   FOLLOW CONTACT SURFACES ALONG Y AT X=0
00          IF (IFACS.LE.1) GO TO 36
00          YCONTS=YCONTS+DTTK*(V(2,LCONT,IPP)+(YCONTS-Y(LCONT))*(V(2,LCONT1,
00         1IPP)-V(2,LCONT,IPP))/(Y(LCONT1)-Y(LCONT)))
00          IF (YCONTS.LT.Y(LCONT1)) GO TO 37
00          LCONT=LCONT1
00          LCONT1=LCONT+1
00       37 IF (TIM.LE.TAU) GO TO 36
00          YCTSR=YCTSR+DTTK*(V(2,LCTR,IPP)+(YCTSR-Y(LCTR))*(V(2,LCTR1,IPP)-
00         1V(2,LCTR,IPP))/(Y(LCTR1)-Y(LCTR)))
00          IF (YCTSR.LT.Y(LCTR1)) GO TO 36
00          LCTR=LCTR1
00          LCTR1=LCTR+1
00     C   PRINT OUT VALUES
00       36 IF (TIM.LT.TIMP.AND.IEND.EQ.1) GO TO 41
00          TIMM = TIM*TIO
00          WRITE (IO,12) TIM,TIMM,NTIME,DTTK
00          IF (IFACS.EQ.1) GO TO 37
00          YCONTP=YCONTS-YO
00          YCONTK=YCONTP*PS/1.E5
00          YCTSP=YCTSR-YO
00          YCTSPK=YCTSP*PS/1.E5
00          PRINT13P,YCONTP,YCONTK,YCTSP,YCTSPK
00     C   CALCULATE ENERGY AND MASS BUILT-UP
00       37 EPOT=0.0
00          EMAS=0.0
00          ETL=0.0
00          EPT1=0.0
00          EKIN=0.0
```

```
      EBLT=0.0
      EBK1=0.0
      EBLK=0.0
      EBK2=0.0
      EBG1=0.0
      EBG2=0.0
      EBLG=0.0
      DBL1=0.0
      DBL2=0.0
      DBLT=0.0
      IMXI=LMX-1
      BT21=BX(2,1,IPP)**2+BY(2,1,IPP)**2
      THE1 =P(2,1,IPP)
      RKE1=D(2,1,IPP)*(U(2,1,IPP)**2+V(2,1,IPP)**2)
      GRE1=D(2,1,IPP)/Y(1)
      RMS1=D(2,1,IPP)
      DO 9 J=2,LMY
      BT22=BX(2,J,IP)**2+BY(2,J,IP)**2
      THE2=P(2,J,IP)
      RKE2=D(2,J,IP)*(U(2,J,IP)**2+V(2,J,IP)**2)
      GRE2=D(2,J,IP)/Y(J)
      RMS2=D(2,J,IP)
      EBM1=EBM1+DYO2*(BT21+BT22)
      EBT1=EBT1+DYO2*(THE1+THE2)
      EBK1=EBK1+DYO2*(RKE1+RKE2)
      EBG1=EBG1+DYO2*(GRE1+GRE2)
      DBL1=DBL1+DYO2*(RMS1+RMS2)
      BT21=BT22
      THE1=THE2
      RKE1=RKE2
      GRE1=GRE2
    9 RMS1=RMS2
      DO 21 I=3,IMXI
      THE1=P(I,1,IPP)
      BT21=BX(I,1,IPP)**2+BY(I,1,IPP)**2
      RKE1=D(I,1,IPP)*(U(I,1,IPP)**2+V(I,1,IPP)**2)
      GRE1=D(I,1,IPP)/Y(1)
      RMS1=D(I,1,IPP)
      DO 22 J=2,LMY
      BT22=BX(I,J,IP)**2+BY(I,J,IP)**2
      THE2=P(I,J,IP)
      RKE2=D(I,J,IP)*(U(I,J,IP)**2+V(I,J,IP)**2)
      GRE2=D(I,J,IP)/Y(J)
      RMS2=D(I,J,IP)
      EBM2=EBM2+DYO2*(BT21+BT22)
      EBT2=EBT2+DYO2*(THE1+THE2)
      EBK2=EBK2+DYO2*(RKE1+RKE2)
      EBG2=EBG2+DYO2*(GRE1+GRE2)
      BT21=BT22
      DBL2=DBL2+DYO2*(RMS1+RMS2)
      THE1=THE2
      RKE1=RKE2
      GRE1=GRE2
   22 RMS1=RMS2
      EBLM=EBLM+DXO2*(EBM1+EBM2)
      EBLT=EBLT+DXO2*(EBT1+EBT2)
      EBLK=EBLK+DXO2*(EBK1+EBK2)
```

```
      EBLG=EBLG+DYO2*(EBG1+EBG2)
      DELT=DELT+DXO2*(DEL1+DEL2)
      EPM1=EPM2
      EPT1=EPT2
      EPM2=0.0
      EPT2=0.0
      EBK1=EBK2
      EBK2=0.0
      EBG1=EBG2
      DEL1=DEL2
      EBG2=0.0
   21 DEL2=0.0
      EBLM=(EBLM-AREAM)*4.E3*RG**2*RS**2
      EBLT=(EBLT-AREAT)*PD*RS**2*1.E5*PI/(PI-1.)
      EBLK=EBLK*DC*AC**2*RS**2*PM*1.E15/2.
      EBLG=(EBLG-AREAG)*CPA*SUMM*DC*PM*RS*1.E5/YJ
      DELT=(DELT-AREAT)*DC*PM*RS**2*1.E5
      DELTP=DELT/PM
      PRINT 23,EBLM,EBLT,EBLK,EBLG,DELT,DELTP
C   FIND CHARACTERISTIC DIRECTIONS AT Y0
      PRINT 27
      DO 26 I=2,LDISMX
      IF (X(I).LT.XTP.AND.I.NE.LDISMX) GO TO 26
      ARY=ABC*-Y(I,1,IPP)/SQRT(D(I,1,IPP))
      ARY2=ARY**2
      ARG1=PRNG2*F(I,1,IPP)/D(I,1,IPP)
      ARG2=ARG1+ARG2*(V X(I,1,IPP)**2                 )/D(I,1,IPP)+ARY2
      ARG1=SQRT(ARG2**2-4.*ARG1*ARY2)
      ARG3=SQRT(.5*(ARG2+ARG1))
      RL3=V(I,1,IPP)+ARG3
      RL5=V(I,1,IPP)-ARG3
      ARG3=SQRT(.5*(ARG2-ARG1))
      RL4=V(I,1,IPP)+ARG3
      RL6=V(I,1,IPP)-ARG3
      PRINT 28,X(I),RL3,RL4,RL5,RL6
      XTP=XTP+DXTP
   26 CONTINUE
      XTP=X(2)-1.E-6
      DO 17 I=2,LDISMX
      IF (X(I).LT.XTP.AND.I.NE.LDISMX) GO TO 17
      XMM=X(I)/TAPCG
      WRITE (I2,15) X(I),XMM,I
      LSUP = LDISMY(I)
      DO 13 J=1,LSUP
      IF (Y(J).LT.YTP.AND.J.NE.LSUP) GO TO 13
      YMYM=(Y(J)-Y0)*RS/1.E5
C   CALCULATE LORENTZ FORCE: ONLY VALID IF BZ=0
      IF (J.GT.1) GO TO 29
      RJCP=((BY(I+1,J,IPP)-BY(I-1,J,IPP))/DXTT2-(Y(J+1)*BX(I,J+1,IPP)-
     1Y(J)*BX(I,J,IPP))/DYT)/Y(J)
      RJCX=-BY(I,J,IPP)*RJCP
      RJCY=BX(I,J,IPP)*RJCP
      GO TO 32
   29 RJCP=(BY(I+1,J,IP)-BY(I-1,J,IP))/DXTT2
      IF (J.GT.F) GO TO 31
      RJCP=(RJCP-(Y(J+1)*BX(I,J+1,IP)-Y(J-1)*BX(I,J-1,IP))/DYTT2)/Y(J)
      GO TO 32
```

```
      00          31 RJCB=(RJCB-(Y(J+1)*BX(I,J+1,IP)-Y(J-1)*BX(I,J-1,IP))/BYTT2)/Y(J)
      00          32 RJCBX=-BY(I,J,IP)*RJCB
      00             RJCBY=BX(I,J,IP)*RJCB
      00          30 IF (J.GT.1) GO TO 19
      00             IF (ICHCK.EQ.1) GO TO 19
      00             TEMPR=P(I,J,IPP)/D(I,J,IPP)
      00             BETA=BETA0*P(I,J,IPP)/(BX(I,J,IPP)**2+BY(I,J,IPP)**2)
      00             WRITE (ID,14) J,YMYO,U(I,J,IPP),V(I,J,IPP),RJCBX,     D(I,J,IPP),
      00            1P(I,J,IPP),BX(I,J,IPP),BY(I,J,IPP),RJCBY,TEMPR,BETA
      00             GO TO 20
      00          19 TEMPR=P(I,J,IP)/D(I,J,IP)
      00             BETA=BETA0*P(I,J,IP)/(BX(I,J,IP)**2+BY(I,J,IP)**2)
      00             WRITE (ID,14) J,YMYO,U(I,J,IP),V(I,J,IP),RJCBX,     D(I,J,IP),
      00            1P(I,J,IP),BX(I,J,IP),BY(I,J,IP),RJCBY,TEMPR,BETA
      00          20 YTP = YTP+DYTP
      00          13 CONTINUE
      00             IF (I.GT.2.OR.IRDTN.EQ.C) GO TO 60
      00             PRINT 62
      00             YTP=Y(1)-1.E-6
      00             DO 61 J=1,LSUB
      00             IF (Y(J).LT.YTP.AND.J.NE.LSUB) GO TO 61
      00             TEMPR=P(2,J,IP)/D(2,J,IP)
      00             QRDN=RADFN(TEMPR*TG)*(D(2,J,IP)*DO)**2*CRADN
      00             QRDNM=QRDN-PADTN(J)
      00             PRINT 63,J,QRDN,QPDNM
      00          61 CONTINUE
      00          60 YTP = Y(1)-1.E-6
      00             XTP = XTP+DXTP
      00          17 CONTINUE
      00             IF (IPTFL.EQ.1) GO TO 86
      00          C  FACII AT WHICH MS=1 AND MA=1
      00             L=IP
      00             PRINT 95
      00             DO 87 I=2,LMXM1
      00             RSE1=YO
      00             RAE1=YO
      00             ISE1=1
      00             IAE1=1
      00             RMS2=V(I,1,L)/SQRT(P(I,1,L)/D(I,1,L))
      00             IF (RMS2.GE.1.) ISE1=2
      00             RMA2=V(I,1,L)*SQRT(D(I,1,L)/(BX(I,1,L)**2+BY(I,1,L)**2))/A=0
      00             IF (RMA2.GE.1.) IAE1=2
      00             DO 88 J=1,LMY
      00             GO TO (89,90) ,ISE1
      00          89 RMS1=RMS2
      00             RMS2=V(I,J,L)/SQRT(P(I,J,L)/D(I,J,L))
      00             IF (RMS2.LT.1.) GO TO 90
      00             ISE1=2
      00             RSE1=Y(J-1)+DYT*(1.-RMS1)/(RMS2-RMS1)
      00          90 GO TO (91,92),IAE1
      00          91 RMA1=RMA2
      00             RMA2=V(I,J,L)*SQRT(D(I,J,L)/(BX(I,J,L)**2+BY(I,J,L)**2))/A=0
      00             IF (RMA2.LT.1.) GO TO 85
      00             IAE1=2
      00             RAE1=Y(J-1)+DYT*(1.-RMA1)/(RMA2-RMA1)
      00          92 IF (ISE1.EQ.2.AND.IAE1.EQ.2) GO TO 93
      00          88 CONTINUE
```

```
393.    00        93 XKM=X(I)/RAPDG
399.    00           PRINT 94,I,XKM ,RSE1,RAE1
400.    00        27 CONTINUE
401.    00        56 XTP=X(2)-1.E-6
402.    00           TIMP = TIMP+DTP
403.    00     C  CREATE PLOT FILES
404.    00        40 IF (IPTVR.EQ.0) GO TO 51
405.    00           IF (TIM.LT.TIMPL.AND.IEND.EQ.1) GO TO 16
406.    00        58 TIMMP=TIM*TIO
407.    00           LDISM1=LDISMX-1
408.    00           DO 57 J=2,LDISMX
409.    00        57 LDIYP1(J)=LDISMY(J)+1
410.    00           GO TO (65,64), IPTVR
411.    00        68 ENCODE (12,47,IHD2) TIMMP
412.    00           WRITE (10) (IHD2(I),I=1,2), LDISM1,(LDIYP1(J),J=2,LDISMX)
413.    00           GO TO 65
414.    00        64 WRITE (10) TIMMP,          LDISM1,(LDIYP1(J),J=2,LDISMX)
415.    00        65 DO 48 I=2,LDISMX
416.    00           LDISM2=LDISMY(I)+1
417.    00           GO TO (66,67),IPTVR
418.    00        66 WRITE (10) (P(I,J,IP),D(I,J,IP),BX(I,J,IP),BY(I,J,IP),U(I,J,IP),
419.    00          1V(I,J,IP),          J=1,LDISM2)
420.    00           GO TO 48
421.    00        67 ARG1=X(I)
422.    00           IF (IMAGF.EQ.1.OR.IMAGF.EQ.5.OR.IMAGF.EQ.7) ARG1=ARG1-PIEC2
423.    00           DO 59 J=1,LDISM2
424.    00        59 AZZ(I-1,J)=AZZ(I-1,J)+Y(J)*SIN(ARG1)
425.    00           WRITE (10) (P(I,J,IP),D(I,J,IP),BX(I,J,IP),BY(I,J,IP),U(I,J,IP),
426.    00          1V(I,J,IP),AZZ(I-1,J),J=1,LDISM2)
427.    00        48 CONTINUE
428.    00           NPTVR=NPTVR+1
429.    00           PRINT 45,NPTVR
430.    00           IF (IPULS6.EQ.1) GO TO 56
431.    00           TIMPL=TIMPL+DTPTL
432.    00        51 IF (IEND.EQ.2) RETURN
433.    00           GO TO 16
434.    00           END
435.    00     *FORTRAN,D=PLIB,DN=STSTC1,FL
436.    00           SUBROUTINE STST (ISTST,DY,IMAGF,AREAG,AREAD,IPTFL,IPTVR,DXIP)
437.    00     C  CALCULATE STEADY-STATE SOLUTION AND FILL TIME-DEPENDENT ARRAYS
438.    00           PARAMETER (IX7=79,IY7=51)
439.    00           COMMON X(IX7),Y(IY7),U(IX7,IY7,2),V(IX7,IY7,2),D(IX7,IY7,2),
440.    00          1P(IX7,IY7,2),LDISMY(IX7),BY(IX7,IY7,2),BX(IX7,IY7,2),AZZ(IX7,IY7),
441.    00          2AZZ(IX7,IY7)
442.    00           COMMON /COMM1/ YO,TO,DO,   IO,AO,RNO,PO,SO,TIO,YEND,DXI,DYT,XMAX,
443.    00          1YMAX,TAU,TMAX,DTP,RS,VO,WO,FO,AEO,APEAK,AREAT
444.    00           COMMON /COMM2/ LDISMX,LMX,LMY,ICHCK,IFULS,XMP,YMP,DTT,STRY,PI,DMP
445.    00           COMMON /COMRDN/IRDTN,RADTN(IY7),CRADN,RADTNC(IX7,IY7)
446.    00           DIMENSION IHD2(2)
447.    00          1 FORMAT ( // ' OUTPUT -' // 10X35H**********************************
448.    00          1** / 11X1H*,' INITIAL STEADY-STATE ATMOSPHERE ',1H*   / 10X
449.    00          235H**********************************)
450.    00          2 FORMAT ( / 7X'VALUES AT YO' / 5X'P =',1PE11.3,' DYNES/CM2'/5X
451.    00          1'A =',E11.3,' KM/SEC' / 5X'TI =',E10.3,' MIN'/5X'% =',E11.3 /
452.    00          25X'S =',E11.3 / 5X'AB =',E10.3/5X'BTA =',E9.3/5X'GAM =',E9.3,' GM3
453.    00          3-S/ERG')
454.    00          6 FORMAT ( / 3X'SOLUTION OF STEADY-STATE EQUATIONS' / 5X
```

```
     1'THERMODYNAMIC VARIABLES' / 14X'R'11X
     1'R'10X'R-RS'10X'P=D'11X'P'12X'D'       / 5X'NO'2X'SOLAR RADII'5X
     2'KM'11X'KM'9X'NON DIM'5X'DYNES/CM2'5X'NO/CM3'2X'BETA')
    7 FORMAT (I7,F11.4,6(1PE13.3))
   13 FORMAT (5X'NEED LARGER DO LOOP LIMIT FOR X - EXECUTION TERMINATED'
     1)
   14 FORMAT(5X'NEED LARGER DO LOOP LIMIT FOR Y - EXECUTION TERMINATED')
   32 FORMAT(/3X'SOLUTION OF STEADY-STATE EQUATIONS' / 5X
     1'NON-DIMENSIONAL VARIABLES'/13X'R'11X'VR'11X'P'11X'D'11X'T'11X'MS'
     2'10X'MA'9X'MFA'9X'BETA')
   34 FORMAT(I7, 9(1PE12.4))
   17 FORMAT ( / 5X'MAGNETIC FIELD' / 9X'R-RO' / (8(1PE14.4)))
   18 FORMAT ($9X'BT(R)' / (8(1PE14.4)))
   19 FORMAT (9X'BR(R)' / (8(1PE14.4)))
   23 FORMAT (7X'T =',1PE12.5)
   25 FORMAT ( / 5X'INITIAL ENERGY (ERGS/KM2):  MAGNETIC =',1PE11.5,
     1', THERMAL =',E11.5,
     2                ', GRAVITATIONAL =',E11.5 / 5X'INITIAL MASS =',
     2E11.5,' GMS/KM2 =',E11.5,' PARTICLES/KM2')
   45 FORMAT (/3X'REVISED VALUES OF TMAX AND RMAX'/5X'TMAX =',1PE9.3,
     1' DEGREES'    /5X'RMAX =' E9.3,' SOLAR RADII'/5X'LMX =',I4/
     25X'LMY =',I4)
   77 FORMAT (/5X'RADIATION'/5X'NO'4X'NON DIM'4X'ERG/CM3-S')
   76 FORMAT (I7,2(1PE12.4))
   82 FORMAT ('T=',1PE9.3,' ')
   83 FORMAT (/' *** NO CONVERGENCE IN STST - EXECUTION TERMINATED ***')
   95 FORMAT (/5X'RADII AT WHICH SOUND AND ALFVEN MACH NUMBERS ARE ONE'
     1/5X'NO'3X'TH(DEG)'6X'RS'10X'RA')
   94 FORMAT (I7,2(1PE12.4))
C  SET CONSTANTS
      BC = 1.32E-16
      PM = 1.67239E-24
      RS = 6.957E10
      SUNM = 1.987E33
      GRA = 6.67E-8
      WRITE (10,1)
      PIEC = 3.141593
      PIEC2=PIEC/2.
      RADDG=.0174533
      TMAX=90.
C  FIND REVISED XMAX AND YMAX, FILL X AND Y ARRAYS
      XMAX=XMAX+DXT
      DO 9 IM=1,1000
      X(IM) = (IM-2)*DXT+TMIN
      IF  (X(IM),GE.XMAX-1.E-5 ) GO TO 10
    9 CONTINUE
      WRITE (10,13)
      CALL EXIT
   10 DO 5 J=1,1000
      Y(J) = Y0+(J-1)*DYT
      IF (Y(J) .GE.YMAX-1.E-5 ) GO TO 12
    5 CONTINUE
      WRITE (10,14)
      CALL EXIT
   12 LMX = IM
      LMY = J
      XMAX=X(LMX-1)
```

```
      YMAX=Y(LMY)
      PRINT 45,XMAX,YMAX,LMX,LMY
      LMXP1=LMX+1
      ARG=PIEC/(2.*(XMAX))
C VALUES AT Y0
      PO = 2.*RO**EC*TC
      AO = SQRT(PI*PO/(PM*DO))/1.E5
      CRADN=RS/(PM*DO*AO**3*1.E15)
      TIO = PS/(AO**3.E5*60.)
      PHO = SQRT(PO**2*1.E10*PM*DO/PC)
      SO = GRA*SQRT(GAO**2*1.E10*RS)
      ABO = 2.2E11*PO/(AO*SQRT(DO)*1.E5)
      BTA=2./(PI*ABO**2)
      WRITE (IO,2) PO,AO,TIO,RNO,SO,ABO,BTA,CRADN
      TAU = TAU/TIO
      TMAX = TMAX/TIO
      DTP = DTP/TIO
      GO TO (64,64,65,66,65,67,69),IMAGE
   64 CONVF=1.
      GO TO 67
   65 CONVF=.5
      GO TO 67
   66 CONVF=1./.75
      GO TO 67
   68 CONVF=8./75.
      GO TO 67
   69 CONVF=1./30.
   67 GO TO (4,71),    ISTST
C  STEADY-STATE SOLUTION, THERMODYNAMIC VARIABLES AND VELOCITIES
    4 C1 = SO*PMO**2
      C2 = RS/1.E5
      WRITE (IO,6)
      GO TO 33
   71 II=-1
      CALL SOLWD (AO,TO,PI,UO,II,AO)
      US=UO
      F=0.0
      UT1=US
      S1=US**2/2.+1./(PI-1.)-SO
      WRITE (IO,32)
   33 DO 5 I=1,100
      GO TO (59,50), ISTST
   59 YS = YO+(I-1)*DY
      PS = EXP(C1*(1./YS-1./YO))
      YSK = YS*C2
      YSKP = YSK-C2
      PSO = PS*PO
      DSL = PS*DO
      GO TO 51
   50 YS = YO+(I-1)*DY
      UT2=UT1
      UT1=US
      US=2.*UT1-UT2
      DO 40 J=1,20
      UT=US
      FT=F
      US=UT-FT/(UT-(UO/YS**2)**(PI-1.)/UT**PI)
```

```
      F=US**2/2.+(U0/(US*YS**2))**(PI-1.)/(PI-1.)-S0/YS-ST
      IF (ABS(US-UT)/UT.GT.1.E-5) GO TO 81
      IF (ABS(F).LT.1.E-5) GO TO 82
   81 CONTINUE
      PRINT 83
      CALL EXIT
   82 DS=U0/(US*YS**2)
      PS=DS**PI
      TS=PS/DS
      AS=   SQRT(YS)
      RMSS=U1/AS
      GO TO (49,51,49,53,53,70,70),IMAGF
   49 BTA0=BTA*PS*YS**6
      GO TO (50,62),ISTST
   51 BTA0=BTA*PS*YS**8
      GO TO (50,62),ISTST
   53 BTA0=BTA*PS*YS**10
      GO TO (50,62),ISTST
   70 BTA0=BTA*PS*YS**14
      GO TO (50,62),ISTST
   50 WRITE (10,7) I,YS,YSK,YSRK,PS,PSD,DSD,BTA0
      GO TO 62
   62 RMAS=RMSS*SQRT(BTA0*PI/2.)
      RMFW=US/(AS*SQRT(1.+2./(PI*BTA0)))
      PRINT 54,I,YS,US,PS,DS,TS,RMSS,RMAS,RMFW,BTA0
   63 U(1,I,1)=YS
      IF (IPOTN.EQ.0) GO TO 73
      IF (ISTST.EQ.1) TSD=TS
      RADTN(I)=RADFN(TSD)*DSD**2
   73 IF (YS.GE.YEND-1.E-5) GO TO 3
    5 CONTINUE
C  STEADY-STATE SOLUTION, MAGNETIC FIELD
    3 XMAXMD=XMAX
C
      IF (IPOTN.EQ.0) GO TO 74
      PRINT 77
      DO 75 K=1,I
      RADTNK=RADTN(K)*CRADK
      PRINT 76,K,RADTNK,RADTN(K)
   75 CONTINUE
C
   74 DO 37 K=1,I
   37 BX(1,K,1)=U(1,K,1)-V0
      PRINT 17,(BX(1,J,1),J=1,I)
      DO 22 K=1,80
      XCLB=XMAX+(K-1)*(XMAX*2.-XMAX)/2.
      IF (XCLB.GT.XMAX+1.E-5) GO TO 24
      PRINT 27, XCLB
      ARG1=XCLB*RADDG
      IF (IMAGF.EQ.3) ARG1=ARG1-PIEC2
      IF (IMAGF.EQ.5) ARG1=ARG1-PIEC2
      IF (IMAGF.EQ.7) ARG1=ARG1-PIEC2
      DO 16 J=1,I
      GO TO (55,47,55,54,56,71,71),IMAGF
   55 ARG2=U(1,J,1)**2
      BX(1,J,1)=SIN(ARG1)/ARG2*COSMF
      BY(1,J,1)=2.*COS(ARG1)/ARG2*COSMF
```

```
      GO TO 16
   47 ARG2=U(1,J,1)**4
      BX(1,J,1)=2.*SIN(ARG1)*COS(ARG1)/ARG2
      BY(1,J,1)=(3.*COS(ARG1)**2-1.)/ARG2
      GO TO 16
   58 ARG2=U(1,J,1)**5
      BX(1,J,1)=3.*SIN(ARG1)*(5.*COS(ARG1)**2-1.)/(2.*ARG2)*CONMF
      BY(1,J,1)=COS(ARG1)*(5.*COS(ARG1)**2-3.)/ARG2*CONMF
      GO TO 16
   71 ARG2=U(1,J,1)**
      BX(1,J,1)=25.*CONMF*SIN(ARG1)*(63.*COS(ARG1)**4/2.-31.*COS(ARG1)
     1**2+1.5)/(4.*ARG2)
      BY(1,J,1)=7.5*CONMF*(63.*COS(ARG1)**4/2.-35.*COS(ARG1)**2+7.5)*
     1COS(ARG1)/(   ARG2)
   16 CONTINUE
      PRINT 15,(BX(1,J,1),J=1,I)
      PRINT 15,(BY(1,J,1),J=1,I)
   22 CONTINUE
C  FILL TIME-DEPENDENT ARRAYS
   24 US=U0
      F=0.0
      UT1=US
      DO 11 J=1,LMY
      Y=YC+(J-1)*DYT
      U(1,J,1) = 0.0
      IF (ISTST.EQ.1) GO TO 35
      UT2=UT1
      UT1=US
      US=2.*UT1-UT2
      DO 34 L=1,50
      UT=US
      FT=F
      US=UT-FT/(UT-(U0/YS**2)**(FI-1.)/UT**FI)
      F=US**2/2.+(U0/(U0*YS**2))**(FI-1.)/(FI-1.)-SQ/YS-C
      IF (ABS(US-UT)/UT.GT.1.E-5) GO TO 34
      IF (ABS(F).LT.1.E-5) GO TO 35
   34 CONTINUE
      PRINT 33
      CALL EXIT
   35 V(1,J,1)=US
      D(1,J,1)=U0/(US*Y(J)**2)
      P(1,J,1)=D(1,J,1)**FI
      GO TO 38
   35 D(1,J,1) = EXP(C1*(1./Y(J)  -1./YC))
      P(1,J,1) = D(1,J,1)
      V(1,J,1) = 0.0
   76 RADTN(J)=RADFN(P(1,J,1)*T0/D(1,J,1))*(D(1,J,1)-TC)**2*CFAD%
      RADTNC(1,J)=RADTN(J)
   78 DO 11 I=2,LMX
      V(I,J,1) = V(1,J,1)
      B(I,J,1) = 0.0
      RADTNC(I,J)=RADTN(J)
      D(I,J,1) = D(1,J,1)
   11 P(I,J,1) = P(1,J,1)
      DO 17 I=1,LMX
      ARG1=X(I)*BARG
      IF (FI*ABS(F).GT.7) ARG=ARG*(1-FI*I)
```

```
      IF (IMAGF.EQ.5) ARG1=ARG1-PIEC2
      IF (IMAGF.EQ.7) ARG1=ARG1-PIEC2
      DO 21 J=1,LMY
      GO TO (57,25,57,58,53,72,72),IMAGF
C  DIPOLE FIELD
   57 ARG2=Y(J)**3
      BX(I,J,1)=SIN(ARG1)/ARG2*CONMF
      IF(I.EQ.1.OR.I.EQ.LMX) GO TO 26
      AZB(I-1,J)=SIN(ARG1)/Y(J)**2*CONMF
      AZZ(I-1,J)=AZB(I-1,J)*Y(J)*SIN(ARG1)
   26 BY(I,J,1)=2.*COS(ARG1)/ARG2*CONMF
      GO TO 21
C  QUADRAPOLE FIELD
   25 ARG2=Y(J)**4
      BX(I,J,1)=2.*SIN(ARG1)*COS(ARG1)/ARG2
      IF (I.EQ.1.OR.I.EQ.LMX) GO TO 48
      AZB(I-1,J)=SIN(ARG1)*COS(ARG1)/Y(J)**3
      AZZ(I-1,J)=AZB(I-1,J)*Y(J)*SIN(ARG1)
   48 BY(I,J,1)=(3.*COS(ARG1)**2-1.)/ARG2
      GO TO 21
C  HEXAPOLE
   58 ARG2=Y(J)**5
      BX(I,J,1)=3.*SIN(ARG1)*(5.*COS(ARG1)**2-1.)/(4.*ARG2)*CONMF
      BY(I,J,1)=COS(ARG1)*(5.*COS(ARG1)**2-3.)/ARG2*CONMF
      IF (I.EQ.1.OR.I.EQ.LMX) GO TO 21
      AZB(I-1,J)=SIN(ARG1)*(5.*COS(ARG1)**2-1.)/(4.*Y(J)**4)*CONMF
      AZZ(I-1,J)=AZB(I-1,J)*Y(J)*SIN(ARG1)
      GO TO 21
C  DECAPOLE
   72 ARG2=Y(J)**7
      BX(I,J,1)=25.*CONMF*SIN(ARG1)*(63.*COS(ARG1)**4/2.-21.*COS(ARG1)**
     12+1.5)/(4.*ARG2)
      BY(I,J,1)=7.5*CONMF*COS(ARG1)*(63.*COS(ARG1)**4/2.-35.*COS(ARG1)**
     12+7.5)/(   ARG2)
      IF (I.EQ.1.OR.I.EQ.LMX) GO TO 21
      AZB(I-1,J)=CONMF*5.*(63.*COS(ARG1)**4/2.-21.*COS(ARG1)**2+1.5)*
     1SIN(ARG1)/(4.*Y(J)**6)
      AZZ(I-1,J)=AZB(I-1,J)*Y(J)*SIN(ARG1)
   21 CONTINUE
   27 IF (IPTFL.EQ.1) GO TO 30
C  RADII AT WHICH MS=1 AND MA=1
      PRINT 95
      LMXM1=LMX-1
      DO 87 I=2,LMXM1
      RSE1=Y0
      RAE1=Y0
      ISE1=1
      IAE1=1
      RMS2=V(I,1,1)/SQRT(P(I,1,1)/D(I,1,1))
      IF (RMS2.GE.1.) ISE1=2
      RMAZ=V(I,1,1)*SQRT(D(I,1,1)/(BX(I,1,1)**2+BY(I,1,1)**2))/AE0
      IF (RMAZ.GE.1.) IAE1=2
      DO 88 J=1,LMY
      GO TO (89,90) ,ISE1
   89 RMS1=RMS2
      RMS2=V(I,J,1)/SQRT(P(I,J,1)/D(I,J,1))
      IF (RMS2.LT.1.) GO TO 59
```


C-2

```
      ISE1=2
      RSE1=Y(J-1)+DYT*(1.-RMS1)/(RMS2-RMS1)
   90 GO TO (91,92),IAE1
   91 RMA1=RMA2
      RMA2=V(I,J,1)*SQRT(D(I,J,1)/(BX(I,J,1)**2+BY(I,J,1)**2))/AEC
      IF (RMA2.LT.1.) GO TO 8?
      IAE1=2
      RAE1=Y(J-1)+DYT*(1.-RMA1)/(RMA2-RMA1)
   92 IF (ISE1.EQ.2.AND.IAE1.EQ.2) GO TO 93
    ? CONTINUE
   93 PRINT 94,I,X(I),RSE1,RAE1
   97 CONTINUE
C  CREATE PLOT FILES
   36 IF (IPTVR.EQ.0) GO TO 41
      TIME=0.0
      LMXM1=LMX-1
      LMXM2=LMX-2
      GO TO (79,80),IPTVR
   79 ENCODE (12,42,IHD2) TIME
      WRITE (10) (IHD2(I),I=1,2),LMXM2,LMY,((P(I,J,1),D(I,J,1),
     1BX(I,J,1),BY(I,J,1),I=2,LMXM1),J=1,LMY),XMAX,Y0,YMAX,
     1(X(I),I=2,LMXM1),(Y(J),J=1,LMY)
      GO TO 41
   80 WRITE (10) TIME,                 LMXM2,LMY,((P(I,J,1),D(I,J,1),
     1BX(I,J,1),BY(I,J,1),I=2,LMXM1),J=1,LMY),XMAX,Y0,YMAX,
     1(X(I),I=2,LMXM1),(Y(J),J=1,LMY),((AZZ(I,J),I=1,LMXM2),J=1,LMY),
     2TO,DO,CRADN
   41 PRMO2=PI/RMO**2
      ARG2=ALO**2
      CHARDX=0.0
      CHARDY=0.0
      XMAX=XMAX*RAPDG
      DXT=DXT*RAPDG
      DXTP=DXTP*RAPDG
      DO 46 I=1,LMX
   46 X(I)=X(I)*RAPDG
      DO 15 I=1,LMX
      DO 15 J=1,LMY
      U(I,J,2) = U(I,J,1)
      V(I,J,2) = V(I,J,1)
      D(I,J,2) = D(I,J,1)
      BX(I,J,2)=BX(I,J,1)
      BY(I,J,2)=BY(I,J,1)
      P(I,J,2) = P(I,J,1)
      ARG1=PRMO2*P(I,J,1)/D(I,J,1)
      ABX2=ARO2*BX(I,J,1)**2/D(I,J,1)
      ABY2=ARO2*BY(I,J,1)**2/D(I,J,1)
      ARG2=ARG1+ABX2+ABY2
      CHARXT=
     1       (U(I,J,1)+SQRT(.5*(ARG2+SQRT(ARG2**2-4.*ARG1*ABX2))))/Y(J)
      IF(CHARXT.GT.CHARDX) CHARDX=CHARXT
      CHARYT=V(I,J,1)+SQRT(.5*(ARG2+SQRT(ARG2**2-4.*ARG1*ABY2)))
      IF (CHARYT.GT.CHARDY) CHARDY=CHARYT
   15 CONTINUE
      CHARXT=DXT/CHARDX
      CHARYT=DYT/CHARDY
      DTT=AMIN1(CHARXT,CHARYT)*CTRY
```

```
797.    00      C  CALCULATE INITIAL ENERGIES AND MASS
798.    00         AREAM1=0.0
799.    00         AREAM2=0.0
800.    00         AREAM=0.0
801.    00         AREAT1=0.0
802.    00         AREAT2=0.0
803.    00         AREAT=0.0
804.    00         AREAG1=0.0
805.    00         AREAG2=0.0
806.    00         AREAG=0.0
807.    00         AREAD1=0.0
808.    00         AREAD2=0.0
809.    00         AREAD=0.0
810.    00         IMXI=LMX-1
811.    00         BT21=BX(2,1,1)**2+BY(2,1,1)**2
812.    00         GRE1=D(2,1,1)/Y(1)
813.    00         DO 29 J=2,LMY
814.    00         BT22=BX(2,J,1)**2+BY(2,J,1)**2
815.    00         GRE2=D(2,J,1)/Y(J)
816.    00         AREAM1=AREAM1+.5*(BT21+BT22)*DYT
817.    00         AREAT1=AREAT1+.5*(P(2,J-1,1)+P(2,J,1))*DYT
818.    00         AREAG1=AREAG1+.5*(GRE1+GRE2)*DYT
819.    00         AREAD1=AREAD1+.5*(D(2,J-1,1)+D(2,J,1))*DYT
820.    00         BT21=BT22
821.    00      29 GRE1=GRE2
822.    00         DO 28 I=3,IMXI
823.    00         BT21=BX(I,1,1)**2+BY(I,1,1)**2
824.    00         GRE1=D(I,1,1)/Y(1)
825.    00         DO 30 J=2,LMY
826.    00         BT22=BX(I,J,1)**2+BY(I,J,1)**2
827.    00         GRE2=D(I,J,1)/Y(J)
828.    00         AREAM2=AREAM2+.5*(BT21+BT22)*DYT
829.    00         AREAT2=AREAT2+.5*(P(I,J-1,1)+P(I,J,1))*DYT
830.    00         AREAG2=AREAG2+.5*(GRE1+GRE2)*DYT
831.    00         AREAD2=AREAD2+.5*(D(I,J-1,1)+D(I,J,1))*DYT
832.    00         BT21=BT22
833.    00      30 GRE1=GRE2
834.    00         AREAM=AREAM+.5*(AREAM1+AREAM2)*DXT
835.    00         AREAT=AREAT+.5*(AREAT1+AREAT2)*DXT
836.    00         AREAG=AREAG+.5*(AREAG1+AREAG2)*DXT
837.    00         AREAD=AREAD+.5*(AREAD1+AREAD2)*DXT
838.    00         AREAM1=AREAM2
839.    00         AREAT1=AREAT2
840.    00         AREAM2=0.0
841.    00         AREAT2=0.0
842.    00         AREAG1=AREAG2
843.    00         AREAD1=AREAD2
844.    00         AREAG2=0.0
845.    00      28 AREAD2=0.0
846.    00         AREAMI=4.E5*PO**2*AREAM*RS**2
847.    00         AREATI=PO*RS**2*AREAT*PI/(PI-1.)*1.E5
848.    00         AREAGI=AREAG*GRA*SQRT*DT*PM*RS*1.E5/VO
849.    00         AREADI=AREAD*PO*PM*RS**2*1.E5
850.    00         AREADP=AREADI/PM
851.    00         PRINT 35,AREAMI,AREATI,AREAGI,AREADI,AREADP
852.    00         RETURN
853.    00         END
```

```
      00    *FORTRAN,D=PLIB,DN=LAXOCT,FL
      00          SUBROUTINE LAX(P1,N,DTTK, ILMX,IFFX,IFPY1,IFPY2)
      00          PARAMETER (IX7=39,IY7=51)
      00          COMMON X(IX7),Y(IY7),U(IX7,IY7,2),V(IX7,IY7,2),P(IX7,IY7,2),
      00         1P(IY7,IY7,2),LDISMY(IX7),PY(IX7,IY7,2),PX(IY7,IY7,2),AZE(IX7,IY7),
      00         2AZ2(IX7,IY7)
      00    C   WATCH DIMENSION OF ILMY IN COMMON/COBDRY/
      00          COMMON /COMX1/ YO,TO,DO,   IO,AO,RNO,PO,SO,TIC,YEND,DXT,DYT,XMAX,
      00         1YMAX,TAU,TMAX,DTP,RS,VO,WO,RO,ARO,AREAM,APE4T
      00          COMMON /COMX2/ LDISMX,LMX,LMY,ICHCK,IFULS,XMP,WMP,DTT,STDY,PI,DMP
      00          COMMON /COMLX/ ISMTH,S4TH,NTMSM,ILOWB
      00          COMMON/LAPID/ N1LAP,C2,ABO2,DTDX,DTDY,CHARDX,CHARDY,C3,ABO2
      00          COMMON /COBDRY/ LKEEP,ILMY(IY7),ILMYT
      00          COMMON /COMRDN/IRDTN,RADTN(IY7),CRADN,RADTNC(IX7,IY7)
      00          DIMENSION F(9,6),G(9,6),S(9,6),Q(9,6),GN(4,6),FN(4,6),GN(4,6),
      00         1SF(4,5),QT(5)
      00       67 FORMAT (/' *** NTMSM MUST BE .LE. 1 ***'/)
      00       57 FORMAT (5X'NNDEN =',I5)
      00       58 FORMAT (5X'NNPRE =',I5)
      00          IHS=0
      00          RADDG=.017453?
      00          LMXM1=LMX-1
      00          IF (X(LMXM1)/RADDG.GT.180.-1.E-2.AND.X(LMXM1)/RADDG.LT.180.+1.E-2)
      00         1IHS=1
      00          IF (ISMTH.EQ.0) GO TO 66
      00          IF (NTMSM.LE.0) GO TO 66
      00          PRINT 67
      00          NTMSM=0
      00       66 RNO2 = RNO**2
      00          ABO2=ABO**2
      00          ABOD2=ABO2/2.
      00          C1 = PI/((PI-1.)*RNO2)
      00          C2 = 1./((PI-1.)*RNO2)
      00          C3 = PI/RNO2
      00          DO 34 M=1,9
      00          F(M,4)=0.0
      00       34 G(M,5)=0.0
      00          DO 35 M=1,4
      00          FN(M,4)=0.)
      00       35 GN(M,5)=0.0
      00          N = 1
      00          N1 = 2
      00          DTTT=0.0
      00          EPSX = DXT**2
      00          EPSY = DYT**2
      00          IDFIX=0
      00          IFFIX=0
      00          IVFIX=0
      00          IFIXPD=1
      00          NNDEN=0
      00          NNPRE=0
      00          IFIXP=1
      00          NTMSMT=0
      00          DO 11 I=1,LMX
      00       11 ILMY(I)=0
      00          CRADI=0.0
      00          IF (IRDTN.EQ.2) CRADI=1.
```

```
      QRADN=C.0
      RETURN
      ENTRY LAX1(N1,N,DTTK,ILMX,IFPX,IFPY1,IFPY2)
      NILSF=N1
      DTDX = DTT/DXT
      DTDX4 = DTDX/4.
      DTDY = DTT/DYT
      DTDY4 = DTDY/4.
      DTZ = DTT/2.
      DTDX2 = DTDX/2.
      DTDY2 = DTDY/2.
      CHARGX=0.0
      CHARGY=0.0
      IF (ICHCK.EQ.1) GO TO 2
      IF (           ILFX.EQ.1) GO TO 25
      LDISMX = LDISMX+1
   25 LKEEP=LDISMX
      DO 10 L=2,LDISMX
      IF (ILMY(L).EQ.1) GO TO 10
      LDISMY(L) = LDISMY(L)+1
   10 CONTINUE
    2 DO 1 I=2,LDISMX
      IM = I-1
      IP = I+1
      LSUB = LDISMY(I)
      DO 1 J=2,LSUB
      JM = J-1
      JP = J+1
C  PREDICTOR STEP
C  CALCULATE F, G, S AND U=G AT THE GRID POINTS
      IF (J.EQ.2) GO TO 3
      DO 4 M=1,3
      M3 = M+3
      M6 = M+6
      DO 4 L=1,4
      F(M,L) = F(M3,L)
      G(M,L) = G(M3,L)
      Q(M,L) = Q(M3,L)
      S(M,L) = S(M3,L)
      F(M3,L) = F(M6,L)
      G(M3,L) = G(M6,L)
      S(M3,L) = S(M6,L)
    4 Q(M3,L) = Q(M6,L)
      M = 6
      LM = JP
      LP=JP
      LPP = 3
      GO TO 16
    3 M = 0
      LM = JM
      LP = JP
      LPP = 4
   16 DO 5 L=LM,LP
      DO 5 K=IM,IP
      M = M+1
      E1=C1*F(K,L,N)
      E2=P(K,L,N)+(U(K,L,N)**2+V(K,L,N)**2)/2.
```

```
      E3=E1+E2
      XPKP=X(K)
      IF (IHS.EQ.1.AND.K.EQ.LMXM1) XPKP=X(K-1)
      E4=1./TAN(XPKP)
      F(M,1)=D(K,L,N)*V(K,L,N)
      F(M,2)=F(M,1)*V(K,L,N)+P(K,L,N)/RHO2+ABOP2*(BX(K,L,N)**2-
     1BY(K,L,N)**2)
      IF (ILOWB.EQ.0) GO TO 69
      F(M,2)=F(M,2)+ABOD2*BY(K,L,N)**2
   69 CONTINUE
      F(M,3)=F(M,1)*U(K,L,N)-ABOZ*BY(K,L,N)*BX(K,L,N)
      F(M,5)=V(K,L,N)*BX(K,L,N)-U(K,L,N)*BY(K,L,N)
      F(M,6)=V(K,L,N)*E3+ABOZ*BX(K,L,N)*F(M,5)
      G(M,1)=D(K,L,N)*U(K,L,N)/Y(L)
      G(M,2)=G(M,1)*V(K,L,N)-ABOZ*BX(K,L,N)*BY(K,L,N)/Y(L)
      G(M,3)=G(M,1)*U(K,L,N)+(P(K,L,N)/RHO2+ABOD2*(BY(K,L,N)**2-
     1BX(K,L,N)**2))/Y(L)
      G(M,4)=(U(K,L,N)*BY(K,L,N)-V(K,L,N)*BX(K,L,N))/Y(L)
      G(M,5)=U(K,L,N)*E3/Y(L)+ABOZ*BY(K,L,N)*G(M,4)
      S(M,1)=-D(K,L,N)*(2.*V(K,L,N)+U(K,L,N)*E4)/Y(L)
      S(M,2)=-D(K,L,N)*(SO/Y(L)+2.*V(K,L,N)**2+V(K,L,N)*U(K,L,N)*E4-
     1U(K,L,N)**2)/Y(L)-ABOZ*(BX(K,L,N)**2-2.*BY(K,L,N)**2-BY(K,L,N)*
     2BX(K,L,N)*E4)/Y(L)
      IF (ILOWB.EQ.0) GO TO 70
      IF (K.NE.1.AND.K.NE.LMX) GO TO 200
      IF (K.EQ.1) DBTDT=(BX(2,L,N)-BX(1,L,N))/DXT
      IF (K.EQ.LMX) DBTDT=(BX(LMX,L,N)-BX(LMX-1,L,N))/DXT
      GO TO 201
  200 DBTDT=(BX(K+1,L,N)-BX(K-1,L,N))/(2.*DXT)
  201 S(M,2)=S(M,2)-ABOZ*(2.*BY(K,L,N)**2+BY(K,L,N)*BY(K,L,N)*E4+
     1BY(K,L,N)*DBTDT)/Y(L)
   70 CONTINUE
      S(M,3)=-G(M,1)*(3.*V(K,L,N)+U(K,L,N)*E4)+ABOZ*BX(K,L,N)*(3.*
     1BY(K,L,N)+BX(K,L,N)*E4)/Y(L)
      S(M,4)=-G(M,4)*E4
      S(M,5)=G(M,4)
      S(M,5)=-E3*(2.*V(K,L,N)+U(K,L,N)*E4)/Y(L)-SO*F(M,1)/Y(L)**2+
     1ABOZ*(-2.*V(K,L,N)*BX(K,L,N)**2-V(K,L,N)*BY(K,L,N)**2+V(K,L,N)*
     2BY(K,L,N)*BX(K,L,N)*E4+2.*U(K,L,N)*BY(K,L,N)*BX(K,L,N)-U(K,L,N)*
     3BY(K,L,N)**2*E4)/Y(L)+CRADI*(RADTN(L)-RADTNC(K,L))
      Q(M,1)=D(K,L,N)
      Q(M,2)=F(M,1)
      Q(M,3)=D(K,L,N)*U(K,L,N)
      Q(M,4)=BY(K,L,N)
      Q(M,5)=BX(K,L,N)
    5 Q(M,6)=C2*P(K,L,N)+E2+ABOD2*(BY(K,L,N)**2+BX(K,L,N)**2)
   36 CONTINUE
C   CALCULATE U=G, F, C AND S AT POINTS A, B, C AND D
      IF (J.EQ.2) GO TO 17
      DO 18 L=1,6
      FN(4,L) = FN(2,L)
      SN(4,L) = SN(2,L)
   18 GN(4,L) = GN(2,L)
   17 DO 6 L=1,6
      QN(1,L) = (Q(5,L)+Q(4,L))/2.-DTDX*(F(5,L)-G(4,L))-DTDY4*(F(7,L)+
     1F(8,L)-F(1,L)-F(2,L))+DT2*(S(5,L)+S(4,L))
      QN(2,L) = (Q(5,L)+Q(5,L))/2.-DTDX4*(G(9,L)+G(6,L)-G(7,L)-G(4,L))-
```

```
      1025.      00          1DTDY*(F(6,L)-F(5,L))+DT2*(S(6,L)+S(5,L))
      1026.      00           GN(3,L) = (G(6,L)+G(5,L))/2.-DTDX*(G(6,L)-G(5,L))-DTDY4*(F(6,L)+
      1027.      00          1F(9,L)-F(2,L)-F(3,L))-DT2*(S(6,L)+S(5,L))
      1028.      00           GN(4,L) = ((5,L)+S(2,L))/2.-DTDX4*(G(6,L)+G(9,L)-S(4,L)-G(1,L))-
      1029.      00          1DTDY*(F(5,L)-F(2,L))+DT2*(S(5,L)+S(2,L))
      1030.      00         6 CONTINUE
      1031.      00           DO 7 L=1,LPP
      1032.      00           IF (L.EQ.1.OR.L.EQ.3) Y2 =Y(J)**2
      1033.      00           IF (L.EQ.2) Y2=((Y(JP)+Y(J))/2.)**2
      1034.      00           IF (L.EQ.4) Y2=((Y(J)+Y(JM))/2.)**2
      1035.      00           YSQ=SQRT(Y2)
      1036.      00           GN(L,2) = GN(L,2)/GN(L,1)
      1037.      00           GN(L,3) = GN(L,3)/GN(L,1)
      1038.      00           GN(L,6) = (GN(L,6)-
      1039.      00          1           (GN(L,1)*(GN(L,2)**2+GN(L,3)**2           )+ABO2*(
      1040.      00          1GN(L,4)**2+GN(L,5)**2           ))/2.)/C2
      1041.      00           FN(L,1) = GN(L,1)*GN(L,2)
      1042.      00           GN(L,1) = GN(L,1)*GN(L,3)/YSQ
      1043.      00           BYBX2=GN(L,5)**2-GN(L,4)**2
      1044.      00           FN(L,2) = FN(L,1)*GN(L,2)+GN(L,6)/RNO2+ABOD2* BYBX2
      1045.      00           IF (ILOWB.EQ.0) GO TO 71
      1046.      00           FN(L,2)=FN(L,2)+ABOD2*GN(L,4)**2
      1047.      00         71 CONTINUE
      1048.      00           GN(L,2) =(FN(L,1)*GN(L,3)-ABO2*GN(L,5)*GN(L,4))/YSQ
      1049.      00           FN(L,3) = GN(L,2)*YSQ
      1050.      00           GN(L,3) = GN(L,1)*GN(L,3)+
      1051.      00          1                          (GN(L,6)/RNO2+ABOD2*(-BYBX2))/YSQ
      1052.      00           GN(L,4)=
      1053.      00          1       (GN(L,3)*GN(L,4)-GN(L,2)*GN(L,5))/YSQ
      1054.      00           FN(L,3)=-GN(L,4)*YSQ
      1055.      00           E1 = C1*GN(L,6)+GN(L,1)*(GN(L,2)**2+GN(L,3)**2           )/2.
      1056.      00           FN(L,6) = E1*GN(L,2)+ABO2* GN(L,5)*FN(L,5)
      1057.      00           GN(L,6) = E1*GN(L,3)/YSQ
      1058.      00          1                          +ABO2* GN(L,4)*GN(L,5)
      1059.      00           IF (L.EQ.2.OR.L.EQ.4) THZA=X(I)
      1060.      00           IF (IHS.EQ.1.AND.I.EQ.LAST) THZA=X(IP)
      1061.      00           IF (L.EQ.1) THZA=(X(I)+X(IP))/2.
      1062.      00           IF (L.EQ.3) THZA=(X(I)+X(IP))/2.
      1063.      00           THZA = 1./TAN(THZA)
      1064.      00           E2=2.*GN(L,2)+GN(L,3)*THZA
      1065.      00           SN(L,1)=-GN(L,1)*E2/YSQ
      1066.      00           SN(L,2)=-GN(L,1)*(SQ/YS.-2.*GN(L,2)**2+SN(L,2)*GN(L,3)*THZA-
      1067.      00          1GN(L,3)**2)/YSQ-ABO2*(GN(L,5)**2-2.*GN(L,4)**2-3N(L,4)*SN(L,5)*
      1068.      00          2THZA)/YSQ
      1069.      00           IF (ILOWB.EQ.0) GO TO 72
      1070.      00           SN(L,2)=SN(L,2)-ABO2*(2.*GN(L,2)**2+GN(L,4)*GN(L,5)*THZA+GN(L,4)*
      1071.      00          1(GN(2,5)-GN(1,5))/DXT)/YSQ
      1072.      00         72 CONTINUE
      1073.      00           SN(L,3)=-SN(L,1)*(3.*GN(L,2)+GF(L,3)*THZA)+ABO2*GN(L,5)*(3.*
      1074.      00          1GN(L,4)+SN(L,5)*THZA)/YSQ
      1075.      00           SN(L,4)=-SN(L,4)*THZA
      1076.      00           SN(L,5)=SN(L,4)
      1077.      00           IF (IFOTN,NE.2) GO TO 7
      1078.      00           IF (L.NE.1) GO TO 21
      1079.      00           SNAJ=FADY(J)-(RFDYNC(IP,J)+RADYNC(I,J))/2.
      1080.      00           GO TO 7
      1081.      00         21 IF (L.NE.2) GO TO 22
```

```
1082.   00          GRADX=(RADTM(JP)+RADTM(J))/2.-(RADTMC(I,JP)+RADTMC(I,J))/2.
1083.   00          GO TO 7
1084.   00       22 IF (L.NE.3) GO TO 23
1085.   00          GRADX=(RADTM(J)-(RADTMC(I,J)+RADTMC(IP,J))/2.
1086.   00          GO TO 7
1087.   00       23 IF (L.NE.4) GO TO 7
1088.   00          GRADX=(RADTM(JM)+RADTM(J))/2.-(RADTMC(I,JM)+RADTMC(I,J))/2.
1089.   00        7 SN(L,6)=-E1+E2/YSQ-SQ+FN(L,1)/YZ+AHD2*(-2.*GN(L,2)*GN(L,5)**2+
1090.   00         1GN(L,2)*GN(L,4)**2+GN(L,2)*GN(L,4)*GN(L,5)*THZA+2.*GN(L,3)*
1091.   00         2GN(L,4)+GN(L,5)-GN(L,3)*GN(L,4)**2*THZA)/YSQ*GRADN
1092.   00    C  CORRECTOR STEP
1093.   00          DO 9 L=1,6
1094.   00        9 DT(L) = -DTDX2*((G(6,L)-G(4,L))/2.+GN(3,L)-GN(1,L))-DTDY2*((
1095.   00         1F(6,L)-F(2,L))/2.+FN(2,L)-FN(4,L))+DT2*(S(5,L)+(SN(1,L)+SN(2,L)+
1096.   00         2SN(3,L)+SN(4,L))/4.)
1097.   00          D(I,J,N1) = D(I,J,N)+DT(1)
1098.   00          IF(IFIXPD.EQ.0) GO TO 29
1099.   00          IF (D(I,J,N1).GT.1.E-5) GO TO 29
1100.   00          DNEW = .5*(D(I,J-1,N1)+D(I,J+1,N1))
1101.   00          ANDER=ANDER+1
1102.   00          IF (IDFIX.EQ.0) GO TO 37
1103.   00          WRITE (IO,35) D(I,J,N1),DNEW,I,J
1104.   00       35 FORMAT (' D.LT.1.E-10',2E12.3,2I5)
1105.   00       37 D(I,J,N1) = DNEW
1106.   00       29 V(I,J,N1) = (Q(5,2)+QT(2))/D(I,J,N1)
1107.   00          U(I,J,N1) = (Q(5,3)+QT(3))/D(I,J,N1)
1108.   00          BY(I,J,N1)=G(5,4)+QT(4)
1109.   00          BX(I,J,N1)=F(5,5)+QT(5)
1110.   00          P(I,J,N1) = (Q(5,6)+QT(6)
1111.   00         1              -D(I,J,N1)*(U(I,J,N1)**2+V(I,J,N1)**2              )/2.
1112.   00         2-AB0D2*(BX(I,J,N1)**2+BY(I,J,N1)**2              ))/C2
1113.   00          IF(IFIXPD.EQ.0) GO TO 31
1114.   00          IF (P(I,J,N1).GT.1.E-5) GO TO 31
1115.   00          PNEW = .5*(P(I,J-1,N1)+P(I,J+1,N1))
1116.   00          NPRE =NPRE+1
1117.   00          IF (IPFIX.EQ.0) GO TO 39
1118.   00          WRITE (IO,32) P(I,J,N1),PNEW,I,J
1119.   00       32 FORMAT (' P.LT.1.E-10',2E12.3,2I5)
1120.   00       39 P(I,J,N1) = PNEW
1121.   00    C  CALCULATE MAGNETIC POTENTIAL
1122.   00       31 IF (ISMTH.EQ.0) GO TO 49
1123.   00          AZB(IM,J)=AZB(IM,J)+DT2*F(5,5)
1124.   00          GO TO 63
1125.   00       49 AZB(IM,J)=AZB(IM,J)+DT2*(F(5,5)+V(I,J,N1)*BX(I,J,N1)-U(I,J,N1)*
1126.   00         1BY(I,J,N1))
1127.   00    C  FIND NEW TIME STEP
1128.   00       63 ARG1=C3*P(I,J,N1)/D(I,J,N1)
1129.   00          ABX2=AB02*BX(I,J,N1)**2/D(I,J,N1)
1130.   00          ABY2=AB02*BY(I,J,N1)**2/D(I,J,N1)
1131.   00          ARG2=ARG1+ABX2+ABY2
1132.   00          CHARXT=           SQRT(.5*(ARG2+SQRT(ABS(ARG2**2-4.*ARG1*ABX2))))
1133.   00          SIGNC=1.
1134.   00          IF(U(I,J,N1).LT.0.0) SIGNC=-1.
1135.   00          CHARXT=
1136.   00         1      (SIGNC*U(I,J,N1)+CHARXT)/X(I)
1137.   00          IF(CHARXT.GT.CHARDX) CHARDX=CHARXT
1138.   00          CHARYT=           SQRT(.5*(ARG2+SQRT(ABS(ARG2**2-4.*ARG1*ABY2))))
```

```
1139.          00            SIGNC=1.
1140.          00            IF(V(I,J,N1).LT.0.0) SIGNC=-1.
1141.          00            CHARYT=SIGNC*V(I,J,N1)+CHARYT
1142.          00            IF(CHARYT.GT.CHARDY) CHARDY=CHARYT
1143.          00          1 CONTINUE
1144.          00            IF(RNDEN.EQ.0) GO TO 39
1145.          00            PRINT 57,RNDEN
1146.          00            NNDEN=0
1147.          00         39 IF (RNPRE.EQ.0.0) GO TO 40
1148.          00            PRINT 58,RNPRE
1149.          00            RNPRE=0
1150.          00      C  SMOOTHING
1151.          00         40 IF (ISMTH.EQ.0                ) GO TO 56
1152.          00            NTMSMT=NTMSPT+1
1153.          00            IF (NTMSMT.LT.NTMSM) GO TO 56
1154.          00            NTMSMT=0
1155.          00            CALL LAPSMH(ILMX)
1156.          00         56 DTTM = DTT
1157.          00            CHARXT=DXT/CHARDX
1158.          00            CHARYT=DYT/CHARDY
1159.          00            DTT=AMIN1(CHAPXT,CHARYT)*STMY
1160.          00      C  RADIATION
1161.          00            IF (IRDTN.NE.2) GO TO 29
1162.          00            DO 12 I=2,LDISMX
1163.          00            LSUB=LDISMY(I)+1
1164.          00            DO 12 J=1,LSUB
1165.          00         12 RADTNC(I,J)=RADFN(P(I,J,N1)*TO/D(I,J,NT))*(D(I,J,N1)*DO)**2*CRADN
1166.          00            LSUB=LDISMY(1)+1
1167.          00            DO 15 J=1,LSUB
1168.          00         15 RADTNC(1,J)=RADTNC(2,J)
1169.          00            LSUB=LDISMY(LDISMX)+1
1170.          00            LSUB1=LDISMX+1
1171.          00            DO 19 J=1,LSUB
1172.          00         19 RADTNC(LSUB1,J)=RADFN(P(LSUB1,J,N)*TO/D(LSUB1,J,N))*(D(LSUB1,J,N)*
1173.          00           1DO)**2*CRADN
1174.          00         20 IF (N.EQ.1) GO TO 13
1175.          00            N = 1
1176.          00            N1 = 2
1177.          00            GO TO 14
1178.          00         13 N = 2
1179.          00            N1 = 1
1180.          00         14 RETURN
1181.          00            END
1182.          00            SUBROUTINE LAPSMH(ILMX)
1183.          00            PARAMETER (IX7=39,IY7=51)
1184.          00            COMMON X(IX7),Y(IY7),D(IX7,IY7,2),V(IX7,IY7,2),P(IX7,IY7,2),
1185.          00           1P(IX7,IY7,2),LDISMY(IX7),RY(IX7,IY7,2),RX(IX7,IY7,2),AZP(IX7,IY7),
1186.          00           2AZZ(IX7,IY7)
1187.          00            COMMON /CONST/ LDISMX,LMX,LMY,ICHCK,IPULS,XMP,WMP,DYY,STEY,PI,DPP
1188.          00            COMMON /CONLK/ ISMTH,SMTH,NTMSM,ILOWS
1189.          00            COMMON/LAPCT/ N1LAP,C2,A2DC2,DTDX,DTDY,CHARDX,CHARDY,C3,A3C2
1190.          00            NT=NTLAP
1191.          00            N=N1
1192.          00      C  SMOOTHING IN X-DIRECTION
1193.          00            DTZ=DTT/2.
1194.          00            DTYC=DTDY*SMTH
1195.          00            DO 1 I=2,LDISMX
```

```
      U1=B(I,1,M)
      U1P=B(I,2,M)
      U2=B(I,1,M)*V(I,1,M)
      U2P=B(I,2,M)*V(I,2,M)
      U3=B(I,1,M)*U(I,1,M)
      U3P=B(I,2,M)*U(I,2,M)
      U5=BX(I,1,M)
      U5P=BX(I,2,M)
      U4=BY(I,1,M)
      U4P=BY(I,2,M)
      U6=C2*P(I,1,M)+B(I,1,M)*(U(I,1,M)**2+V(I,1,M)**2              )/2.
     1+ABOD2*(BX(I,1,M)**2+BY(I,1,M)**2)
      U6P=C2*P(I,2,M)+B(I,2,M)*(U(I,2,M)**2+V(I,2,M)**2              )/2.
     1+ABOD2*(BX(I,2,M)**2+BY(I,2,M)**2)
      DVP=ABS(V(I,2,M)-V(I,1,M))
      LSUB=LDIS*Y(I)
      DO 1 J=2,LSUB
      JM=J-1
      JP=J+1
      DVM=DVP
      DVP=ABS(V(I,JP,M)-V(I,J,M))
      U1M=U1
      U1=U1P
      U1P=B(I,JP,M)
      B(I,J,M)=B(I,J,M)+DTYC*(DVP*(U1P-U1)-DVM*(U1-U1M))
      U2M=U2
      U2=U2P
      U2P=U1P*V(I,JP,M)
      V(I,J,M)=(U2+DTYC*(DVP*(U2P-U2)-DVM*(U2-U2M)))/B(I,J,M)
      U3M=U3
      U3=U3P
      U3P=U1P*U(I,JP,M)
      U(I,J,M)=(U3+DTYC*(DVP*(U3P-U3)-DVM*(U3-U3M)))/B(I,J,M)
      U4M=U4
      U4=U4P
      U4P=BY(I,JP,M)
      BY(I,J,M)=BY(I,J,M)+DTYC*(DVP*(U4P-U4)-DVM*(U4-U4M))
      U5M=U5
      U5=U5P
      U5P=BX(I,JP,M)
      BX(I,J,M)=BX(I,J,M)+DTYC*(DVP*(U5P-U5)-DVM*(U5-U5M))
      U6M=U6
      U6=U6P
      U6P=C2*P(I,JP,M)+U1P*(U(I,JP,M)**2+V(I,JP,M)**2)
     1/2.+ABOD2*(U4P**2+U5P**2)
    1 P(I,J,M)=(U6+DTYC*(DVP*(U6P-U6)-DVM*(U6-U6M))-B(I,J,M)*(
     1U(I,J,M)**2+V(I,J,M)**2              )/2.-ABOD2*(BX(I,J,M)**2+
     2BY(I,J,M)**2              ))/C2
C  SMOOTHING IN X-DIRECTION
      DTYC=DTDX*SMTH
      JMAX=0
      DO 2 I=2,LDISMX
      IF (LDIS*Y(I).GT.JMAX) JMAX=LDIS*Y(I)
    2 CONTINUE
      IMAX=LDIS*X
      DO 3 J=2,JMAX
      U1=B(1,J,M)
```

```
      U1P=D(2,J,M)
      U2=D(1,J,M)*V(1,J,M)
      U2P=D(2,J,M)*V(2,J,M)
      U3=D(1,J,M)*U(1,J,M)
      U3P=D(2,J,M)*U(2,J,M)
      U5=BX(1,J,M)
      U5P=BX(2,J,M)
      U4=BY(1,J,M)
      U4P=BY(2,J,M)
      U6=C2*P(1,J,M)+D(1,J,M)*(U(1,J,M)**2+V(1,J,M)**2                    )/2.
     1+ABOD2*(BX(1,J,M)**2+BY(1,J,M)**2)
      U6P=C2*P(2,J,M)+D(2,J,M)*(U(2,J,M)**2+V(2,J,M)**2                   )/2.
     1+ABOD2*(BX(2,J,M)**2+BY(2,J,M)**2)
      DVP=ABS(U(2,J,M)-U(1,J,M))
      DO 3 I=2,IMAX
      IF (I.LT.IMAX) GO TO 7
      IMAX=IMAX-1
      GO TO 3
    7 IM=I-1
      IP=I+1
      DVM=DVP
      DVP=ABS(U(IP,J,M)-U(I,J,M))
      U1M=U1
      U1=U1P
      U1P=D(IP,J,M)
      D(I,J,M)=D(I,J,M)+DTYC*(DVP*(U1P-U1)-DVM*(U1-U1M))
      U2M=U2
      U2=U2P
      U2P=U1P*V(IP,J,M)
      V(I,J,M)=(U2+DTYC*(DVP*(U2P-U2)-DVM*(U2-U2M)))/D(I,J,M)
      U3M=U3
      U3=U3P
      U3P=U1P*U(IP,J,M)
      U(I,J,M)=(U3+DTYC*(DVP*(U3P-U3)-DVM*(U3-U3M)))/D(I,J,M)
      U4M=U4
      U4=U4P
      U4P=BY(IP,J,M)
      BY(I,J,M)=BY(I,J,M)+DTYC*(DVP*(U4P-U4)-DVM*(U4-U4M))
      U5M=U5
      U5=U5P
      U5P=BX(IP,J,M)
      BX(I,J,M)=BX(I,J,M)+DTYC*(DVP*(U5P-U5)-DVM*(U5-U5M))
      U6M=U6
      U6=U6P
      U6P=C2*P(IP,J,M)+U1P*(U(IP,J,M)**2+V(IP,J,M)**2)
     1/2.*ABOD2*((IP**2+U6P**2)
      P(I,J,M)=(U6+DTYC*(DVP*(U6P-U6)-DVM*(U6-U6M))-D(I,J,M)*(
     1U(I,J,M)**2+V(I,J,M)**2                    )/2.-ABOD2*(BX(I,J,M)**2+
     2BY(I,J,M)**2                    ))/C2
C  CALCULATE THE MAGNETIC POTENTIAL
      AZ(IM,J)=AZ(IM,J)+DT2*(V(I,J,M1)*EX(I,J,M1)-U(I,J,M1)*
     1BY(I,J,M1))
C  FIND NEW TIME STEP
      ARG1=C2*D(I,J,M1)/D(I,J,M1)
      ARX2=ABOD2*BX(I,J,M1)**2/D(I,J,M1)
      ARY2=ABOD2*BY(I,J,M1)**2/D(I,J,M1)
      ARG2=ARG1+ARX2+ARY2
```

```
      CHARXT=          SQRT(.5*(ARG2+SQRT(ABS(ARG2**2-4.*ARG1*ABX2))))
      SIGNC=1.
      IF(U(I,J,N1).LT.0.0) SIGNC=-1.
      CHARXT=
     1        (SIGNC*U(I,J,N1)+CHARXT)/Y(J)
      IF(CHARXT.GT.CHARDX) CHARDX=CHARXT
      CHARYT=          SQRT(.5*(ARG2+SQRT(ABS(ARG2**2-4.*ARG1*ABY2))))
      SIGNC=1.
      IF(V(I,J,N1).LT.0.0) SIGNC=-1.
      CHARYT=SIGNC*V(I,J,N1)+CHARYT
      IF(CHARYT.GT.CHARDY) CHARDY=CHARYT
    3 CONTINUE
      RETURN
      END
      FUNCTION RADFN(TS)
      DIMENSION T(49),G(49)
      DATA T/9.2E3,1.E4,1.05E4,1.15E4,1.25E4,1.45E4,1.65E4,2.E4,2.2E4,
     12.3E4,2.45E4,2.E4,3.5E4,4.1E4,4.9E4,5.6E4,6.17E4,7.2E4,8.5E4,
     21.1E5,1.3E5,1.65E5,1.9E5,2.17E5,2.63E5,3.35E5,3.95E5,5.3E5,
     36.9E5,4.7E5,5.63E5,6.2E5,6.9E5,7.4E5,8.07E5,9.07E5,1.06E6,1.3E6,
     41.75E6,2.25E6,3.1E6,4.3E6,7.03E6,9.55E6,1.25E7,2.23E7,3.7E7,
     56.02E7,1.E8/
      DATA G/1.1E-24,3.6E-24,8.05E-24,1.6E-23,3.5E-23,5.25E-23,
     18.75E-23,1.1E-22,1.07E-22,9.5E-23,8.3E-23,1.E-22,1.3E-22,1.65E-22,
     22.25E-22,3.15E-22,4.3E-22,6.05E-22,7.25E-22,8.04E-22,8.35E-22,
     38.3E-22,9.3E-22,1.02E-21,1.E-21,8.5E-22,7.6E-22,6.02E-22,5.1E-22,
     44.7E-22,4.2E-22,3.2E-22,2.84E-22,1.9E-22,1.24E-22,9.3E-23,
     57.3E-23,6.E-23,5.7E-23,5.3E-23,4.9E-23,3.75E-23,2.4E-23,1.9E-23,
     61.7E-23,1.9E-23,2.25E-23,2.9E-23,3.47E-23/
    3 FORMAT (3X'*** T.GT.1.E8, RADIATION EXTRAPOLATED ***')
      IF (TS.GE.T(1)) GO TO 1
      RADFN=0.0
      RETURN
    1 IF (TS.LT.T(49)) GO TO 2
      PRINT 3
      RADFN=G(47)+(G(49)-G(47))*(TS-T(47))/(T(49)-T(47))
      RETURN
    2 DO 4 I=1,48
      IP=I+1
      IF (TS.GE.T(I).AND.TS.LT.T(IP)) GO TO 5
    4 CONTINUE
    5 RADFN=G(I)+(G(IP)-G(I))*(TS-T(I))/(T(IP)-T(I))
      RETURN
      END
*FORTRAN,D=PLI2,DN=PULSC1,FL
      SUBROUTINE PULSIN(IENDT,IIM,IF,YMXP1,YMXP2,LMAPY,LMPY1,TALT)
C  CALCULATE INITIAL PULSE
      PARAMETER (IX7=39,IY7=51)
      COMMON X(IX7),Y(IY7),U(IX7,IY7,2),V(IX7,IY7,2),R(IX7,IY7,2),
     1P(IX7,IY7,2),LDISMY(IX7),DY(IX7,IY7,2),EK(IX7,IY7,2),AZE(IX7,IY7),
     2AZZ(IX7,IY7)
      COMMON /COMM1/ YL,T0,DO,  IO,FC,RRC,PO,SC,TIC,YEND,DXT,DYT,XMAX,
     1YMAX,TAU,TMAX,DTF,RS,VO,RO,PC,AEO,AREAF,AREAT
      COMMON /COMM2/ LDISMX,LMX,LMY,ICHCK,IPULS,XMP,RMF,DTT,STAY,PI,BPF
      COMMON /COMP3/ INXPU,IMXPU
      DIMENSION EXK(IX7),EYK(IX7)
    3 FORMAT ( / 10X17H***************** / 10X1H*,' INITIAL PULSE ',1H*
```

```
00        1/ 10X17H*****************  )
00     12 FORMAT ( / 6X'T-DEG'11X'DT'12X'DD')
00      4 FORMAT(3E14.3)
00     17 FORMAT (5X'DTT REDUCED FROM',E10.3,' TO',E10.3,' IN PULSIN')
00     13 FORMAT (/5X'*** NEED LARGER XMAX IN PULSIN ***')
00     16 FORMAT (/6X'T-DEG'10X'DET'11X'DER')
00   C
00   C  NOTE - IF PUT IN TIME-DEPENDENT PULSE, NEED CHANGES IN BBRY
00   C
00        CHARDX=1.E-10
00        CHARDY=1.E-10
00        PIE = 3.14159
00        RAPDG=.0174533
00        ABO2=ABO**2
00        C3=PI/RNG**2
00        DTINC=XMXPT/TIO
00        ITHPU=0
00        WRITE (IO,3)
00      5 IENDT=1
00        GO TO (8,8,9),IPULS
00      8 WRITE (IO,12)
00        GO TO 15
00      9 PRINT 16
00     15 XMP=(XMP-90.)*RAPDG
00        IF (IPULS.EQ.3) GO TO 2
00        XDIV=XMP/19.
00        DO 13 I=1,20
00        XCP = (I-1)*XDIV
00        XCPN=(XCP+PIE/2.)/RAPDG
00        C1 = COS(PIE*XCP/(XMP*2.))
00        VCP=1.+(VMP-1.)*C1
00        DCP=1.+(DMP-1.)*C1
00        IF (IPULS.EQ.2) VCP=-VMP*C1
00        IF (IPULS.EQ.2) VCP=VMP*C1
00        IF (IPULS.EQ.2) DCP=-DMP      *SIN(PIE*XCP/(XMP*2.))
00        WRITE (IO,4)XCPN,VCP,DCP
00     13 CONTINUE
00      2 DMP=DMP*1.E5/PS
00        DO 20 I=2,LMX
00        THTA=X(I)-PIE/2.
00        IF (THTA.GT.XMP) GO TO 34
00        RR=SQRT((SIN(THTA))**2+(ABS(DMP-1.+COS(THTA)))**2)
00        ALPA=ASIN(SIN(THTA)/RR)
00        PHIA=THTA+PIE/2.-ALPA
00        IF (COS(THTA).LT.(1.-DMP)) PHIA=THTA-PIE/2.+ALPA
00        BAC=DMP*WCP/RR
00        BAT=BAC*SIN(PHIA)
00        BAR=BAC*COS(PHIA)
00        XCPN=X(I)/RAPDG
00        PRINT  4,XCPN,BAT,BAR
00     20 CONTINUE
00     14 CONTINUE
00        IF (DTT.LT.DTINC) GO TO 24
00     27 TTST=TI+DTT
00        IF (TTST.GT.DTINC) TTST=DTINC
00        TCNST=TTST/DTINC
00        GO TO 26
```

```
1424.          00          24 TCNST=1.
1425.          00          26 J=1
1426.          00             N1=IP
1427.          00             DO 14 I=1,LMX
1428.          00             II=I
1429.          00             XRAD=X(I)-PIE/2.
1430.          00             IF (XRAD.ST.XMP) GO TO 1C
1431.          00             C1 = COS(PIE*XRAD/(XMP*2.))
1432.          00             GO TO (21,22,22),IPULS
1433.          00          21 D(I,1,1) = 1.+(DMP-1.)*C1*TCNST
1434.          00             D(I,2,2) = D(I,1,1)
1435.          00             P(I,1,1)=D(I,1,1)*(1.+(DMP-1.)*C1*TCNST)
1436.          00             P(I,1,2)=P(I,1,1)
1437.          00             GO TO 23
1438.          00          22 IF (ITHRU.EQ.0) DXK(I)=PX(I,1,1)
1439.          00             IF (IPULS.EQ.2) GO TO 32
1440.          00             PX(I,1,2)=DXK(I)-AMP      *C1*TCNST
1441.          00             PX(I,1,1)=DXK(I)+AMP      *C1*TCNST
1442.          00             GO TO 33
1443.          00          32 THTA=X(I)-PIE/2.
1444.          00             RR=SQRT((SIN(THTA))**2+(ABS(DMP-1.+COS(THTA)))**2)
1445.          00             ALPA=ASIN(SIN(THTA)/RR)
1446.          00             PHIA=THTA+PIE/2.-ALPA
1447.          00             IF (COS(THTA).LT.(1.-DMP)) PHIA=THTA-PIE/2.+ALPA
1448.          00             BAO=DMP**MP/RR
1449.          00             BAT=BAO*SIN(PHIA)
1450.          00             BAP=BAO*COS(PHIA)
1451.          00             PX(I,1,1)=DXK(I)+BAT*TCNST
1452.          00          33 PX(I,1,2)=PX(I,1,1)
1453.          00             IF (ITHRU.EQ.0) PYK(I)=PY(I,1,1)
1454.          00             IF (IPULS.EQ.2) GO TO 30
1455.          00             PY(I,1,1)=PYK(I)-DMP         *SIN(PIE*XRAD/(2.*XMP))*TCNST
1456.          00             GO TO 31
1457.          00          30 PY(I,1,1)=PYK(I)-BAP*TCNST
1458.          00          31 PY(I,1,2)=PY(I,1,1)
1459.          00          23 ARG1=C1*D(I,J,N1)/D(I,J,N1)
1460.          00             ABX2=AB02*PX(I,J,N1)**2/D(I,J,N1)
1461.          00             ABY2=AB02*BY(I,J,N1)**2/D(I,J,N1)
1462.          00             ARG2=ARG1+ABX2+ABY2
1463.          00             GO TO 35
1464.          00             CHARXT=          SQRT(.5*(ARG2+SQRT(ABS(ARG2**2-4.*ARG1*ABX2))))
1465.          00             SIGNC=1.
1466.          00             IF(U(I,J,N1).LT.0.0) SIGNC=-1.
1467.          00             CHARXT=
1468.          00            1       (SIGNC*U(I,J,N1)+CHARXT)/Y(J)
1469.          00             IF(CHARXT.GT.CHARDX) CHARDX=CHARXT
1470.          00          35 CONTINUE
1471.          00             CHARYT=          SQRT(.5*(ARG2+SQRT(ABS(ARG2**2-4.*ARG1*ABY2))))
1472.          00             SIGNC=1.
1473.          00             IF(V(I,J,N1).LT.0.0) SIGNC=-1.
1474.          00             CHARYT=SIGNC*V(I,J,N1)+CHARYT
1475.          00             IF(CHARYT.GT.CHARDY) CHARDY=CHARYT
1476.          00          14 CONTINUE
1477.          00          18 CHARXT=DXT/CHARDX
1478.          00             CHARYT=DYT/CHARDY
1479.          00             DTTT=AMIN1(CHARXT,CHARYT)*STBY
1480.          00             IF (DTTT.GE.DTT) GO TO 4
```

```
00          WRITE (10,15) DTT,DTTT
00          DTT = DTTT
00        6 I=II
00          ITHRU=ITHRU+1
00          IF (ITHRU.GT.1) RETURN
00          LDISMX = I
00          LKP = I-1
00          IYXPU=LKP
00          IF ((XXP+PIE/2.).GT.X(LMX)) LDISMX=LMX-1
00          DO 5 I=1,LMX
00        5 LDISMY(I)=1
00          RETURN
00          ENTRY PULSIA(IEND1,TIM,IP,YMXP1,YMXP2,LMXPY,LMXPYT,TAU1)
00          IF (TIM+DTT.GT.DTINC) GO TO 25
00          GO TO 27
00       25 IF (TIM.LT.TAU) RETURN
00          IEND1=2
00          DO 1 I=1,LKP
00          GO TO (10,11),IPULS
00       10 P(I,1,1)=1.
00          P(I,1,2)=1.
00          D(I,1,1)=1.
00          D(I,1,2)=1.
00          GO TO 1
00       11 BX(I,1,1)=BXK(I)
00          BX(I,1,2)=BX(I,1,1)
00          BY(I,1,1)=BYK(I)
00          BY(I,1,2)=BY(I,1,1)
00        1 CONTINUE
00          RETURN
00          END
00    *FORTRAN,D=PLIB,DN=BDRYC1,FL
00          SUBROUTINE BDRY(N,NTIME,IBDRY,ILMX,TIM,N1,LMXPY)
00          PARAMETER (IX7=79,IY7=51)
00          COMMON X(IX7),Y(IY7),U(IX7,IY7,2),V(IX7,IY7,2),P(IX7,IY7,2),
00         1P(IX7,IY7,2),LDISMY(IX7),BY(IX7,IY7,2),BX(IX7,IY7,2),AZP(IX7,IY7),
00         2AZZ(IX7,IY7)
00          COMMON /COMM1/ Y0,T0,D0,   I0,A0,RHO,P0,S0,TIC,YEND,DXT,DYT,XMAX,
00         1YMAX,TAU,TMAX,DTP,RS,V0,X0,B0,AB0,AREAK,AREAT
00          COMMON /COMM2/ LDISMX,LMX,LMY,ICHCK,IPULS,XPP,XPP,DTT,STBY,PI,DPP
00          COMMON /COMM3/ IYXPU,IMXPU
00          COMMON /COMBDY/IBDY
00       25 FORMAT (' IVLIM =',I3)
00        5 FORMAT (5X'RL1.GT.0 IN BDRY')
00        4 FORMAT (5X'DTT REDUCED FROM',E10.3,' TO',E10.3,' FOR TIME CYCLE NO
00         *',I5)
00       10 FORMAT (' R.LT.1.E-10 AT BOUNDARY',2E10.3,I5)
00          C1 = SQRT(PI)/RHO
00          C5 = RHO*SQRT(PI)
00          C11 = C1**2
00          C6 = 1./(2.*DX)
00          A=C1*A30**2
00          IEXTR=0
00          DELP=P(1,1,1)-P(1,2,1)
00          DELD=D(1,1,1)-D(1,2,1)
00          RETURN
00          ENTRYBDRY1(N,NTIME,IBDRY,ILMX,TIM,N1,LMXPY)
```

```
      IF (IBDRY.EQ.0.AND.IRBDY.EQ.0) RETURN
      IVLIM=0
      LSUB=LDIS+X
      DTSY = DTT/DYY
      DT2=DTT/2.
      C4 = SC*DTT/Y(1)**2
      CHARDX=1.E-10
      CHARDY=1.E-10
      DO 1 I=1,LSUB
      ICHDY=
      IF (IBDRY.EQ.0) GO TO 20
      U (I,1,N)=U (I,2,N)
      IF (IEXTR.EQ.0) GO TO 19
      IF (U (I,2,N).GT.U (I,3,N).AND.U (I,3,N).GT.U (I,4,N).OR.
     1U (I,2,N).LT.U (I,3,N).AND.U (I,3,N).LT.U (I,4,N)) U (I,1,N)=
     2.+U (I,2,N)-U (I,3,N)
   19 IVRD=0
      IPRS=0
      IDNS=0
      GO TO (15,8,16,8,8,23,23),IBDRY
   15 IVRD=1
      GO TO 17
    8 IF (I.GT.IMXPU) GO TO 13
      IVRD=1
      IF (IBDRY.EQ.2) GO TO 17
      IF (IBDRY.EQ.4.AND.TIM.LT.TAU) GO TO 17
      IF (IBDRY.EQ.5.AND.TIM.LT.TAU) GO TO 17
      V(I,1,N)=0.0
      IVRD=0
      GO TO 17
   13 IPRS=1
      IDNS=1
      IF (IBDRY.EQ.5) IVRD=1
      GO TO 17
   16 IVRD=1
      IF (I.GT.IMXPU) GO TO 13
      IF (TIM.GT.TAU) GO TO 13
      GO TO 17
   23 IF (IBDRY.EQ.6) IVRD=1
      IF (IBDRY.EQ.7.AND.I.LE.IMXPL) IVRD=1
      IF (IPLLS.EQ.2.OR.IPLLS.EQ.3) GO TO 32
      IF (I.LE.IMXPU.AND.TIM.LT.TAU) GO TO 17
   32 IPRS=1
      IDNS=1
   17 IF (IPRS.EQ.0) GO TO 18
      P (I,1,N)=P (I,2,N)+DELP
      IF (IEXTR.EQ.0) GO TO 14
      IF (P (I,2,N).GT.P (I,3,N).AND.P (I,3,N).GT.P (I,4,N).OR.
     1P (I,2,N).LT.P (I,3,N).AND.P (I,3,N).LT.P (I,4,N)) P (I,1,N)=
     22.*P (I,2,N)-P (I,3,N)
   18 IF (IDNS.EQ.0) GO TO 20
      D (I,1,N)=D (I,2,N)*DELD
      IF (IEXTR.EQ.0) GO TO 21
      IF (D (I,2,N).GT.D (I,3,N).AND.D (I,3,N).GT.D (I,4,N).OR.
     1D (I,2,N).LT.D (I,3,N).AND.D (I,3,N).LT.D (I,4,N)) D (I,1,N)=
     22.*D (I,2,N)-D (I,3,N)
   20 IF (IVRD.EQ.0) GO TO 14
```

```
1595.          00            V (I,1,N)=V (I,2,N)
1596.          00            IF (IEXTR.EQ.0) GO TO 14
1597.          00            IF (V (I,2,N).GT.V (I,3,N).AND.V (I,3,N).GT.V (I,4,N).OR.
1598.          00           1V (I,2,N).LT.V (I,3,N).AND.V (I,3,N).LT.V (I,4,N)) V (I,1,N)=
1599.          00           2.*V (I,2,N)-V (I,3,N)
1600.          00        14 IF (IBDRY.EQ.6.OR.IBDRY.EQ.7) GO TO 26
1601.          00           GO TO 24
1602.          00        26 IF (IBDRY.EQ.7.AND.I.GT.IMXPU) GO TO 24
1603.          00           TT=P(I,1,N)*TO/D(I,1,N)
1604.          00           AA=A0*SQRT(TT/TO)
1605.          00           CALL SOLWD(AA,TT,PI,Z,I,A0)
1606.          00           IF (IPULS.EQ.2) GO TO 29
1607.          00           IF (IPULS.EQ.3) GO TO 29
1608.          00           IF (V(I,1,N).LE.Z) GO TO 24
1609.          00           V(I,1,N)=Z
1610.          00           IVLIM=IVLIM+1
1611.          00           GO TO 24
1612.          00        29 ICHVT=1
1613.          00        24 IBTH=0
1614.          00           IERD=0
1615.          00           IF (IMBDY.EQ.0) GO TO 30
1616.          00           GO TO (21,27,34),IMBDY
1617.          00        21 IBTH=1
1618.          00           IERD=1
1619.          00           GO TO 28
1620.          00        27 IF (I.LE.IMXPU) GO TO 33
1621.          00           IBTH=1
1622.          00        33 IERD=1
1623.          00           GO TO 28
1624.          00        34 IF (I.LE.IMXPU) GO TO 28
1625.          00           IBTH=1
1626.          00           IERD=1
1627.          00        28 IF (IBTH.EQ.0) GO TO 32
1628.          00           BY(I,1,N)=BY(I,2,N)
1629.          00        32 IF (IBFC.EQ.0) GO TO 30
1630.          00           BY(I,1,N)=BY(I,2,N)
1631.          00        30 IF (ICHVT.EQ.0) GO TO 6
1632.          00           IF (IPULS.EQ.2) GO TO 36
1633.          00           ALFA=ATAN(ABS(BY(I,1,N))/ABS(BX(I,1,N)))
1634.          00           VTH=Z*SIN(ALFA)
1635.          00           IF (V(I,1,N).LE.VTH) GO TO 31
1636.          00           V(I,1,N)=VTH
1637.          00           IVLIM=IVLIM+1
1638.          00        31 VTTH=Z*COS(ALFA)
1639.          00           BXYP=BY(I,1,N)*BX(I,1,N)
1640.          00           IF (BXYP.LT.0.0) VTTH=-VTTH
1641.          00           IF (ABS(U(I,1,N)).LE.ABS(VTTH)) GO TO 6
1642.          00           U(I,1,N)=VTTH
1643.          00           IVLIM=IVLIM+1
1644.          00           GO TO 6
1645.          00        36 IF (ABS(V(I,1,N)).LT.Z) GO TO 6
1646.          00           IVLIM=IVLIM+1
1647.          00           CIVTR=1.
1648.          00           IF (V(I,1,N).LT.0.0) CIVTR=-1.
1649.          00           CIVTH=1.
1650.          00           IF (U(I,1,N).LT.0.0) CIVTH=-1.
1651.          00           V(I,1,N)=CIVTR*Z
```

```
      IF (ABS(V(I,1,N)).LT.1.E-3) GO TO 6
      IF (ABS(U(I,1,N)).LT.1.E-3) GO TO 6
      ALFA=ATAN(ABS(V(I,1,N))/ABS(U(I,1,N)))
      C(I,1,N)=CIVT**2/TAN(ALFA)
    4 IF (I.EQ.1.OR.I.EQ.LSUB) GO TO 2
      IY=I-1
      AZB(IY,1)=AZB(IY,1)+DTZ*(V(I,1,N1)*BX(I,1,N1)-U(I,1,N1)*
     *BY(I,1,N1))+V(I,1,N)*BY(I,1,N)-U(I,1,N)*BY(I,1,N))
    2 IF (P(I,1,N).GT.1.E-10) GO TO 9
      WRITE (IW,17) P(I,1,N),P(I,2,N),I
      P(I,1,N) = P(I,2,N)
    9 ARG1= C11*P(I,1,N)/D(I,1,N)
      ABX2=ARG2+BX(I,1,N)**2/D(I,1,N)
      ABY2=ARG2+BY(I,1,N)**2/D(I,1,N)
      ARG2=ARG1+ABX2+ABY2
      GO TO 77
      CHARXT=          SQRT(.5*(ARG2+SQRT(ABS(ARG2**2-4.*ARG1*ABY2))))
      SIGNC=1.
      IF (U(I,1,N).LT.0.0) SIGNC=-1.
      CHARXT=
     1      (SIGNC*U(I,1,N)+CHARXT)/V(1)
      IF(CHARXT.GT.CHARMX) CHARMX=CHARXT
   77 CONTINUE
      CHARYT=          SQRT(.5*(ARG2+SQRT(ABS(ARG2**2-4.*ARG1*ABY2))))
      SIGNC=1.
      IF(V(I,1,N).LT.0.0) SIGNC=-1.
      CHARYT=SIGNC*V(I,1,N)+CHARYT
      IF (CHARYT.GT.CHARDY) CHARDY=CHARYT
    1 CONTINUE
      CHARXT=DXT/CHARDX
      CHARYT=DYT/CHARDY
      DTTT=AMIN1(CHARXT,CHARYT)*STBY
      IF(DTTT.GT.DTT) GO TO 3
      W ITE (IW,4) TT,DTT,NTIME
      TIN = TIN-DTT-DTTT
      DTT = DTTT
    3 CONTINUE
      IF (IVLIM.EQ.0) RETURN
      IF (IBDRY.EQ.0.OR.IBDRY.EQ.7) PRINT 25,IVLIM
      RETURN
      END
*FORTRAN,D=PLIM,D=SHOW1.FL
      SUBROUTINE OLDRY(ILMX,IEND,N,N1)
C  WATCH DIMENSION OF ILMY IN COMMON/COBDRY/
      PARAMETER (IX7=39,IY7=51)
      COMMON X(IX7),Y(IY7),U(IX7,IY7,2),V(IX7,IY7,2),P(IX7,IY7,2),
     1P(IX7,IY7,2),LDISMY(IX7),BY(IX7,IY7,2),BX(IX7,IY7,2),AZB(IX7,IY7),
     2AZZ(IX7,IY7)
      COMMON /ECOM2/ LDISMX,LMX,LMY,ICHCK,IPULS,XMP,WMP,DTT,STBY,PI,DPP
      COMMON /COBDRY/ LKEEP,ILMY(IY7),ILMYT
      COMMON /COBDR2/IBDX0,IBDX4,IBDY0
    2 FORMAT ( / 35H *** DISTURBANCE PROPAGATED TO XMAX ***)
   10 FORMAT ( / 3XH *** DISTURBANCE PROPAGATED TO XMAX ***
     1                , 5HJMAX =,I4)
      ILMYT=1
      LMY1=LMY-1
      ICTYP=0
```

```
1709.   00          EPP=.001
1710.   00          EPV=.001
1711.   00          RETURN
1712.   00          ENTRY OBSRV1(ILMX,IEND,N,N1)
1713.   00      C   NOTE - N1 AND N CHANGED IN LAX, N IS THE NEW VALUE
1714.   00      C   FIND MAXIMUM DISTANCE DISTURBANCE PROPAGATED TO
1715.   00          IF (ICHCK.EQ.1) GO TO 12
1716.   00          IF (              ILMX.EQ.1) GO TO 26
1717.   00          LSUB = LDISMY(2)
1718.   00          DO 55 L=3,LDISMX
1719.   00          IF (LDISMY(L).GT.LSUB) LSUB=LDISMY(L)
1720.   00       55 CONTINUE
1721.   00          DO 33 L=2,LSUB
1722.   00          VTST=SQRT(U(LDISMX,L,N1)**2+V(LDISMX,L,N1)**2)
1723.   00          IF(                                          ABS((P(LDISMX,L,N1)-P(
1724.   00         1LDISMX,L,N))/P(LDISMX,L,N1)).LT.  EPP.AND.ABS((VTST-SQRT(
1725.   00         2U(LDISMX,L,N)**2+V(LDISMX,L,N)**2))     ).LT.  EPV) GO TO 33
1726.   00          GO TO 26
1727.   00       33 CONTINUE
1728.   00          LDISMX = LDISMX-1
1729.   00       26 DO 11 L=2,LKEEP
1730.   00          IF (ILMY(L).EQ.1) GO TO 11
1731.   00          LSUB = LDISMY(L)
1732.   00          VTST=SQRT(U(L,LSUB,N1)**2+V(L,LSUB,N1)**2)
1733.   00          IF (                                    ABS((P(L,LSUB,N1)-P(L,LSUB,N))/
1734.   00         1P(L,LSUB,N1)).LT.  EPP.AND.ABS((VTST-SQRT(U(L,LSUB,N)**2+V(L,LSUB,
1735.   00         2N)**2))     ).LT.  EPV)LDISMY(L)=LDISMY(L)-1
1736.   00       11 CONTINUE
1737.   00          GO TO 31
1738.   00          LL=0
1739.   00          LIN=1
1740.   00          DO 29 L=3,LKEEP
1741.   00          LL=LL+1
1742.   00          LS=LKEEP-LL
1743.   00          IF (ILMY(LS).EQ.1) GO TO 31
1744.   00          LFN=LDISMY(LS)
1745.   00          IF (LFN.EQ.LIN) GO TO 29
1746.   00          DO 30 I=LIN,LFN
1747.   00          IF (ABS((P(LS,I,N1)-P(LS,I,N))/P(LS,I,N1)).LT.  EPP.AND.ABS(
1748.   00         1SQRT(U(LS,I,N1)**2+V(LS,I,N1)**2)-SQRT(U(LS,I,N)**2+V(LS,I,N)**2
1749.   00         2)).LT.  EPV) GO TO 30
1750.   00          LDISMY(LS+1)=I
1751.   00       30 CONTINUE
1752.   00          LIN=LFN
1753.   00       29 CONTINUE
1754.   00       31 IF (LDISMX+2.LE.LMX.OR.ILMX.EQ.1) GO TO 6
1755.   00          PRINT 7
1756.   00          IF (IBDRN.EQ.0) IEND=2
1757.   00          ILMX = 1
1758.   00          LDISMX = LMX-1
1759.   00        6 GO TO (1,2,12),ILMYT
1760.   00        1 DO 7 I=2,LDISMX
1761.   00          IF (LDISMY(I)+2.LE.LMX) GO TO 7
1762.   00          PRINT 10,I
1763.   00          IF (IBDYN.EQ.0) IEND=2
1764.   00          ILMYT=2
1765.   00          GO TO 2
```

```
      8 CONTINUE
        GO TO 12
      2 DO 3 I=2,LDISMX
        IF (ILMY(I).EQ.1) GO TO 3
        IF (LDISMY(I)+2.LE.LMY) GO TO 3
        ICTYM=ICTYM+1
        ILMY(I)=1
        LDISMY(I)=LMYM1
        IF (ICTYM.EQ.LMX-2) ILMYT=3
      3 CONTINUE
C     BOUNDARY AT Y=YX
     12 IF (ILMYT.EQ.1.OR.IBDYM.EQ.0) GO TO 18
        DO 19 I=2,LDISMX
        IF (ILMY(I).EQ.0) GO TO 19
        LSUB1=LDISMY(I)-1
        LSUB2=LDISMY(I)+1
        LSUB=LDISMY(I)
        GO TO (21,27), IBDYM
     21  U(I,LSUB2,N1)=2.* U(I,LSUB,N1)- U(I,LSUB1,N1)
       - V(I,LSUB2,N1)=2.* V(I,LSUB,N1)- V(I,LSUB1,N1)
         D(I,LSUB2,N1)=2.* D(I,LSUB,N1)- D(I,LSUB1,N1)
        BX(I,LSUB2,N1)=2.*BX(I,LSUB,N1)-BX(I,LSUB1,N1)
        BY(I,LSUB2,N1)=2.*BY(I,LSUB,N1)-BY(I,LSUB1,N1)
         P(I,LSUB2,N1)=2.* P(I,LSUB,N1)- P(I,LSUB1,N1)
        GO TO 19
     27  U(I,LSUB2,N1)= U(I,LSUB,N1)
         V(I,LSUB2,N1)= V(I,LSUB,N1)
         D(I,LSUB2,N1)= D(I,LSUB,N1)
        BX(I,LSUB2,N1)=BX(I,LSUB,N1)
        BY(I,LSUB2,N1)=BY(I,LSUB,N1)
         P(I,LSUB2,N1)= P(I,LSUB,N1)
     19 CONTINUE
C    BOUNDARY AT XC
     18 LSUB = LDISMY(2)+1
        GO TO (4,5,22,17),IBDXC
      4 DO 9 J=1,LSUB
        U(1,J,N1) = U(3,J,N1)
        V(1,J,N1) =-V(3,J,N1)
        D(1,J,N1) = D(3,J,N1)
        BX(1,J,N1)=BX(3,J,N1)
        BY(1,J,N1)=-BY(3,J,N1)
      9 P(1,J,N1) = P(3,J,N1)
        GO TO 17
      5 DO 20 J=1,LSUB
        U(1,J,N1) =-U(3,J,N1)
        V(1,J,N1) = V(3,J,N1)
        D(1,J,N1) = D(3,J,N1)
        BX(1,J,N1)=BX(3,J,N1)
        BY(1,J,N1)=-BY(3,J,N1)
     20 P(1,J,N1) = P(3,J,N1)
        U(2,LMY,N1)=0.0
        GO TO 17
     22 DO 23 J=1,LSUB
        U(1,J,N1) =-U(3,J,N1)
        U(2,J,N1)=0.0
        V(1,J,N1) = V(3,J,N1)
        D(1,J,N1) = D(3,J,N1)
```

```
      1823.   00            BX(1,J,N1)=-BX(3,J,N1)
      1824.   00            BX(2,J,N1)=0.0
      1825.   00            BY(1,J,N1)= BY(3,J,N1)
      1826.   00         23 P(1,J,N1)=P(3,J,N1)
      1827.   00      C  BOUNDARY AT XMAX
      1828.   00         17 IF(ILMX.EQ.1.OR.IBDYM.EQ.0) GO TO 16
      1829.   00            LSUB1 = LDISMX-1
      1830.   00            LSUB2 = LDISMX+1
      1831.   00            LSUB=LDISMY(LDISMX)+1
      1832.   00            GO TO (24,17),IBDYM
      1833.   00         24 DO 25 J=1,LSUB
      1834.   00             U(LSUB2,J,N1)= U(LDISMX,J,N1)
      1835.   00             V(LSUB2,J,N1)= V(LDISMX,J,N1)
      1836.   00             D(LSUB2,J,N1)= D(LDISMX,J,N1)
      1837.   00            BX(LSUB2,J,N1)=BX(LDISMX,J,N1)
      1838.   00            BY(LSUB2,J,N1)=BY(LDISMX,J,N1)
      1839.   00         25  P(LSUB2,J,N1)= P(LDISMX,J,N1)
      1840.   00            GO TO 16
      1841.   00         13 DO 15 J=1,LSUB
      1842.   00             U(LSUB2,J,N1)=2.* U(LDISMX,J,N1)- U(LSUB1,J,N1)
      1843.   00             V(LSUB2,J,N1)=2.* V(LDISMX,J,N1)- V(LSUB1,J,N1)
      1844.   00             D(LSUB2,J,N1)=2.* D(LDISMX,J,N1)- D(LSUB1,J,N1)
      1845.   00            BX(LSUB2,J,N1)=2.*BX(LDISMX,J,N1)-BX(LSUB1,J,N1)
      1846.   00            BY(LSUB2,J,N1)=2.*BY(LDISMX,J,N1)-BY(LSUB1,J,N1)
      1847.   00         15  P(LSUB2,J,N1)=2.* P(LDISMX,J,N1)- P(LSUB1,J,N1)
      1848.   00         16 RETURN
      1849.   00            END
      1850.   00            SUBROUTINE SOLVE (AC,TO,W,V,L,AN)
      1851.   00          5 FORMAT( 50H *** NO CONVERGENCE FOR VO AT CRITICAL POINT - I =,
      1852.   00           1I3,10H V = 0 ***)
      1853.   00         11 FORMAT ( / 3X'CRITICAL POINT ITERATION' / 4X'N'6X'X'10X'F(X)')
      1854.   00         13 FORMAT (I5,2( E13.4))
      1855.   00         19 FORMAT ( 49H *** NO SUBSONIC CRITICAL POINT SOLUTION - I =,I3,
      1856.   00           11OH V = 0 *** )
      1857.   00          8 FORMAT (5X'VR =',1PE10.3,' KM/SEC')
      1858.   00         10 FORMAT (/3X'CRITICAL POINT'/5X'R =',1PE11.3,' SOLAR RADII'/5X
      1859.   00           1'VR =',E10.3,' KM/SEC')
      1860.   00            IPRNT=0
      1861.   00            IF (IPRNT.EQ.1) PRINT 11
      1862.   00            EC = 1.38E-16
      1863.   00            PM = 1.6721E-24
      1864.   00            RS = 6.957E10
      1865.   00            SUNM = 1.987E33
      1866.   00            GRA = 6.67E-8
      1867.   00            IT=1
      1868.   00            C4=0-1.
      1869.   00            C5=2./(5.-3.*G)
      1870.   00            V=1.
      1871.   00      C  ITERATION - SECANT METHOD ONCE SOLUTION ISOLATED
      1872.   00            DO 1 I=1,200
      1873.   00            GO TO (15,14,16),IT
      1874.   00         14 V=V+4.
      1875.   00            IF (V.LT.40) GO TO 16
      1876.   00            PRINT 19,L
      1877.   00            V=0.0
      1878.   00            RETURN
      1879.   00         16 S=GRA*SUNM/(V **2*1.E10*RS)
```

```
1937.    00          COMMON /COM2/ LDISMX,LMX,LMY,ICHCK,IPULS,XMP,WMP,DTT,STBY,PI,DMP
1938.    00          DIMENSION BTCGL(IX7),BTCGU(IX7),VCGL(IX7),VCGU(IX7),BRCGU(IX7),
1939.    00         1PCGU(IX7),DCGU(IX7)
1940.    00         11 FORMAT (3X'DTT REDUCED IN HSBDY FROM',1PE12.4,' TO',E12.4)
1941.    00          LMYM1=LMY-1
1942.    00          LMXM1=LMX-1
1943.    00          LMXM2=LMX-2
1944.    00          ABO2=ABO**2
1945.    00          C3=PI/RNO**2
1946.    00          DO 1 I=2,LMXM1
1947.    00          BTCGL(I)=BX(I,1,1)-BX(I,2,1)
1948.    00          BTCGU(I)=BX(I,LMY,1)-BX(I,LMYM1,1)
1949.    00          VCGL(I)=V(I,1,1)-V(I,2,1)
1950.    00          VCGU(I)=V(I,LMY,1)-V(I,LMYM1,1)
1951.    00          BRCGU(I)=BY(I,LMY,1)-BY(I,LMYM1,1)
1952.    00          PCGU(I)=P(I,LMY,1)-P(I,LMYM1,1)
1953.    00        1 DCGU(I)=D(I,LMY,1)-D(I,LMYM1,1)
1954.    00          ENTRY HSBDY1(N)
1955.    00     C  INNER BOUNDARY,R=RS
1956.    00          DO 2 I=2,LMXM1
1957.    00          V(I,1,N)=V(I,2,N)+VCGL(I)
1958.    00          IF (I.EQ.LMXM1) GO TO 4
1959.    00          BX(I,1,N)=BX(I,2,N)+BTCGL(I)
1960.    00        4 IF (V(I,1,N).LT.0.0) GO TO 3
1961.    00          IF (I.EQ.2.OR.I.EQ.LMXM1) GO TO 2
1962.    00          U(I,1,N)=V(I,1,N)*BX(I,1,N)/BY(I,1,N)
1963.    00          GO TO 2
1964.    00        3 V(I,1,N)=0.0
1965.    00          U(I,1,N)=0.0
1966.    00        2 CONTINUE
1967.    00     C  UPPER BOUNDARY, R=RMAX
1968.    00          DO 5 I=2,LMXM1
1969.    00          V(I,LMY,N)=V(I,LMYM1,N)+VCGU(I)
1970.    00          IF (I.EQ.LMXM1) GO TO 6
1971.    00          BX(I,LMY,N)=BX(I,LMYM1,N)+BTCGU(I)
1972.    00        6 IF (I.EQ.2) GO TO 7
1973.    00          BY(I,LMY,N)=BY(I,LMYM1,N)+BRCGU(I)
1974.    00        7 IF (I.EQ.2.OR.I.EQ.LMXM1) GO TO 8
1975.    00          U(I,LMY,N)=U(I,LMYM1,N)
1976.    00        8 P(I,LMY,N)=P(I,LMYM1,N)+PCGU(I)
1977.    00        5 D(I,LMY,N)=D(I,LMYM1,N)+DCGU(I)
1978.    00     C  SYMMETRY BOUNDARIES, EQUATOR AND POLE
1979.    00          DO 4 J=1,LMY
1980.    00          U(1,J,N)=-U(3,J,N)
1981.    00          V(1,J,N)= V(3,J,N)
1982.    00          P(1,J,N)= P(3,J,N)
1983.    00          D(1,J,N)= D(3,J,N)
1984.    00          BX(1,J,N)= BX(3,J,N)
1985.    00          BY(1,J,N)=-BY(3,J,N)
1986.    00          U(LMX,J,N)=-U(LMXM2,J,N)
1987.    00          V(LMX,J,N)= V(LMXM2,J,N)
1988.    00          P(LMX,J,N)= P(LMXM2,J,N)
1989.    00          D(LMX,J,N)= D(LMXM2,J,N)
1990.    00          BX(LMX,J,N)=-BX(LMXM2,J,N)
1991.    00        4 BY(LMX,J,N)= BY(LMXM2,J,N)
1992.    00     C  CHECK TIME
1993.
```

```
1994.          00            CHARDY=1.E-6
1995.          00            N1=N
1996.          00            DO 10 I=2,LMXM1
1997.          00            J=1
1998.          00            ARG1=CZ*P(I,J,N1)/D(I,J,N1)
1999.          00            ABX2=AB02*BX(I,J,N1)**2/D(I,J,N1)
2000.          00            ABY2=AB02*BY(I,J,N1)**2/D(I,J,N1)
2001.          00            ARG2=ARG1+ABX2+ABY2
2002.          00            GO TO 12
2003.          00            CHARXT=          SQRT(.5*(ARG2+SQRT(ABS(ARG2**2-4.*ARG1*ABX2))))
2004.          00            SIGNC=1.
2005.          00            IF(U(I,J,N1).LT.0.0) SIGNC=-1.
2006.          00            CHARXT=
2007.          00           1      (SIGNC*U(I,J,N1)+CHARXT)/Y(J)
2008.          00            IF(CHARXT.GT.CHARDX) CHARDX=CHARXT
2009.          00           12 CONTINUE
2010.          00            CHARYT=          SQRT(.5*(ARG2+SQRT(ABS(ARG2**2-4.*ARG1*ABY2))))
2011.          00            SIGNC=1.
2012.          00            IF(V(I,J,N1).LT.0.0) SIGNC=-1.
2013.          00            CHARYT=SIGNC*V(I,J,N1)+CHARYT
2014.          00            IF(CHARYT.GT.CHARDY) CHARDY=CHARYT
2015.          00            GO TO 10
2016.          00            J=LMY
2017.          00            ARG1=CZ*P(I,J,N1)/D(I,J,N1)
2018.          00            ABX2=AB02*BX(I,J,N1)**2/D(I,J,N1)
2019.          00            ABY2=AB02*BY(I,J,N1)**2/D(I,J,N1)
2020.          00            ARG2=ARG1+ABX2+ABY2
2021.          00            CHARXT=          SQRT(.5*(ARG2+SQRT(ABS(ARG2**2-4.*ARG1*ABX2))))
2022.          00            SIGNC=1.
2023.          00            IF(U(I,J,N1).LT.0.0) SIGNC=-1.
2024.          00            CHARXT=
2025.          00           1      (SIGNC*U(I,J,N1)+CHARXT)/Y(J)
2026.          00            IF(CHARXT.GT.CHARDX) CHARDX=CHARXT
2027.          00            CHARYT=          SQRT(.5*(ARG2+SQRT(ABS(ARG2**2-4.*ARG1*ABY2))))
2028.          00            SIGNC=1.
2029.          00            IF(V(I,J,N1).LT.0.0) SIGNC=-1.
2030.          00            CHARYT=SIGNC*V(I,J,N1)+CHARYT
2031.          00            IF(CHARYT.GT.CHARDY) CHARDY=CHARYT
2032.          00           10 CONTINUE
2033.          00            CHARXT=DXT/CHARDX
2034.          00            CHARYT=DYT/CHARDY
2035.          00            DTTCK=AMIN1(CHARXT,CHARYT)*STBY
2036.          00            IF(DTTCK.GE.DTT) RETURN
2037.          00            PRINT 11,DTT,DTTCK
2038.          00            DTT=DTTCK
2039.          00            RETURN
2040.          00            END
2041.          00        *END

END ELT.  ERRORS: NONE. TIME: 19.429 SEC. IMAGE COUNT: 2041

@PRT,S SAMPLE
FURPUR 2HR1.1 U1 E35 S74T11 04/25/79 09:39:32
```

APPENDIX B. COMPUTER CODE FOR COMPUTER-GENERATED PLOTS

One outstanding advantage of a computing facility such as that at the National Center for Atmospheric Research in Boulder, Colorado, which is where these simulations were performed, is the capability of quickly producing multi-dimensional plots of the physical variables. A listing of the code we used to obtain computer-generated plots (some of which are presented in this report) is given here along with a description of the variables that must be input to the code. The routines in the listing that actually generate the plots are, in general, unique to the NCAR Computing Facility; however, the remaining logic should be applicable to any facility.

Since the plots are placed on microfilm, this introduces the possibility of producing computer-generated movies. We have produced movies of the evolving magnetic field lines for the streamer and transient simulations for both $\beta = 0.5$ and $\beta = 4$.

R. S. Steinolfson
25 April 1980

Description of Input Variables for Plot Routine PLTPTS for Codes MHDHS and MHDCT (CRAY-1)

Variable	Columns	Definition	Comments	Units
			Card 1	
NDS	1-4	Number of data sets to be plotted	NDS should be set equal to the last value of NPTVR printed out by code MHDMP	- - -
			Card 2	
ANGH	1-8	Angular orientation of surface plots	See NCAR manual "NCAR Software Support Library, Vol. 3" for write-up on Subroutine SRFACE.	degrees
ANGV	9-16			

Options (Card 2)

Variable	Columns	Definition	Value	Comments
IPSU	17-20	Surface plots of non-dimensional pressure, density, velocity magnitude and temperature	0	Produce plots - see write-up on SRFACE in above manual.
			1	No plots
IPHT	21-24	Half-tone plots of non-dimensional density, temperature and pressure	0	Produce plots - see write-up on HAFTON in above manual.
			1	No plots
IPVV	25-28	Velocity vector plot	0	Produce plots - see write-up on VELVEC in above manual.
			1	No plots
IPFL	29-32	Contour plots of magnetic field lines and the non-dimensional density less the ambient value	0	Produce plots - see write-up on CONREC in above manual.
			1	No plots
IPRN	33-36	Half-tone plots of total radiation (Cox-Tucker) and the total radiation minus the background value	0	Produce plots - see write-up on HAFTON in above manual.
			1	No plots
IPTO	37-40	Plots at t = 0	0	Produce plots
			1	No plots

Variable	Columns	Definition	Value	Comments
IPFLO	41-44	If IPFLO=0, determines which contour polar plots.	0	All contour polar plots.
			1	Only do calculated field line contour polar plot.
IPRSA	45-48	MS=1 and MA=1 curves on calculated field line contour polar plots.	0	Include on plots.
			1	Not on plots.
ICLCK	49-52	Clock on calculated field line contour polar plots.	0	No clock.
			1	Include clock.
IMOVY	53-56	Use flash buffers if making a movie.	0	No flash buffers used.
			1	Use flash buffers, Set all variables to 1 except IPFLO=IPTO=IPRSA=0.
IDISP	57-60	Disposing dd80 instructions to 7600	0	Less than 1000 frames so use usual DISPOSE card procedure.
			1	More than 1000 frames so remove DISPOSE cards and use Fortran call to dispose.

FORM [illegible] Rev. 1-62

FORTRAN CODING FORM

ANALYST R. S. Steinolfson ENGINEER _____ EXT. _____

JOB NO. PLTPTS Input Format - 25 April 1980 COST CONTROL NO _____

C | NO. | X | FORTRAN STATEMENT | LABEL

1 2 3 4 5 6 7 8 9 10 11 12 13 14 15 16 17 18 19 20 21 22 23 24 25 26 27 28 29 30 31 32 33 34 35 36 37 38 39 40 41 42 43 44 45 46 47 48 49 50 51 52 53 54 55 56 57 58 59 60 61 62 63 64 65 66 67 68 69 70 71 72 73 74 75 76 77 78 79 80

Card 1. (right-adjusted integer):

N D S

Card 2:

ANGV	ANGH	IPSU	IPHT	IPVV	IPFL	IPRN	IPTO	IPFLO	IPRSA	ICLCK	IMOVY	IDISP

Right-adjusted integers

1 2 3 4 5 6 7 8 9 10 11 12 13 14 15 16 17 18 19 20 21 22 23 24 25 26 27 28 29 30 31 32 33 34 35 36 37 38 39 40 41 42 43 44 45 46 47 48 49 50 51 52 53 54 55 56 57 58 59 60 61 62 63 64 65 66 67 68 69 70 71 72 73 74 75 76 77 78 79 80

Listing of Computer Code PLTPTS

```
@ELT,IDL .SAMPLE,,STOP
ELT 8R1 S740IC 04/25/80 11:18:44 (->0)
     1.          00      *JOB,5346,35881000,STEINOLFSON
     2.          00      *FORTRAN,D=PLIB,DN=PLTCY2,AF,FL
     3.          00            PROGRAM PLTPTS
     4.          00      C  1. II AND JJ MUST BE AT LEAST AS LARGE AS ARRAYS READ ON TAPE,
     5.          00      C        II.GE.LMX-2, JJ.GE.LMY, II=IX7, JJ=IY7
     6.          00      C  2. DIMENSIONS OF Z MUST BE EQUAL TO ACTUAL NUMBER OF POINTS PLOTTED,
     7.          00      C        M7 AND N7, M7=IMXP, N7=JMXP
     8.          00      C  3. DIMENSIONS OF WORK MUST BE AT LEAST AS LARGE AS 2*M7*N7+M7+N7
     9.          00      C  4. IWK=2*IMXP*JMXP+IMXP+JMXP, IIV=IMXP/2+1, JJV=JMXP/2+1
    10.          00      C  5. NMFL=3*JMXP
    11.          00            PARAMETER (IX7=37,IY7=41,IMXP=37,JMXP=41,IWK=2614,IIV=19,JJV=21,
    12.          00           1NMFL=123)
    13.          00            REAL LAB1,LAB
    14.          00            DIMENSION P(IX7,IY7),D(IX7,IY7),V(IX7,IY7),U(IX7,IY7),BX(IX7,IY7),
    15.          00           1BY(IX7,IY7),X(IX7),LY(IX7),        Y(IY7),        FL(IX7,IY7),
    16.          00           2IA(IY7),DA(IY7),RADIN(IY7)
    17.          00            DIMENSION Z(IMXP,JMXP),WORK(IWK),VU(IIV,JJV),VV(IIV,JJV),SPV(2),
    18.          00           1LAB1(3),LAB(6),ZC(JMXP,IMXP),ZZ(JMXP,IMXP),VUC(JJV,IIV),
    19.          00           2VVC(JJV,IIV),XXL(IX7),YYL(IX7),XXU(IX7),YYU(IX7),VUD(JJV,IIV),
    20.          00           3VVD(JJV,IIV),XXM(NMFL),YYM(NMFL)
    21.          00            COMMON /TRANS/Y1,Y2,X1,X2
    22.          00           56 FORMAT (' *** INCREASE NMFL ***')
    23.          00            4 FORMAT (I3/2F8.0,6I4)
    24.          00            3 FORMAT ('1INPUT -'//3X'NDS ='I4 /
    25.          00           23X'ANGH ='E11.4 / 3X'ANGV ='E11.4 / 3X'IPSU =',I3 / 3X'IPHT =',
    26.          00           3I3/3X'IPVV =',I3/3X'IPFL =',I3/3X'IPRN =',I3/3X'IPTO =',I3)
    27.          00           31 FORMAT ('TIME =',1PE10.3,' MIN.,  ')
    28.          00            SPV(1)=0.0
    29.          00            SPV(2)=0.0
    30.          00            IMXPV=IMXP/2
    31.          00            IF (2*IMXPV.LT.IMXP) IMXPV=IMXPV+1
    32.          00            JMXPV=JMXP/2
    33.          00            IF (2*JMXPV.LT.JMXP) JMXPV=JMXPV+1
    34.          00      C  PLOT OPTION - WATCH Z DIMENSION
    35.          00            IPLOT=1
    36.          00      C
    37.          00            NDST=1
    38.          00            PIEC=3.1415926
    39.          00            RLTIC=.05
    40.          00            RADDG=.0174533
    41.          00            READ (10) TIME,M,N,((P(I,J),D(I,J),U(I,J),V(I,J),BX(I,J),BY(I,J),
    42.          00           1I=1,M),J=1,N),XMAX,YO,YMAX,(X(I),I=1,M),(Y(J),J=1,N),((FL(I,J),
    43.          00           2I=1,M),J=1,N),TO,DO,CRADN
    44.          00            Y1=Y(1)
    45.          00            Y2=Y(JMXP)-Y1
    46.          00            AB=Y1+Y2
    47.          00            DO 49 I=1,IMXP
    48.          00            X(I)=X(I)*RADDG
    49.          00            XXL(I)=Y(1)*COS(PIEC-X(I))
    50.          00            YYL(I)=Y(1)*SIN(PIEC-X(I))
    51.          00            XXU(I)=Y(JMXP)*COS(PIEC-X(I))
    52.          00           49 YYU(I)=Y(JMXP)*SIN(PIEC-X(I))
    53.          00            Y1Y2=Y1+Y2
    54.          00            X2=X(IMXP)-X(1)
    55.          00            X1=0.0
```

```
      00            READ (5,4) NDS,ANGH,ANGV,IPSU,IPHT,IPVV,IPFL,IPRN,IPTO
      00            PRINT 3,   NDS,ANGH,ANGV,IPSU,IPHT,IPVV,IPFL,IPRN,IPTO
      00            DO 22 J=1,N
      00            TA(J)=P(1,J)/D(1,J)
      00         22 DA(J)=D(1,J)
      00            IF (IPRN.EQ.1) GO TO 44
      00            DO 25 J=1,N
      00         25 RADTN(J)=RADFN(TA(J)*TO)*(DA(J)*DO)**2*CRADN
      00         44 IF (IPTO.EQ.1) GO TO 16
      00            ENCODE (24,31,LAB1) TIME
      00            LAB(1)=LAB1(1)
      00            LAB(2)=LAB1(2)
      00            LAB(3)=LAB1(3)
      00            GO TO 26
      00         46 IPTO=1
      00         16 READ (10) TIME,            LX,(LY(J),J=1,LX)
      00            ENCODE (24,31,LAB1) TIME
      00            LAB(1)=LAB1(1)
      00            LAB(2)=LAB1(2)
      00            LAB(3)=LAB1(3)
      00            DO 14 I=1,LX
      00            L =LY(I)
      00            READ (10)  (P(I,J),D(I,J),BX(I,J),BY(I,J),U(I,J),V(I,J),FL(I,J),
      00           1J=1,L)
      00         14 CONTINUE
      00      C  SURFACE PLOTS
      00            IF (IPSU.EQ.1) GO TO 13
      00            DO 7 MM=1,4
      00            DO 6 I=1,IMXP
      00            DO 6 J=1,JMXP
      00            GO TO (8,9,17,18),MM
      00         8  Z(I,J)=P(I,J)
      00            GO TO 6
      00         9  Z(I,J)=D(I,J)
      00            GO TO 6
      00         17 IF (NDST.EQ.1) GO TO 7
      00            Z(I,J)=SQRT(U(I,J)**2+V(I,J)**2)
      00            GO TO 6
      00         18 Z(I,J)=P(I,J)/D(I,J)
      00         6  CONTINUE
      00            GO TO (32,33,34,35),MM
      00         32 LAB(4)=8HPRESSURE
      00            LAB(5)=1H
      00            LAB(6)=1H
      00            GO TO 36
      00         33 LAB(4)=7HDENSITY
      00            GO TO 36
      00         34 LAB(4)=8HVELOCITY
      00            LAB(5)=5H MAGNITU
      00            LAB(6)=2HDE
      00            GO TO 36
      00         35 LAB(4)=8HTEMPERAT
      00            LAB(5)=3HURE
      00            LAB(6)=1H
      00         36 CALL PWRY(66,1008,LAB,48,2,0,2)
      00            CALL EZSRFC(Z,IMXP,JMXP,ANGH,ANGV,WORK)
      00         7  CONTINUE
```

```
      00      C  HALFTON PLOTS
      00         13 IF (IPHT.EQ.1) GO TO 15
      00            DO 2 MM=1,3
      00            DO 5 I=1,IMXP
      00            DO 5 J=1,JMXP
      00            GO TO (11,12,24),MM
      00         11 Z(I,J)=D(I,J)/DA(J)
      00            GO TO 5
      00         12 Z(I,J)=P(I,J)/(D(I,J)*TA(J))
      00            GO TO 5
      00         24 Z(I,J)=P(I,J)/(TA(J)*DA(J))
      00          5 CONTINUE
      00            GO TO (37,38,39),MM
      00         37 LAB(4)=4HD/D0
      00            LAB(5)=1H
      00            LAB(6)=1H
      00            GO TO 40
      00         38 LAB(4)=4HT/T0
      00            GO TO 40
      00         39 LAB(4)=4HP/P0
      00         40 CALL PWRY(136,1008,LAB,48,2,0,2)
      00            CALL EZHFTN(Z,IMXP,JMXP)
      00          2 CONTINUE
      00      C  RADIATION PLOTS
      00         15 IF (IPRN.EQ.1) GO TO 26
      00            DO 27 MM=1,2
      00            DO 28 I=1,IMXP
      00            DO 28 J=1,JMXP
      00            GO TO (29,30),MM
      00         29 Z(I,J)=RADFN(P(I,J)*T0/D(I,J))*(D(I,J)*D0)**2*CRADN
      00            GO TO 28
      00         30 Z(I,J)=Z(I,J)-RADTN(J)
      00         28 CONTINUE
      00            GO TO (41,42),MM
      00         41 LAB(4)=8HRADIATIO
      00            LAB(5)=1HN
      00            LAB(6)=1H
      00            GO TO 43
      00         42 LAB(5)=8HN - AMBI
      00            LAB(6)=3HENT
      00         43 CALLPWRY(136,1008,LAB,48,2,0,2)
      00            CALL EZHFTN(Z,IMXP,JMXP)
      00         27 CONTINUE
      00      C  VELOCITY VECTOR PLOTS
      00         26 IF (IPVV.EQ.1) GO TO 10
      00            KI=-1
      00            DO 19 I=1,IMXPV
      00            KI=KI+2
      00            KJ=-1
      00            DO 19 J=1,JMXPV
      00            KJ=KJ+2
      00            YYM(I)=X(KI)
      00            VU(I,J)=U(KI,KJ)
      00         19 VV(I,J)=V(KI,KJ)
      00            DO 48 I=1,IMXPV
      00            DO 48 J=1,JMXPV
      00            VVC(J,I)=VV(I,J)
```

```
      00        48 VUC(J,I)=VD(I,J)
      00           DO 58 J=1,JMXPV
      00           DO 58 I=1,IMXPV
      00           K=IMXPV+1-I
      00           XXM(I)=YYM(K)
      00           VVD(J,I)=VVC(J,K)
      00        58 VUD(J,I)=VUC(J,K)
      00           DO 59 J=1,JMXPV
      00           DO 59 I=1,IMXPV
      00           IF (VUD(J,I).LT.1.E-4.AND.VVD(J,I).LT.1.E-4) GO TO 60
      00           IF (VUD(J,I).GT.1.E-4*VVD(J,I)) GO TO 67
      00           ALP=0.0
      00           GO TO 68
      00        67 IF (VVD(J,I).GT.1.E-4*VUD(J,I)) GO TO 69
      00           ALP=PIEC/2.
      00           GO TO 68
      00        69 ALP=ATAN(ABS(VUD(J,I)/VVD(J,I)))
      00        68 IF (VUD(J,I).GE.0.0) PHI=PIEC-XXM(I)+ALP
      00           IF (VUD(J,I).LE.0.0) PHI=PIEC-XXM(I)-ALP
      00           CC1=SQRT(VUD(J,I)**2+VVD(J,I)**2)
      00           VVC(J,I)=CC1*COS(PHI)
      00           VUC(J,I)=CC1*SIN(PHI)
      00           GO TO 59
      00        60 VVC(J,I)=VVD(J,I)
      00           VUC(J,I)=VUD(J,I)
      00        59 CONTINUE
      00           LAB(4)=8HVELOCITY
      00           LAB(5)=8H VECTORS
      00           LAB(6)=1H
      00           IPFL1=2
      00           GO TO 73
      00        72 CALL EZVEC (VVC,VUC,JMXPV,IMXPV)
      00         C CONTOUR PLOTS
      00        10 IF (IPFL.EQ.1) GO TO 21
      00           DO 74 MM=1,5
      00           DO 20 I=1,IMXP
      00           DO 20 J=1,JMXP
      00           GO TO (75,76,77,78,79),MM
      00        75 ZZ(J,I)=FL(I,J)
      00           GO TO 20
      00        76 ZZ(J,I)=P(I,J)/(TA(J)*DA(J))
      00           GO TO 20
      00        77 ZZ(J,I)=D(I,J)/DA(J)
      00           GO TO 20
      00        78 ZZ(J,I)=D(I,J)-DA(J)
      00           GO TO 20
      00        79 ZZ(J,I)=P(I,J)/(D(I,J)*TA(J))
      00        20 CONTINUE
      00           DO 47 J=1,JMXP
      00           DO 47 I=1,IMXP
      00           K=IMXP+1-I
      00        47 ZC(J,I)=ZZ(J,K)
      00           GO TO (80,81,82,83,84),MM
      00        80 LAB(4)=8HMAGNETIC
      00           LAB(5)=8H FIELD L
      00           LAB(6)=4HINES
      00           GO TO 85
```

```
227.          00        81 LAB(4)=4HP/PO
228.          00           LAB(5)=1H
229.          00           LAB(6)=1H
230.          00           GO TO 85
231.          00        82 LAB(4)=4HD/DO
232.          00           GO TO 85
233.          00        83 LAB(4)=8HMASS EXC
234.          00           LAB(5)=8HESS (D-D
235.          00           LAB(6)=2HO)
236.          00           GO TO 85
237.          00        84  LAB(4)=4HT/TO
238.          00           LAB(5)=1H
239.          00           LAB(6)=1H
240.          00        85 CALL PWRY(66,1008,LAB,48,2,0,2)
241.          00           CALL SET (.05,.95,.05,.95,0.0,AB,0.0,AB,1)
242.          00           DO 89 I=1,2
243.          00           CALL LINE (0.0,0.0,AB,0.0)
244.          00           CALL LINE (0.0,0.0,0.0,AB)
245.          00        89 CONTINUE
246.          00           DO 86 I=2,15
247.          00           RI=I
248.          00           IF (RI.GE.AB-1.E-5) GO TO 87
249.          00           CALL LINE (RI,0.0,RI,RLTIC)
250.          00           CALL LINE (0.0,RI,RLTIC,RI)
251.          00        86 CONTINUE
252.          00        87 CALL CURVE(XXL,YYL,IMXP)
253.          00           CALL CURVE (XXU,YYU,IMXP)
254.          00           CALL EZCNTR(ZC,JMXP,IMXP)
255.          00           IF (IPTO.EQ.0) GO TO 88
256.          00        74 CONTINUE
257.          00        88 IPFL1=1
258.          00        73 CALL PWRY(66,1008,LAB,48,2,0,2)
259.          00           CALL SET (.05,.95,.05,.95,0.0,AB,0.0,AB,1)
260.          00           DO 90 I=1,2
261.          00           CALL LINE (0.0,0.0,AB,0.0)
262.          00           CALL LINE (0.0,0.0,0.0,AB)
263.          00        90 CONTINUE
264.          00           DO 61 I=2,15
265.          00           RI=I
266.          00           IF (RI.GE.AB-1.E-5) GO TO 62
267.          00           CALL LINE (RI,0.0,RI,RLTIC)
268.          00           CALL LINE (0.0,RI,RLTIC,RI)
269.          00        61 CONTINUE
270.          00        62 CALL CURVE(XXL,YYL,IMXP)
271.          00           CALL CURVE (XXU,YYU,IMXP)
272.          00           GO TO (71,72),IPFL1
273.          00        71 DL=Y(2)-Y(1)
274.          00           DO 50 I=1,IMXP
275.          00           DO 50 J=1,JMXP
276.          00           BX(I,J)=-BX(I,J)
277.          00        50 BY(I,J)=-BY(I,J)
278.          00           LAB(4)=8HMAGNETIC
279.          00           LAB(5)=8H FIELD L
280.          00           LAB(6)=4HINES
281.          00           IMXPM1=IMXP-1
282.          00           DO 70 L=4,IMXPM1,2
283.          00           R1=Y(1)
```

```
      00          T1=X(L)
      00          XXM(1)=R1*COS(PIEC-T1)
      00          YYM(1)=R1*SIN(PIEC-T1)
      00          ICOMP=0
      00          BR1=BY(L,1)
      00          BT1=BX(L,1)
      00          DO 51 K=2,NMFL
      00          KK=K
      00          DR=DL
      00          IF (ABS(BT1).GT.1.E-5*ABS(BR1)) DR=DL*AES(BR1/BT1)/SQRT(1.+(BR1/
      00         1BT1)**2)
      00          IF (BR1.LT.0.0) DR=-DR
      00          DT=DL/R1
      00          IF (ABS(BR1).GT.1.E-5*ABS(BT1)) DT=ABS(DR*BT1/BR1)/R1
      00          IF (BT1.LT.0.0) DT=-DT
      00          R1=R1+DR
      00          T1=T1+DT
      00          IF (R1.GT.Y(1)) GO TO 63
      00          R1=Y(1)
      00          ICOMP=1
      00       63 IF (R1.LT.Y(JMXP)) GO TO 64
      00          R1=Y(JMXP)
      00          ICOMP=1
      00       64 IF (T1.GT.X(1)) GO TO 65
      00          T1=X(1)
      00          ICOMP=1
      00       65 IF (T1.LT.X(IMXP))GO TO 66
      00          T1=X(IMXP)
      00          ICOMP=1
      00       66 XXM(K)=R1*COS(PIEC-T1)
      00          YYM(K)=R1*SIN(PIEC-T1)
      00          IF (ICOMP.EQ.1) GO TO 57
      00          DO 52 I=2,IMXP
      00          II=I
      00          IF (X(I).GT.T1) GO TO 53
      00       52 CONTINUE
      00       53 I=II-1
      00          IP1=I+1
      00          DO 54 J=2,JMXP
      00          JJ=J
      00          IF (Y(J).GT.R1) GO TO 55
      00       54 CONTINUE
      00       55 J=JJ-1
      00          JP1=J+1
      00          BR1=BY(I,J)+(R1-Y(J))*(BY(I,JP1)-BY(I,J))/(Y(JP1)-Y(J))+(T1-X(I))*
      00         1(BY(IP1,J)-BY(I,J)+(R1-Y(J))*(BY(IP1,JP1)-BY(IP1,J)-BY(I,JP1)+
      00         2BY(I,J))/(Y(JP1)-Y(J)))/(X(IP1)-X(I))
      00          BT1=BX(I,J)+(R1-Y(J))*(BX(I,JP1)-BX(I,J))/(Y(JP1)-Y(J))+(T1-X(I))*
      00         1(BX(IP1,J)-BX(I,J)+(R1-Y(J))*(BX(IP1,JP1)-BX(IP1,J)-BX(I,JP1)+
      00         2BX(I,J))/(Y(JP1)-Y(J)))/(X(IP1)-X(I))
      00       51 CONTINUE
      00          PRINT 56
      00       57 CALL CURVE (XXM,YYM,KK)
      00       70 CONTINUE
      00          CALL FRAME
      00          IF (IPTO.EQ.0) GO TO 46
      00       21 NDST=NDST+1
```

```
      IF (NDST.LE.NDS) GO TO 16
      END
      FUNCTION RADFN(TS)
      DIMENSION T(49),Q(49)
      DATA T/9.2E3,1.E4,1.08E4,1.15E4,1.26E4,1.45E4,1.85E4,2.E4,2.2E4,
     12.3E4,2.65E4,3.E4,3.5E4,4.1E4,4.9E4,5.6E4,6.17E4,7.02E4,8.5E4,
     21.1E5,1.3E5,1.65E5,1.9E5,2.17E5,2.63E5,2.85E5,2.98E5,3.3E5,
     33.9E5,4.7E5,5.63E5,6.2E5,6.9E5,7.4E5,8.07E5,9.08E5,1.06E6,1.3E6,
     41.75E6,2.28E6,3.1E6,4.3E6,7.03E6,9.85E6,1.25E7,2.23E7,3.7E7,
     56.02E7,1.E8/
      DATA Q/1.1E-24,3.6E-24,8.05E-24,1.65E-23,3.5E-23,5.85E-23,
     18.15E-23,1.1E-22,1.07E-22,9.5E-23,8.8E-23,1.E-22,1.2E-22,1.65E-22,
     22.23E-22,3.15E-22,4.3E-22,6.05E-22,7.25E-22,8.04E-22,8.08E-22,
     38.3E-22,9.3E-22,1.02E-21,1.E-21,8.8E-22,7.6E-22,6.02E-22,5.1E-22,
     44.7E-22,4.2E-22,3.8E-22,2.84E-22,1.9E-22,1.24E-22,9.3E-23,
     57.1E-23,6.E-23,5.7E-23,5.3E-23,4.9E-23,3.25E-23,2.4E-23,1.9E-23,
     61.7E-23,1.9E-23,2.25E-23,2.9E-23,3.47E-23/
    3 FORMAT (2X'*** T.GT.1.E8, RADIATION EXTRAPOLATED ***')
      IF (TS.GE.T(1)) GO TO 1
      RADFN=0.0
      RETURN
    1 IF (TS.LT.T(49)) GO TO 2
      PRINT 3
      RADFN=Q(47)+(Q(49)-Q(47))*(TS-T(47))/(T(49)-T(47))
      RETURN
    2 DO 4 I=1,48
      IP=I+1
      IF (TS.GE.T(I).AND.TS.LT.T(IP)) GO TO 5
    4 CONTINUE
    5 RADFN=Q(I)+(Q(IP)-Q(I))*(TS-T(I))/(T(IP)-T(I))
      RETURN
      END
*END

END ELT.  ERRORS: NONE. TIME:  3.532 SEC. IMAGE COUNT: 373

@PRT,S SAMPLE
FURPUR 28R1.1 U1 E35 S74T11 04/25/80 11:18:46
```

APPENDIX C. SAMPLE RUN

A listing of a typical computer run for a coronal streamer simulation is presented. The input variables are listed first followed by the initial ambient atmosphere and the time-dependent solution. The time-dependent solution is given at selected time intervals along radial lines at selected meridional increments. For this example the solution is only shown for the first time increment.

INPUT -

```
 RUN IDENTIFICATION
   RUN NUMBER =  1
   HELMET STREAMER SIMULATION

 OPTIONS
   ISIGI =  3
   IFUL_S =  3
   ICHCK =  1
   IBDRY =  6
   IMAGE =  1
   IFNCS =  6
   IPIEL =  2
   IFTAR =  2
   ISISL =  1
   ISMTH =  1
   NIMSM =  0
   IBDXO =  2
   IBDXM =  2
   IBDYM =  2
   IBDIN =  2
   ILOWB =  1
   IWBDY =  2

 STEADY-STATE PARAMETERS AT RO
   RO = 1.0000E+00 SOLAR RADII
   T =  1.8600E+06 K
   D =  2.2453E+08 ELECTRONS/CM3
   BI =     1.1500
   B =  5.2533E-01 GAUSS

 PULSE PARAMETERS
   TAU = 1.8000E+02 MINUTES
   TM =  1.0400E+02 DEGREES
   BI =  6.4623E+01 GAUSS
   DD =  7.0000E+03 KM
   DTT = 1.0000E+01 MINUTES

 STEADY-STATE SOLUTION PARAMETERS
   RBND =5.0000E+00 SOLAR RADII
   DR =  1.0000E-01 SOLAR RADII

 TIME-DEPENDENT SOLUTION PARAMETERS
   DTT = 2.5000E+00 DEGREES
   DRI = 1.0000E-01 SOLAR RADII
   TMAX =1.8000E+02 DEGREES
   RMAX =5.0000E+00 SOLAR RADII
   DITP =4.5000E+01 DEGREES
   DRTP =0.0000E+00 SOLAR RADII
   TMAX =1.4400E+03 MINUTES
   DIP = 1.2000E+02 MINUTES
   DTPI =1.2000E+02 MINUTES
   SIBY =1.0000E+00
   SMTH =2.0000E+00
   ISIP =1.4400E+03 MINUTES
```

OUTPUT -

```
          **********************************
          * INITIAL STEADY-STATE SOLUTION *
```

REVISED VALUES OF TMAX AND RMAX
TMAX =1.8[illegible]E+02 DEGREES
RMAX =5.000E+00 SOLAR RADII
LMX = 39
LMY = 41

VALUES AT YO
P = 1.117E-01 DYNES/CM2
A = 1.766E+02 KM/SEC
TI = 6.565E+01 MIN
N = 1.025E+00
S = 6.178E+05
AB = 4.364E-01
BTA =1.[illegible]E+01
ORD =3.359E+14 CM3-S/ERG
VR = 8.242E+01 KM/SEC

CRITICAL POINT
R = 4.266E+00 SOLAR RADII
VR = 1.531E+02 KM/SEC

SOLUTION OF STEADY-STATE EQUATIONS
NON-DIMENSIONAL VARIABLES

	R	VR	P	D	T	MS	MA	MFM	BETA
1	1.000[illegible]E+00	4.6669E-02	1.0[illegible]E+00	1.0[illegible]E+00	1.0[illegible]E+00	4.6669E-02	1.3693E-01	4.2773E-02	1.0[illegible]E+01
2	1.10[illegible]E+00	6.7019E-02	5.5292E-01	5.6874E-01	9.7219E-01	6.8773E-02	1.5597E-01	8.2932E-02	9.7955E+00
3	1.2000E+00	9.2438E-02	3.3270E-01	3.5065E-01	9.4894E-01	9.4892E-02	2.1671E-01	8.6424E-02	9.9347E+00
4	1.30[illegible]E+00	1.1398E-01	2.1435E-01	2.3036E-01	9.2922E-01	1.2436E-01	2.8964E-01	1.1427E-01	1.0332E+01
5	1.4000E+00	1.4947E-01	1.4533E-01	1.5931E-01	9.1224E-01	1.5649E-01	3.7508E-01	1.4442E-01	1.0943E+01
6	1.50[illegible]E+00	1.8059E-01	1.0306E-01	1.1436E-01	9.0765E-01	1.9962E-01	4.7526E-01	1.7632E-01	1.1742E+01
7	1.6000E+00	2.1269E-01	7.5834E-02	8.5712E-02	8.8441E-01	2.2616E-01	5.8440E-01	2.1592E-01	1.2719E+01
8	1.70[illegible]E+00	2.4535E-01	5.7447E-02	6.5819E-02	8.7231E-01	2.6262E-01	7.0858E-01	2.4625E-01	1.3867E+01
9	1.8000E+00	2.7819E-01	4.4652E-02	5.1777E-02	8.6240E-01	2.9957E-01	8.4594E-01	2.8238E-01	1.5197E+01
10	1.90[illegible]E+00	3.1096E-01	3.5462E-02	4.1574E-02	8.5298E-01	3.3665E-01	9.9645E-01	3.1897E-01	1.6684E+01
11	2.0000E+00	3.4342E-01	2.5683E-02	3.3973E-02	8.4462E-01	3.7373E-01	1.1603E+00	3.5573E-01	1.8360E+01
12	2.10[illegible]E+00	3.7544E-01	2.3531E-02	2.8187E-02	8.3657E-01	4.1048E-01	1.3375E+00	3.9241E-01	2.0229E+01
13	2.2000E+00	4.0669E-01	1.9654E-02	2.3698E-02	8.2935E-01	4.4679E-01	1.5282E+00	4.2984E-01	2.2284E+01
14	2.30[illegible]E+00	4.3769E-01	1.6532E-02	2.0156E-02	8.2266E-01	4.8256E-01	1.7324E+00	4.6436E-01	2.4547E+01
15	2.4000E+00	4.6779E-01	1.4141E-02	1.7320E-02	8.1645E-01	5.1771E-01	1.9501E+00	5.0138E-01	2.7025E+01
16	2.50[illegible]E+00	4.9716E-01	1.2175E-02	1.5019E-02	8.1065E-01	5.5215E-01	2.1824E+00	5.3530E-01	2.9726E+01
17	2.6000E+00	5.2573E-01	1.0573E-02	1.3130E-02	8.0522E-01	5.8594E-01	2.4263E+00	5.6957E-01	3.2661E+01
18	2.70[illegible]E+00	5.5366E-01	9.2514E-03	1.1563E-02	8.0012E-01	6.1897E-01	2.6850E+00	6.0315E-01	3.5843E+01
19	2.8000E+00	5.8079E-01	8.1514E-03	1.0249E-02	7.9531E-01	6.5125E-01	2.9575E+00	6.3601E-01	3.9282E+01
20	2.90[illegible]E+00	6.0717E-01	7.2272E-03	9.1395E-03	7.9078E-01	6.8279E-01	3.2438E+00	6.6815E-01	4.2990E+01
21	3.0000E+00	6.3285E-01	6.4443E-03	8.1941E-03	7.8649E-01	7.1359E-01	3.5439E+00	6.9955E-01	4.6981E+01
22	3.10[illegible]E+00	6.5777E-01	5.7762E-03	7.3829E-03	7.8243E-01	7.4365E-01	3.8586E+00	7.3021E-01	5.1265E+01
23	3.20[illegible]E+00	6.8203E-01	5.2020E-03	6.6822E-03	7.7860E-01	7.7301E-01	4.1866E+00	7.6015E-01	5.5857E+01
24	3.30[illegible]E+00	7.0563E-01	4.7154E-03	6.0734E-03	7.7477E-01	8.0166E-01	4.5281E+00	7.8938E-01	6.0778E+01
25	3.4000E+00	7.2857E-01	4.2734E-03	5.5411E-03	7.7122E-01	8.2963E-01	4.8842E+00	8.1791E-01	6.6048E+01
26	3.50[illegible]E+00	7.5100E-01	3.8956E-03	5.0735E-03	7.6783E-01	8.5693E-01	5.2544E+00	8.4576E-01	7.1613E+01
27	3.6000E+00	7.7262E-01	3.5635E-03	4.6698E-03	7.6459E-01	8.8360E-01	5.6398E+00	8.7295E-01	7.7572E+01
28	3.70[illegible]E+00	7.9376E-01	3.2752E-03	4.2347E-03	7.6146E-01	9.0964E-01	6.0374E+00	8.9948E-01	8.3937E+01
29	3.80[illegible]E+00	8.1435E-01	3.0181E-03	3.9687E-03	7.5846E-01	9.3507E-01	6.4502E+00	9.2540E-01	9.0634E+01
30	3.90[illegible]E+00	8.3446E-01	2.7734E-03	3.6772E-03	7.5557E-01	9.5993E-01	6.8773E+00	9.5071E-01	9.7768E+01
31	4.0000E+00	8.5394E-01	2.5713E-03	3.4157E-03	7.5279E-01	9.8422E-01	7.3137E+00	9.7544E-01	1.0532E+02
32	4.10[illegible]E+00	8.7349E-01	2.3941E-03	3.1784E-03	7.5008E-01	1.0[illegible]E+00	7.7767E+00	1.0[illegible]E+00	1.1325E+02
33	4.20[illegible]E+00	8.9152E-01	2.2183E-03	2.9675E-03	7.4751E-01	1.0511E+00	8.2445E+00	1.0232E+00	1.2177E+02
34	4.30[illegible]E+00	9.0955E-01	2.0674E-03	2.7751E-03	7.4501E-01	1.0[illegible]E+00	8.7287E+00	1.0462E+00	1.3089E+02
35	4.40[illegible]E+00	9.2729E-01	1.9304E-03	2.5995E-03	7.4258E-01	1.0761E+00	9.2331E+00	1.0688E+00	1.4063E+02
36	4.50[illegible]E+00	9.4492E-01	1.8162E-03	2.4400E-03	7.4027E-01	1.0979E+00	9.7416E+00	1.0909E+00	1.4099E+02
37	4.60[illegible]E+00	9.6135E-01	1.6930E-03	2.2942E-03	7.3796E-01	1.1191E+00	1.0270E+01	1.1125E+00	1.6941E+02
38	4.70[illegible]E+00	9.7775E-01	1.5887E-03	2.1597E-03	7.3575E-01	1.1398E+00	1.0812E+01	1.1336E+00	1.7136E+02
39	4.80[illegible]E+00	9.9394E-01	1.4951E-03	2.0361E-03	7.3359E-01	1.1603E+00	1.1369E+01	1.1543E+00	1.8287E+02
40	[illegible]	[illegible]	[illegible]	1.9254E-03	7.3162E-01	1.1803E+00	1.1941E+01	1.1745E+00	1.9495E+02

40	4.8000E+00	1.2099E+01	1.4084E-03	1.9264E-03	7.3152E-01	1.1033E+00	1.1941E+01	1.1746E+00	1.9495E+02
41	5.0000E+00	1.2249E+01	1.3287E-03	1.8214E-03	7.2949E-01	1.1999E+00	1.2528E+01	1.1945E+00	2.0762E+02

MAGNETIC FIELD

R=20

0.0000E+00	1.0000E-01	2.0000E-01	3.0000E-01	4.0000E-01	5.0000E-01	6.0000E-01	7.0000E-01
8.0000E-01	9.0000E-01	1.0000E+00	1.1000E+00	1.2000E+00	1.3000E+00	1.4000E+00	1.5000E+00
1.6000E+00	1.7000E+00	1.8000E+00	1.9000E+00	2.0000E+00	2.1000E+00	2.2000E+00	2.3000E+00
2.4000E+00	2.5000E+00	2.6000E+00	2.7000E+00	2.8000E+00	2.9000E+00	3.0000E+00	3.1000E+00
3.2000E+00	3.3000E+00	3.4000E+00	3.5000E+00	3.6000E+00	3.7000E+00	3.8000E+00	3.9000E+00
4.0000E+00							

T = 9.0000E+01

BT(R)

1.0000E+00	7.5131E-01	5.7872E-01	4.5517E-01	3.6443E-01	2.9635E-01	2.4414E-01	2.0354E-01
1.7147E-01	1.4677E-01	1.2562E-01	1.0798E-01	9.3914E-02	8.2190E-02	7.2331E-02	6.4000E-02
5.6836E-02	5.0639E-02	4.5554E-02	4.1072E-02	3.7037E-02	3.3567E-02	3.0513E-02	2.7826E-02
2.5443E-02	2.3324E-02	2.1433E-02	1.9742E-02	1.8224E-02	1.6858E-02	1.5625E-02	1.4509E-02
1.3497E-02	1.2578E-02	1.1739E-02	1.0974E-02	1.0274E-02	9.6318E-03	9.0422E-03	8.4994E-03
8.0011E-03							

BR(R)

-1.3464E-06	-1.0116E-06	-7.7917E-07	-6.1284E-07	-4.9067E-07	-3.9894E-07	-3.2871E-07	-2.7405E-07
-2.3037E-07	-1.9633E-07	-1.6833E-07	-1.4537E-07	-1.2643E-07	-1.1066E-07	-9.7397E-08	-8.6172E-08
-7.6615E-08	-6.8461E-08	-6.1334E-08	-5.5206E-08	-4.9867E-08	-4.5135E-08	-4.1089E-08	-3.7466E-08
-3.4256E-08	-3.1413E-08	-2.8858E-08	-2.6581E-08	-2.4577E-08	-2.2698E-08	-2.1048E-08	-1.9536E-08
-1.8173E-08	-1.6934E-08	-1.5806E-08	-1.4775E-08	-1.3833E-08	-1.2966E-08	-1.2179E-08	-1.1444E-08
-1.0771E-08							

T = 1.3500E+02

BT(R)

7.0711E-01	5.3126E-01	4.0920E-01	3.2195E-01	2.5763E-01	2.0951E-01	1.7267E-01	1.4393E-01
1.2135E-01	1.0384E-01	8.8399E-02	7.6353E-02	6.6407E-02	5.8117E-02	5.1151E-02	4.5255E-02
4.0231E-02	3.5865E-02	3.2211E-02	2.9098E-02	2.6389E-02	2.3736E-02	2.1579E-02	1.9685E-02
1.7991E-02	1.6463E-02	1.5156E-02	1.3985E-02	1.2946E-02	1.1998E-02	1.1049E-02	1.0260E-02
9.5441E-03	8.8936E-03	8.3063E-03	7.7597E-03	7.2646E-03	6.8127E-03	6.3938E-03	6.0103E-03
5.6569E-03							

BP(R)

-1.4142E+00	-1.0563E+00	-8.1841E-01	-6.4771E-01	-5.1538E-01	-4.1903E-01	-3.4527E-01	-2.8785E-01
-2.4249E-01	-2.0618E-01	-1.7679E-01	-1.5271E-01	-1.3262E-01	-1.1623E-01	-1.0223E-01	-9.0910E-02
-8.0463E-02	-7.1802E-02	-6.4423E-02	-5.7966E-02	-5.2377E-02	-4.7471E-02	-4.3159E-02	-3.9353E-02
-3.5991E-02	-3.2959E-02	-3.0312E-02	-2.7920E-02	-2.5773E-02	-2.3841E-02	-2.2097E-02	-2.0519E-02
-1.9033E-02	-1.7787E-02	-1.6642E-02	-1.5620E-02	-1.4529E-02	-1.3821E-02	-1.2798E-02	-1.2021E-02
-1.1314E-02							

T = 1.8000E+02

BT(R)

-1.3464E-06	-1.0116E-06	-7.7917E-07	-6.1284E-07	-4.9067E-07	-3.9894E-07	-3.2871E-07	-2.7405E-07
-2.3037E-07	-1.9633E-07	-1.6833E-07	-1.4537E-07	-1.2643E-07	-1.1066E-07	-9.7397E-08	-8.6172E-08
-7.6615E-08	-6.8461E-08	-6.1334E-08	-5.5206E-08	-4.9867E-08	-4.5135E-08	-4.1089E-08	-3.7466E-08
-3.4256E-08	-3.1413E-08	-2.8858E-08	-2.6581E-08	-2.4577E-08	-2.2698E-08	-2.1048E-08	-1.9536E-08
-1.8173E-08	-1.6934E-08	-1.5806E-08	-1.4775E-08	-1.3833E-08	-1.2966E-08	-1.2179E-08	-1.1444E-08
-1.0771E-08							

BP(R)

-2.0000E+00	-1.5026E+00	-1.1574E+00	-9.1633E-01	-7.2849E-01	-5.9259E-01	-4.8829E-01	-4.0708E-01
-3.4294E-01	-2.9153E-01	-2.5000E-01	-2.1596E-01	-1.8765E-01	-1.6438E-01	-1.4466E-01	-1.2800E-01
-1.1379E-01	-1.0161E-01	-9.1118E-02	-8.2074E-02	-7.4074E-02	-6.7134E-02	-6.1035E-02	-5.5653E-02
-5.0845E-02	-4.6047E-02	-4.2447E-02	-3.9494E-02	-3.6449E-02	-3.3716E-02	-3.1253E-02	-2.9019E-02
-2.6993E-02	-2.5159E-02	-2.3473E-02	-2.1908E-02	-2.0567E-02	-1.9284E-02	-1.8094E-02	-1.7000E-02
-1.6000E-02							

RADII AT WHICH SOUND AND ALFVEN MACH NUMBERS ARE ONE

NO	TH(DEG)	RS	RA
2	9.0000E+01	4.2644E+00	1.9022E+00
3	3.2500E+01	4.2644E+00	1.8438E+00
4	9.5000E+01	4.2644E+00	1.9041E+00
5	9.7500E+01	4.2644E+00	1.9076E+00
6	1.0000E+02	4.2644E+00	1.9292E+00
7	1.1250E+02	4.2644E+00	1.9436E+00
8	1.0500E+02	4.2644E+00	1.9367E+00
9	1.0750E+02	4.2644E+00	1.9401E+00

11	1.1250E+02	4.0648E+00	2.0222E+00
12	1.1500E+02	4.0648E+00	2.0446E+00
13	1.1750E+02	4.0648E+00	2.0673E+00
14	1.2000E+02	4.0648E+00	2.0917E+00
15	1.2250E+02	4.0648E+00	2.1156E+00
16	1.2500E+02	4.0648E+00	2.1378E+00
17	1.2750E+02	4.0648E+00	2.1617E+00
18	1.3000E+02	4.0648E+00	2.1834E+00
19	1.3250E+02	4.0648E+00	2.2054E+00
20	1.3500E+02	4.0648E+00	2.2259E+00
21	1.3750E+02	4.0648E+00	2.2459E+00
22	1.4000E+02	4.0648E+00	2.2653E+00
23	1.4250E+02	4.0648E+00	2.2839E+00
24	1.4500E+02	4.0648E+00	2.3016E+00
25	1.4750E+02	4.0648E+00	2.3174E+00
26	1.5000E+02	4.0648E+00	2.3323E+00
27	1.5250E+02	4.0648E+00	2.3463E+00
28	1.5500E+02	4.0648E+00	2.3592E+00
29	1.5750E+02	4.0648E+00	2.3712E+00
30	1.6000E+02	4.0648E+00	2.3817E+00
31	1.6250E+02	4.0648E+00	2.3912E+00
32	1.6500E+02	4.0648E+00	2.3998E+00
33	1.6750E+02	4.0648E+00	2.4063E+00
34	1.7000E+02	4.0648E+00	2.4118E+00
35	1.7250E+02	4.0648E+00	2.4160E+00
36	1.7500E+02	4.0648E+00	2.4191E+00
37	1.7750E+02	4.0648E+00	2.4216E+00
38	1.8000E+02	4.0648E+00	2.4216E+00

INITIAL ENERGY (ERGS/KMZ)= MAGNETIC =4.29834E+24, THERMAL =4.05501E+26, GRAVITATIONAL =1.04634E+26
INITIAL MASS =6.95533E+10 GMS/KMZ =4.15892E+34 PARTICLES/KMZ

****
* TIME-DEPENDENT SOLUTION *
****

TIME = 1.348E+03 = 1.213E+02 MINUTES, TIME CYCLE NO 52, DTT = 3.521E-02
RCONTS-RO =5.594JE-01 SOLAR RADII =3.892CE+04 KM, RCONTSR-RO =0.000JE+00 SOLAR RADII =0.000JE+00 KM
ENERGY BUILD-UP (ERGS/KMZ)= MAGNETIC =5.15599E+23, THERMAL =2.75997E+25, KINETIC =7.16808E+23, GRAVITATIONAL =5.33026E+24
MASS BUILD-UP =4.130019E+09 GMS/KMZ =2.469863E+33 PARTICLES/KMZ
R CHARACTERISTIC DIRECTIONS AT RO

T	L3	L4	L5	L6
1.5708E+00	1.0565E+00	5.4312E-07	-1.0565E+00	-5.4312E-07
2.3562E+00	1.0491E+00	6.3310E-01	-1.0058E+00	-5.3977E-01
3.1416E+00	1.0487E+00	9.1953E-01	-9.5333E-01	-8.2619E-01

T = 1.571E+00 RAD = 9.000E+01 DEG, T-PRIO NO 2

NO	R	VT	VP	JXBT	D	P	BT	BR	JXBR	T	BETA
1	1.0000E+00	0.0000E+00	0.0000E+00	-6.4778E-08	1.0440E+00	1.0472E+00	7.8893E-01	-1.3464E-06	-4.9892E-02	1.3025E+00	1.6824E+01
2	1.1000E+00	1.4011E-04	1.5936E-02	1.8796E-03	9.1324E-01	9.1007E-01	2.4025E-01	2.5611E-03	-3.4373E-01	9.7553E-01	2.0560E+01
3	1.2000E+00	-3.3799E-05	1.6869E-02	2.0257E-03	7.8232E-01	7.8653E-01	3.9653E-01	2.4543E-03	-3.2730E-01	9.5975E-01	2.7336E+01
4	1.3000E+00	-1.7353E-04	2.5018E-02	7.2811E-04	2.5597E-01	2.4124E-01	2.9792E-01	1.1296E-03	-1.9203E-01	9.4246E-01	2.7181E+01
5	1.4000E+00	-1.4939E-04	4.9812E-02	-5.4499E-06	1.4008E-01	1.6679E-01	2.3792E-01	-9.1369E-06	-1.4191E-01	9.2545E-01	2.9466E+01
6	1.5000E+00	-1.7405E-04	6.7636E-02	-3.6491E-04	1.3121E-01	1.1963E-01	1.9942E-01	-5.9883E-04	-1.0820E-01	9.1172E-01	3.4083E+01
7	1.6000E+00	-2.2371E-04	1.3438E-01	-4.2763E-04	9.6581E-02	8.8543E-02	1.7316E-01	-6.7604E-04	-8.1725E-02	8.9822E-01	2.9532E+01
8	1.7000E+00	-2.4027E-04	1.8503E-01	-3.4380E-04	7.5965E-02	6.7296E-02	1.5431E-01	-9.2765E-04	-6.0398E-02	8.8588E-01	2.8373E+01
9	1.8000E+00	-2.1228E-04	2.3612E-01	-2.4853E-04	5.9789E-02	5.2284E-02	1.3896E-01	-8.5224E-04	-4.3460E-02	8.7458E-01	2.7077E+01
10	1.9000E+00	-1.5911E-04	2.8519E-01	-1.7157E-04	4.7910E-02	4.1405E-02	1.2632E-01	-7.1199E-04	-3.0442E-02	8.6423E-01	2.5946E+01
11	2.0000E+00	-9.7629E-05	3.3094E-01	-1.0115E-04	3.8996E-02	3.3332E-02	1.1516E-01	-5.5263E-04	-2.0871E-02	8.5474E-01	2.5132E+01
12	2.1000E+00	-4.2175E-05	3.7319E-01	-5.4716E-05	3.2194E-02	2.7237E-02	1.0539E-01	-4.0531E-04	-1.4186E-02	8.4603E-01	2.4665E+01
13	2.2000E+00	-3.3604E-06	4.1251E-01	-2.9137E-05	2.6942E-02	2.2578E-02	9.5976E-02	-2.8652E-04	-9.7264E-03	8.3805E-01	2.4512E+01
14	2.3000E+00	1.7522E-05	4.5111E-01	-1.5424E-05	2.2842E-02	1.8975E-02	8.7821E-02	-1.9947E-04	-6.8113E-03	8.3176E-01	2.4635E+01
15	2.4000E+00	2.4932E-05	4.8595E-01	-8.2055E-06	1.9500E-02	1.6152E-02	8.0561E-02	-1.3744E-04	-4.6682E-03	8.2606E-01	2.4887E+01
16	2.5000E+00	2.4504E-05	5.2577E-01	-4.5383E-06	1.6986E-02	1.3893E-02	7.4062E-02	-9.5712E-05	-3.2118E-03	8.1791E-01	2.5330E+01
17	2.6000E+00	2.1349E-05	5.6093E-01	-2.5167E-06	1.4836E-02	1.2049E-02	6.8182E-02	-6.7991E-05	-2.2548E-03	8.1215E-01	2.5929E+01

NO	R	VT	VR	JXBT	D	P	BT	BR	JXBR	T	BETA
19	[illegible]	[illegible]	[illegible]	[illegible]	[illegible]	[illegible]	[illegible]	[illegible]	[illegible]	[illegible]	[illegible]
20	2.9000E+00	1.3334E-05	6.5559E-01	-5.3676E-07	1.0276E-02	8.1878E-03	5.3561E-02	-2.5864E-05	-1.1157E-03	7.9681E-01	2.8542E+01
21	3.0000E+00	1.1532E-05	6.8623E-01	-3.5474E-07	9.2364E-03	7.3132E-03	4.9788E-02	-1.8759E-05	-9.4157E-04	7.9243E-01	2.9527E+01
22	3.1000E+00	9.4342E-06	7.2373E-01	-2.2872E-07	8.3782E-03	6.6057E-03	4.6643E-02	-1.2966E-05	-8.1383E-04	7.8844E-01	3.0435E+01
23	3.2000E+00	6.7152E-06	7.6195E-01	-1.2209E-07	7.6629E-03	6.0140E-03	4.3730E-02	-7.7933E-06	-6.9174E-04	7.8482E-01	3.1449E+01
24	3.3000E+00	3.7874E-06	8.0131E-01	-4.1971E-08	7.0507E-03	5.5098E-03	4.1209E-02	-3.1730E-06	-5.4508E-04	7.8146E-01	3.2447E+01
25	3.4000E+00	1.3363E-06	8.3326E-01	-9.1053E-09	6.4962E-03	5.0569E-03	3.8785E-02	-1.0009E-06	-3.5284E-04	7.7820E-01	3.3617E+01
26	3.5000E+00	2.2315E-06	8.6773E-01	-7.2832E-09	5.9622E-03	4.6173E-03	3.6233E-02	-2.0425E-06	-1.2778E-04	7.7478E-01	3.5176E+01
27	3.6000E+00	1.2706E-06	8.8371E-01	2.5906E-09	5.4079E-03	4.1694E-03	3.2417E-02	-1.4497E-06	5.9708E-05	7.7096E-01	3.7359E+01
28	3.7000E+00	9.2142E-07	8.8642E-01	3.2159E-09	4.8585E-03	3.7256E-03	3.0439E-02	-7.4674E-07	1.3109E-04	7.6681E-01	4.0211E+01
29	3.8000E+00	1.3735E-06	8.8418E-01	7.3914E-09	4.3656E-03	3.3235E-03	2.7693E-02	-1.9209E-06	1.0650E-04	7.6266E-01	4.3415E+01
30	3.9000E+00	2.5564E-06	8.8461E-01	5.0824E-09	3.9484E-03	2.9960E-03	2.5330E-02	-2.4141E-06	5.3328E-05	7.5878E-01	4.6635E+01
31	4.0000E+00	2.5325E-06	8.9053E-01	1.1427E-09	3.6078E-03	2.7250E-03	2.3378E-02	-2.3635E-06	1.1363E-05	7.5531E-01	4.9861E+01
32	4.1000E+00	2.2852E-06	9.0380E-01	-7.6524E-10	3.3226E-03	2.4992E-03	2.1722E-02	-2.0803E-06	-8.0323E-06	7.5217E-01	5.2966E+01
33	4.2000E+00	1.9858E-06	9.1348E-01	-1.2297E-09	3.0767E-03	2.3052E-03	2.0272E-02	-1.7447E-06	-1.4405E-05	7.4924E-01	5.6096E+01
34	4.3000E+00	1.6371E-06	9.2738E-01	-1.1475E-09	2.8605E-03	2.1354E-03	1.8975E-02	-1.4304E-06	-1.5219E-05	7.4649E-01	5.9309E+01
35	4.4000E+00	1.4353E-06	9.4136E-01	-9.0695E-10	2.6681E-03	1.9847E-03	1.7860E-02	-1.1624E-06	-1.3888E-05	7.4387E-01	6.2643E+01
36	4.5000E+00	1.2053E-06	9.5662E-01	-6.7275E-10	2.4953E-03	1.8499E-03	1.6727E-02	-9.4095E-07	-1.1953E-05	7.4136E-01	6.6122E+01
37	4.6000E+00	1.0320E-06	9.7148E-01	-4.7731E-10	2.3393E-03	1.7296E-03	1.5742E-02	-7.6084E-07	-9.8759E-06	7.3895E-01	6.9755E+01
38	4.7000E+00	8.5555E-07	9.8634E-01	-3.3678E-10	2.1978E-03	1.6193E-03	1.4634E-02	-6.1251E-07	-8.1565E-06	7.3663E-01	7.3573E+01
39	4.8000E+00	6.6209E-07	1.0011E+00	-2.3202E-10	2.0689E-03	1.5193E-03	1.3998E-02	-4.8380E-07	-6.7136E-06	7.3438E-01	7.7530E+01
40	4.9000E+00	3.7648E-07	1.0155E+00	-2.8702E-11	1.9527E-03	1.4299E-03	1.3226E-02	-3.4363E-07	-1.1047E-06	7.3228E-01	8.1745E+01
41	5.0000E+00	3.6100E+03	1.0308E+00	-2.8702E-11	1.8365E-03	1.3405E-03	1.2493E-02	-1.0771E-08	-1.1047E-06	7.2991E-01	8.6442E+01

T = 2.356E+00 RAD = 1.350E+02 DEG. T-GRID NO 20

NO	R	VT	VR	JXBT	D	P	BT	BR	JXBR	T	BETA
1	1.0000E+00	-2.0103E-02	4.6669E-02	-1.1705E-01	1.0000E+00	1.0000E+00	6.0919E-01	-1.4142E+00	-9.4716E-02	1.0000E+00	4.2179E+00
2	1.1000E+00	-3.2790E-02	7.8449E-02	2.2657E-02	5.8704E-01	5.7484E-01	4.3334E-01	-1.1783E+00	4.5003E-03	9.7922E-01	3.6909E+00
3	1.2000E+00	-3.6500E-02	1.0899E-01	-9.4525E-02	3.6952E-01	3.5493E-01	3.1704E-01	-9.3760E-01	-3.1963E-02	9.6252E-01	3.6233E+00
4	1.3000E+00	-4.6713E-02	1.4010E-01	-9.4713E-02	2.4678E-01	2.3249E-01	2.4741E-01	-7.5280E-01	-3.0994E-02	9.4361E-01	3.7020E+00
5	1.4000E+00	-5.2401E-02	1.7295E-01	-4.9429E-02	1.7232E-01	1.5932E-01	1.9360E-01	-6.1900E-01	-1.5554E-02	9.2804E-01	3.8473E+00
6	1.5000E+00	-5.8496E-02	2.0617E-01	-3.4439E-02	1.2521E-01	1.1440E-01	1.5461E-01	-5.1382E-01	-1.0563E-02	9.1370E-01	4.0165E+00
7	1.6000E+00	-6.3479E-02	2.4018E-01	-2.4345E-02	9.4000E-02	8.4655E-02	1.2567E-01	-4.3052E-01	-7.1161E-03	9.0359E-01	4.2089E+00
8	1.7000E+00	-6.7360E-02	2.7341E-01	-1.7150E-02	7.2445E-02	6.4372E-02	1.0346E-01	-3.6699E-01	-4.6348E-03	8.8857E-01	4.4277E+00
9	1.8000E+00	-7.2576E-02	3.0619E-01	-1.2733E-02	5.7094E-02	5.0133E-02	8.6374E-02	-3.1608E-01	-3.7527E-03	8.7756E-01	4.6667E+00
10	1.9000E+00	-7.2133E-02	3.3693E-01	-1.1812E-02	4.5972E-02	3.9884E-02	7.3383E-02	-2.7491E-01	-3.0996E-03	8.6755E-01	4.9265E+00
11	2.0000E+00	-7.2427E-02	3.7229E-01	-9.2271E-03	3.7687E-02	3.2351E-02	6.3419E-02	-2.4092E-01	-2.4236E-03	8.5842E-01	5.2125E+00
12	2.1000E+00	-7.2683E-02	4.0395E-01	-7.2524E-03	3.1288E-02	2.6593E-02	5.5400E-02	-2.1232E-01	-1.8924E-03	8.4992E-01	5.5232E+00
13	2.2000E+00	-7.2405E-02	4.3356E-01	-6.7516E-03	2.6279E-02	2.2127E-02	4.8982E-02	-1.8812E-01	-1.7580E-03	8.4200E-01	5.8556E+00
14	2.3000E+00	-6.9494E-02	4.6457E-01	-7.0945E-03	2.2392E-02	1.8692E-02	4.4330E-02	-1.6762E-01	-1.8763E-03	8.3476E-01	6.2182E+00
15	2.4000E+00	-6.2931E-02	4.9364E-01	-7.1119E-03	1.9369E-02	1.6047E-02	4.1338E-02	-1.5062E-01	-1.9597E-03	8.2822E-01	6.6253E+00
16	2.5000E+00	-5.3870E-02	5.3737E-01	-6.3046E-03	1.6938E-02	1.3926E-02	3.9463E-02	-1.3456E-01	-1.8548E-03	8.2221E-01	7.0823E+00
17	2.6000E+00	-4.4723E-02	5.7378E-01	-4.9961E-03	1.4885E-02	1.2153E-02	3.7141E-02	-1.2072E-01	-1.5743E-03	8.1646E-01	7.5657E+00
18	2.7000E+00	-3.7466E-02	6.0572E-01	-3.6780E-03	1.3098E-02	1.0620E-02	3.6625E-02	-1.0824E-01	-1.2444E-03	8.1282E-01	8.1339E+00
19	2.8000E+00	-3.2229E-02	6.3379E-01	-2.7494E-03	1.1554E-02	9.3051E-03	3.5095E-02	-9.7104E-02	-9.9332E-04	8.0534E-01	8.7284E+00
20	2.9000E+00	-2.7851E-02	6.6165E-01	-2.1626E-03	1.0264E-02	8.2133E-03	3.3597E-02	-8.7338E-02	-8.3960E-04	8.0020E-01	9.3793E+00
21	3.0000E+00	-2.3341E-02	6.9274E-01	-1.7951E-03	9.2128E-03	7.3291E-03	3.2237E-02	-7.8844E-02	-7.3395E-04	7.9553E-01	1.0101E+01
22	3.1000E+00	-1.8533E-02	7.2825E-01	-1.4535E-03	8.3607E-03	6.6163E-03	3.1004E-02	-7.1446E-02	-6.3073E-04	7.9135E-01	1.0908E+01
23	3.2000E+00	-1.3775E-02	7.6719E-01	-1.1161E-03	7.6574E-03	6.0307E-03	2.9913E-02	-6.4959E-02	-5.1223E-04	7.8757E-01	1.1806E+01
24	3.3000E+00	-9.5311E-03	8.0691E-01	-7.7588E-04	7.0523E-03	5.5294E-03	2.8562E-02	-5.9222E-02	-3.7420E-04	7.8406E-01	1.2791E+01
25	3.4000E+00	-6.1470E-03	8.4303E-01	-4.3423E-04	6.4958E-03	5.0705E-03	2.7132E-02	-5.4163E-02	-2.1776E-04	7.8056E-01	1.3842E+01
26	3.5000E+00	-4.0126E-03	8.6973E-01	-1.2201E-04	5.9431E-03	4.6172E-03	2.5407E-02	-4.9511E-02	-6.3126E-05	7.7690E-01	1.4910E+01
27	3.6000E+00	-3.2519E-03	8.8253E-01	3.7524E-05	5.3753E-03	4.1541E-03	2.3369E-02	-4.5395E-02	4.2997E-05	7.7280E-01	1.5936E+01
28	3.7000E+00	-3.4693E-03	8.8375E-01	1.3705E-04	4.8247E-03	3.7075E-03	2.1239E-02	-4.1747E-02	6.9725E-05	7.6844E-01	1.6899E+01
29	3.8000E+00	-3.6810E-03	8.8252E-01	9.4588E-05	4.3413E-03	3.3176E-03	1.9317E-02	-3.8519E-02	4.7636E-05	7.6420E-01	1.7868E+01
30	3.9000E+00	-4.3584E-03	8.8505E-01	3.7497E-05	3.9384E-03	2.9945E-03	1.7726E-02	-3.5628E-02	1.8632E-05	7.6032E-01	1.8914E+01
31	4.0000E+00	-3.9413E-03	8.9259E-01	2.5791E-07	3.6061E-03	2.7292E-03	1.6373E-02	-3.3030E-02	1.2593E-07	7.5682E-01	2.0052E+01
32	4.1000E+00	-3.6531E-03	9.0352E-01	-1.5116E-05	3.3243E-03	2.5062E-03	1.5236E-02	-3.0675E-02	-7.5629E-06	7.5361E-01	2.1356E+01
33	4.2000E+00	-3.3382E-03	9.1633E-01	-1.9243E-05	3.0795E-03	2.3115E-03	1.4234E-02	-2.8529E-02	-9.6615E-06	7.5060E-01	2.2741E+01
34	4.3000E+00	-2.9405E-03	9.3011E-01	-1.8741E-05	2.8635E-03	2.1412E-03	1.3336E-02	-2.6572E-02	-9.4059E-06	7.4776E-01	2.4225E+01
35	4.4000E+00	-2.5402E-03	9.4441E-01	-1.6536E-05	2.6709E-03	1.9920E-03	1.2530E-02	-2.4789E-02	-8.3529E-06	7.4506E-01	2.5802E+01
36	4.5000E+00	-2.2635E-03	9.5895E-01	-1.3972E-05	2.4979E-03	1.8546E-03	1.1774E-02	-2.3159E-02	-7.1635E-06	7.4247E-01	2.7477E+01
37	4.6000E+00	-1.9581E-03	9.7361E-01	-1.1240E-05	2.3416E-03	1.7324E-03	1.1089E-02	-2.1665E-02	-5.8044E-06	7.3999E-01	2.9253E+01
38	4.7000E+00	-1.6906E-03	9.8827E-01	-9.2301E-06	2.1999E-03	1.6227E-03	1.0455E-02	-2.0291E-02	-4.7404E-06	7.3761E-01	3.1144E+01
39	4.8000E+00	-1.4421E-03	1.0029E+00	-7.3568E-06	2.0713E-03	1.5226E-03	9.8712E-03	-1.9013E-02	-3.7676E-06	7.3528E-01	3.3184E+01
40	4.9000E+00	-1.0947E-03	1.0170E+00	-1.5013E-06	1.9544E-03	1.4329E-03	9.3271E-03	-1.7725E-02	-7.6977E-07	7.3312E-01	3.5719E+01
41	5.0000E+00	-7.3624E-04	1.0324E+00	[illegible]	[illegible]	1.3431E-03	8.7846E-03	-1.6440E-02	-7.3977E-07	7.3363E-01	3.8654E+01

NO	R	VT	VR	VADJ	D	P	BT	BR	JXBR	T	BETA
1	1.0000E+00	0.0000E+00	4.6669E-02	-3.8269E-04	1.0000E+00	1.0000E+00	-1.3464E-06	-2.0000E+00	2.3743E-10	1.0000E+00	2.5001E+00
2	1.1000E+00	-2.1944E-06	7.4878E-02	-2.7832E-04	5.8705E-01	5.7576E-01	1.4807E-05	-1.6283E+00	-2.5329E-09	9.9077E-01	2.1716E+00
3	1.2000E+00	-2.1699E-06	1.0480E-01	-7.8921E-05	3.6926E-01	3.5577E-01	3.0214E-05	-1.2966E+00	-1.0391E-09	9.6346E-01	2.1163E+00
4	1.3000E+00	-2.5262E-06	1.3955E-01	-1.2823E-04	3.4727E-01	2.3431E-01	2.3766E-05	-1.0762E+00	-7.5286E-10	9.4761E-01	2.1022E+00
5	1.4000E+00	-2.9551E-06	1.7568E-01	-2.7947E-04	2.7311E-01	1.6146E-01	2.0015E-05	-8.3843E-01	-6.5761E-10	9.3267E-01	2.2469E+00
6	1.5000E+00	-4.0947E-06	2.1330E-01	-1.8617E-03	2.2603E-01	1.1989E-01	2.6730E-05	-6.8915E-01	-7.2173E-10	9.1879E-01	2.4395E+00
7	1.6000E+00	-3.2930E-06	2.5215E-01	1.4131E-03	3.4926E-02	8.5999E-02	2.2576E-05	-5.7408E-01	5.5568E-10	9.0595E-01	2.6095E+00
8	1.7000E+00	-2.7342E-06	2.9015E-01	-5.1652E-06	7.3254E-02	6.5408E-02	1.8952E-05	-4.8328E-01	-2.4177E-10	8.9402E-01	2.6041E+00
9	1.8000E+00	-2.5912E-06	3.2602E-01	-2.4823E-03	5.7734E-02	5.0974E-02	2.2477E-05	-4.1106E-01	-1.3573E-09	8.8291E-01	3.0168E+00
10	1.9000E+00	-4.7044E-06	3.6157E-01	-2.2418E-05	4.6467E-02	4.0553E-02	2.8799E-05	-3.5325E-01	-1.8623E-09	8.7274E-01	3.2499E+00
11	2.0000E+00	-8.3889E-06	3.9721E-01	-1.3153E-05	3.8071E-02	3.2871E-02	3.2287E-05	-3.0616E-01	-1.4186E-09	8.6341E-01	3.5065E+00
12	2.1000E+00	-1.3241E-05	4.3082E-01	-8.9183E-06	3.1601E-02	2.7010E-02	3.4064E-05	-2.6730E-01	-9.8043E-10	8.5471E-01	3.7802E+00
13	2.2000E+00	-1.8597E-05	4.6191E-01	-2.6267E-06	2.6533E-02	2.2466E-02	3.4286E-05	-2.3504E-01	-3.8311E-10	8.4653E-01	4.0671E+00
14	2.3000E+00	-2.6717E-05	4.9321E-01	-4.3011E-07	2.2594E-02	1.8959E-02	3.3239E-05	-2.0806E-01	-6.8769E-11	8.3913E-01	4.3791E+00
15	2.4000E+00	-3.4319E-05	5.2676E-01	-2.6599E-07	1.9500E-02	1.6233E-02	3.1625E-05	-1.8520E-01	-4.5719E-11	8.3232E-01	4.7322E+00
16	2.5000E+00	-3.5941E-05	5.6075E-01	-7.9550E-07	1.6983E-02	1.4232E-02	3.0856E-05	-1.6546E-01	-1.4435E-10	8.2598E-01	5.1257E+00
17	2.6000E+00	-3.4797E-05	5.9150E-01	-8.3478E-07	1.4863E-02	1.2186E-02	3.0302E-05	-1.4830E-01	-1.7057E-10	8.1989E-01	5.5412E+00
18	2.7000E+00	-4.0222E-05	6.1694E-01	-5.9182E-07	1.3038E-02	1.3612E-02	2.9654E-05	-1.3339E-01	-1.3157E-10	8.1395E-01	5.9646E+00
19	2.8000E+00	-5.0964E-05	6.4123E-01	-7.2173E-07	1.1517E-02	9.3102E-03	2.6993E-05	-1.2047E-01	-1.7376E-10	8.0836E-01	6.4153E+00
20	2.9000E+00	-5.2242E-05	6.6358E-01	-6.9437E-07	1.0297E-02	8.2713E-03	2.8766E-05	-1.0913E-01	-1.8311E-10	8.0331E-01	6.9390E+00
21	3.0000E+00	-3.5022E-05	7.0462E-01	6.6826E-07	9.3283E-03	7.4518E-03	2.8291E-05	-9.9178E-02	1.9005E-10	7.9884E-01	7.5760E+00
22	3.1000E+00	-8.2385E-06	7.4571E-01	2.8666E-06	8.5464E-03	6.7932E-03	2.5618E-05	-9.0225E-02	3.1937E-10	7.9487E-01	8.3452E+00
23	3.2000E+00	1.1273E-05	7.9030E-01	4.1794E-06	7.8902E-03	6.2430E-03	2.0324E-05	-8.2147E-02	1.0340E-09	7.9123E-01	9.2516E+00
24	3.3000E+00	1.6066E-05	8.3447E-01	3.7935E-06	7.3062E-03	5.7555E-03	1.4191E-05	-7.4846E-02	7.1925E-10	7.8775E-01	1.0274E+01
25	3.4000E+00	9.4482E-06	8.7247E-01	2.6110E-06	6.7416E-03	5.2866E-03	9.2895E-06	-6.8263E-02	3.5396E-10	7.8417E-01	1.1345E+01
26	3.5000E+00	-2.7206E-05	8.9737E-01	1.5976E-06	6.1504E-03	4.7986E-03	5.9771E-06	-6.2742E-02	1.5317E-10	7.8021E-01	1.2347E+01
27	3.6000E+00	-6.7949E-06	9.0526E-01	1.0792E-06	5.5288E-03	4.2888E-03	3.7935E-06	-5.7066E-02	7.1061E-11	7.7571E-01	1.3161E+01
28	3.7000E+00	-8.8833E-06	9.0228E-01	6.6139E-07	4.9422E-03	3.8104E-03	2.0059E-06	-5.2505E-02	2.5291E-11	7.7104E-01	1.3623E+01
29	3.8000E+00	-8.5116E-06	8.9842E-01	4.6775E-07	4.4327E-03	3.3978E-03	1.1358E-06	-4.8426E-02	1.0954E-12	7.6654E-01	1.4490E+01
30	3.9000E+00	-6.6719E-06	8.9871E-01	-4.5726E-07	4.0079E-03	3.0597E-03	1.7151E-06	-4.4754E-02	-1.7524E-11	7.6240E-01	1.5257E+01
31	4.0000E+00	-4.7228E-06	9.0497E-01	-5.6556E-07	3.6644E-03	2.7804E-03	3.0714E-06	-4.1476E-02	-4.1510E-11	7.5874E-01	1.6163E+01
32	4.1000E+00	-3.8706E-06	9.1531E-01	-3.8386E-07	3.3759E-03	2.5502E-03	4.2686E-06	-3.8506E-02	-4.2552E-11	7.5541E-01	1.7200E+01
33	4.2000E+00	-3.8623E-06	9.2771E-01	-1.4046E-07	3.1263E-03	2.3520E-03	4.8714E-06	-3.5799E-02	-1.9114E-11	7.5231E-01	1.8353E+01
34	4.3000E+00	-3.9132E-06	9.4113E-01	5.3273E-08	2.9064E-03	2.1780E-03	4.8365E-06	-3.3336E-02	-9.1799E-12	7.4933E-01	1.9600E+01
35	4.4000E+00	-3.4773E-06	9.5506E-01	1.6935E-07	2.7104E-03	2.0235E-03	4.2790E-06	-3.1092E-02	2.6058E-11	7.4659E-01	2.0932E+01
36	4.5000E+00	-2.8374E-06	9.6921E-01	2.4663E-07	2.5341E-03	1.8852E-03	3.4306E-06	-2.9042E-02	2.9134E-11	7.4392E-01	2.2351E+01
37	4.6000E+00	-1.9992E-06	9.8339E-01	2.3496E-07	2.3746E-03	1.7604E-03	2.4214E-06	-2.7164E-02	2.1031E-11	7.4136E-01	2.3858E+01
38	4.7000E+00	-2.0544E-06	9.9750E-01	2.1264E-07	2.2295E-03	1.6478E-03	1.5915E-06	-2.5439E-02	1.3506E-11	7.3889E-01	2.5497E+01
39	4.8000E+00	-1.2729E-06	1.0115E+00	1.0619E-07	2.0971E-03	1.5445E-03	6.9281E-07	-2.3836E-02	3.0861E-12	7.3649E-01	2.7179E+01
40	4.9100E+00	-2.3446E-06	1.0248E+00	7.6741E-08	1.9777E-03	1.4522E-03	6.8383E-07	-2.2255E-02	2.2548E-12	7.3426E-01	2.9322E+01
41	5.0000E+00	0.0000E+00	1.0402E+00	7.6741E-08	1.8584E-03	1.3598E-03	-1.3771E-08	-2.0671E-02	2.2548E-12	7.3173E-01	3.1826E+01

RADII AT WHICH SOUND AND ALFVEN MACH NUMBERS ARE ONE

NO	TH(DEG)	RS	RA
2	9.0000E+01	3.5668E+00	1.8267E+00
3	9.2500E+01	3.5679E+00	1.8316E+00
4	9.5000E+01	3.5683E+00	1.8501E+00
5	9.7500E+01	3.5666E+00	1.8751E+00
6	1.0000E+02	3.5605E+00	1.9050E+00
7	1.0250E+02	3.5516E+00	1.9475E+00
8	1.0500E+02	3.5705E+00	1.9779E+00
9	1.0750E+02	3.5737E+00	2.0203E+00
10	1.1000E+02	3.5843E+00	2.0618E+00
11	1.1250E+02	3.5943E+00	2.0984E+00
12	1.1500E+02	3.6140E+00	2.1335E+00
13	1.1750E+02	3.6267E+00	2.1742E+00
14	1.2000E+02	3.6286E+00	2.2097E+00
15	1.2250E+02	3.6227E+00	2.2398E+00
16	1.2500E+02	3.6113E+00	2.2707E+00
17	1.2750E+02	3.5962E+00	2.3024E+00
18	1.3000E+02	3.5916E+00	2.3307E+00
19	1.3250E+02	3.5845E+00	2.3559E+00
20	1.3500E+02	3.5772E+00	2.3773E+00
21	1.3750E+02	3.5693E+00	2.3955E+00

22	1.4000E+02	3.5635E+00	2.4112E+00
23	1.4250E+02	3.5591E+00	2.4271E+00
24	1.4500E+02	3.5478E+00	2.4453E+00
25	1.4750E+02	3.5416E+00	2.4663E+00
26	1.5000E+02	3.5337E+00	2.4862E+00
27	1.5250E+02	3.5271E+00	2.5047E+00
28	1.5500E+02	3.5208E+00	2.5239E+00
29	1.5750E+02	3.5149E+00	2.5346E+00
30	1.6000E+02	3.5091E+00	2.5463E+00
31	1.6250E+02	3.5044E+00	2.5551E+00
32	1.6500E+02	3.4396E+00	2.5644E+00
33	1.6750E+02	3.4390E+00	2.5719E+00
34	1.7000E+02	3.4366E+00	2.5769E+00
35	1.7250E+02	3.4366E+00	2.5815E+00
36	1.7500E+02	3.4935E+00	2.5815E+00
37	1.7750E+02	3.4973E+00	2.5733E+00
38	1.8000E+02	3.4481E+00	2.4581E+00

NPTVR = 1

TIME = 3.665E+03 = 2.436E+02 MINUTES, TIME CYCLE NO 104, DTT = 3.473E-02

RCONTS-RO =8.5761E-02 SOLAR RADII =5.9664E+04 KM, RCONTSR-RO =8.535E-03 SOLAR RADII =5.937E+03 KM

ENERGY BUILD-UP (ERGS/KM2)S MAGNETIC =8.53920E+23, THERMAL =3.15416E+24, KINETIC =6.15955E+23, GRAVITATIONAL =5.66324E+24

MASS BUILD-UP =4.51146E+09 GMS/KM2 =2.69762E+33 PARTICLES/KM2

R CHARACTERISTIC DIRECTIONS AT RO

T	L3	L4	L5	L6
1.5708E+00	1.0517E+00	5.4332E-07	-1.0517E+00	-5.4332E-07
2.3562E+00	1.0997E+00	6.3283E-01	-1.0963E+00	-5.3946E-01
3.1416E+00	1.0467E+00	9.1953E-01	-9.5333E-01	-8.2619E-01

T = 1.571E+00 RAD = 9.000E+01 DEG, T-GRID NO 2

NO	R	VT	VR	JXBT	D	P	BT	BP	JXBR	T	BETA
1	1.0000E+00	0.0000E+00	0.0000E+00	-9.4397E-09	1.0538E+00	1.0562E+00	7.5764E-01	-1.3464E-06	-5.3220E-03	1.0020E+00	1.8336E+01
2	1.1000E+00	3.2385E-05	1.4788E-02	2.2933E-04	6.2254E-01	6.0887E-01	5.0386E-01	8.6337E-04	-1.3523E-02	9.7864E-01	2.3536E+01
3	1.2000E+00	2.6691E-05	2.4233E-02	3.5534E-04	3.9175E-01	3.7568E-01	3.7608E-01	4.7625E-04	-2.7946E-02	9.5893E-01	2.6553E+01
4	1.3000E+00	8.5543E-05	4.0336E-02	5.8692E-04	2.6597E-01	2.4594E-01	2.6682E-01	1.2522E-03	-1.5942E-02	9.4256E-01	2.9468E+01
5	1.4000E+00	-2.1060E-06	4.9401E-02	3.6642E-04	1.8193E-01	1.6892E-01	2.1125E-01	1.3444E-03	-5.7575E-02	9.2814E-01	3.7828E+01
6	1.5000E+00	-1.8476E-06	5.5320E-02	4.2595E-04	1.3323E-01	1.2190E-01	1.5092E-01	1.6773E-03	-3.8327E-02	9.1491E-01	5.3512E+01
7	1.6000E+00	-2.1276E-05	7.2036E-02	3.0376E-04	1.0130E-01	9.1461E-02	1.1433E-01	1.1206E-03	-3.1425E-02	9.0290E-01	5.9362E+01
8	1.7000E+00	-1.6006E-05	9.6593E-02	1.5709E-04	7.8648E-02	7.0124E-02	9.0617E-02	5.3376E-04	-2.7156E-02	8.9163E-01	6.1750E+01
9	1.8000E+00	-7.0195E-05	1.2415E-01	6.8943E-05	6.2116E-02	5.4727E-02	7.7854E-02	2.2935E-04	-2.3506E-02	8.8104E-01	9.0291E+01
10	1.9000E+00	-5.5355E-05	1.5645E-01	3.1180E-05	5.0026E-02	4.3530E-02	6.7534E-02	1.0415E-04	-2.0231E-02	8.7130E-01	9.5401E+01
11	2.0000E+00	1.9333E-05	1.9477E-01	1.5766E-05	4.1133E-02	3.5477E-02	6.2291E-02	5.4914E-05	-1.7310E-02	8.6249E-01	9.7602E+01
12	2.1000E+00	7.0130E-05	2.3799E-01	-8.6671E-07	3.4402E-02	2.9335E-02	5.4907E-02	-3.2440E-06	-1.4704E-02	8.5445E-01	9.7505E+01
13	2.2000E+00	5.0886E-05	2.8237E-01	-2.1637E-05	2.9036E-02	2.4542E-02	5.1717E-02	-8.4665E-05	-1.2424E-02	8.4693E-01	9.5606E+01
14	2.3000E+00	-9.3250E-06	3.2499E-01	-3.7913E-05	2.4797E-02	2.0820E-02	4.7292E-02	-1.7182E-04	-1.0437E-02	6.3977E-01	9.3137E+01
15	2.4000E+00	-5.6456E-05	3.6553E-01	-4.5233E-05	2.1236E-02	1.7730E-02	4.4441E-02	-2.2833E-04	-8.8094E-03	8.3294E-01	8.9775E+01
16	2.5000E+00	-7.4531E-05	4.0533E-01	-4.5900E-05	1.8423E-02	1.5227E-02	4.2084E-02	-2.5670E-04	-7.4068E-03	8.2653E-01	8.5976E+01
17	2.6000E+00	-8.2217E-05	4.4532E-01	-4.3534E-05	1.6079E-02	1.3193E-02	4.0152E-02	-2.7503E-04	-6.3556E-03	8.2050E-01	8.1832E+01
18	2.7000E+00	-9.8980E-05	4.8541E-01	-4.0068E-05	1.4138E-02	1.1521E-02	3.8557E-02	-2.8524E-04	-5.4154E-03	8.1481E-01	7.7463E+01
19	2.8000E+00	-1.2375E-04	5.2491E-01	-3.6013E-05	1.2508E-02	1.0124E-02	3.7212E-02	-2.9074E-04	-4.6093E-03	8.0942E-01	7.3110E+01
20	2.9000E+00	-1.6630E-04	5.6319E-01	-3.1460E-05	1.1121E-02	8.9441E-03	3.6045E-02	-2.8959E-04	-3.9144E-03	8.0427E-01	6.8838E+01
21	3.0000E+00	-2.0566E-04	5.9993E-01	-2.6594E-05	9.9316E-03	7.9336E-03	3.5006E-02	-2.8082E-04	-3.3151E-03	7.9934E-01	6.4780E+01
22	3.1000E+00	-2.3521E-04	6.3512E-01	-2.1716E-05	8.9073E-03	7.0780E-03	3.4061E-02	-2.6434E-04	-2.7984E-03	7.9463E-01	6.1008E+01
23	3.2000E+00	-2.5332E-04	6.6890E-01	-1.7135E-05	8.0222E-03	6.3385E-03	3.3181E-02	-2.4168E-04	-2.3526E-03	7.9012E-01	5.7569E+01
24	3.3000E+00	-2.5607E-04	7.0136E-01	-1.3166E-05	7.2548E-03	5.7010E-03	3.2343E-02	-2.1483E-04	-1.9875E-03	7.8582E-01	5.4496E+01
25	3.4000E+00	-2.4885E-04	7.3252E-01	-9.6412E-06	6.5867E-03	5.1490E-03	3.1524E-02	-1.8591E-04	-1.6348E-03	7.8173E-01	5.1812E+01
26	3.5000E+00	-2.2659E-04	7.6234E-01	-6.8920E-06	6.0023E-03	4.6687E-03	3.0713E-02	-1.5690E-04	-1.3486E-03	7.7781E-01	4.9526E+01
27	3.6000E+00	-1.9428E-04	7.9273E-01	-4.7675E-06	5.4855E-03	4.2499E-03	2.9953E-02	-1.2946E-04	-1.1044E-03	7.7405E-01	4.7638E+01
28	3.7000E+00	-1.5593E-04	8.1756E-01	-3.2464E-06	5.0345E-03	3.8791E-03	2.8957E-02	-1.0477E-04	-8.9853E-04	7.7050E-01	4.6133E+01
29	3.8000E+00	-1.1710E-04	8.4314E-01	-2.1622E-06	4.6316E-03	3.5526E-03	2.8103E-02	-8.3514E-05	-7.2759E-04	7.6707E-01	4.4986E+01
30	3.9000E+00	-8.1753E-05	8.6724E-01	-1.4247E-06	4.2727E-03	3.2634E-03	2.7134E-02	-6.5883E-05	-5.8787E-04	7.6378E-01	4.4162E+01
31	4.0000E+00	-5.2474E-05	8.9310E-01	-9.3587E-07	3.9521E-03	3.0061E-03	2.6251E-02	-5.1637E-05	-4.7530E-04	7.6062E-01	4.3624E+01
32	4.1000E+00	-3.0112E-05	9.1198E-01	-6.1704E-07	3.6643E-03	2.7765E-03	2.5313E-02	-4.0514E-05	-3.8553E-04	7.5759E-01	4.3332E+01
33	4.2000E+00	-1.4228E-05	9.3251E-01	-4.1072E-07	3.4059E-03	2.5711E-03	2.4382E-02	-3.1866E-05	-3.1425E-04	7.5468E-01	4.3231E+01
34	4.3000E+00	-3.6632E-06	9.5296E-01	-2.7756E-07	3.1746E-03	2.3869E-03	2.3466E-02	-2.5245E-05	-2.5753E-04	7.5188E-01	4.3349E+01
35	4.4000E+00	2.5352E-06	9.7244E-01	-1.8974E-07	2.9647E-03	2.2211E-03	2.2571E-02	-2.0206E-05	-2.1193E-04	7.4916E-01	4.3601E+01
36	4.5000E+00	6.5212E-06	9.9127E-01	-1.3216E-07	2.7744E-03	2.0713E-03	2.1639E-02	-1.6333E-05	-1.7494E-04	7.4653E-01	4.3931E+01
37	4.6000E+00	[illegible]	[illegible]	[illegible]	2.6013E-03	[illegible]	[illegible]	[illegible]	[illegible]	7.4407E-01	4.4522E+01